ISTC Project #3345

Source Term Assessment at Ex-vessel Stage of Severe Accident

Final Project Activity Report

on the work performed from 01.10.2007 to 31.12.2007

Federal State Unitary Enterprise "St.Petersburg Research and Design Institute ATOMENERGOPROEKT"
(FSUE SPAEP)

191036, Russia, St.Petersburg, 2nd Sovetskaya street, 9/2a

Project Manager
SPAEP Deputy Director for R&D
Doctor of Science (Power Engineering)

Vladimir Bezlepkin

31.12.2007

Signature / Date

1. Objectives of the Project, Scope of Work and Technical Approach

Objectives of the Project

The "Ex-vessel Source Term Analysis" (EVAN) ISTC project includes theoretical and experimental research of the processes affecting the late phase fission product release to the PWR containment atmosphere at the late stage of the hypothetical severe accident with core meltdown. The main results expected to be obtained within the framework of the proposed project are listed below:

1. Experimental data and numerical analysis of core melt fission product release, applicable to different designs of power units, taking into account corium transition from sub-oxidized to fully-oxidized state and water supply onto the melt surface.
2. Experimental data and numerical analysis of processes of modeling aerosol transport and deposition in primary circuit pipelines at different flow conditions of the medium-carrier, aerosol species characteristics.
3. Experimental data and numerical analysis on how composition of containment sump solution and sludge affects content and partitioning of volatile iodine species in the containment atmosphere at different temperature, irradiation dose, ambient parameters and covering characteristics.

The scope of the project may be extended by additional adaptation and validation of computer models, continuation of experimental programmes and radiological consequences calculation for selected severe accident scenarios.

This research is a sort of applied investigations. Theoretical and experimental research results can be used for computer codes validation for application to new designs, for safety assessment of both existing Russian and foreign NPP designs, including probabilistic safety analyses of 2 and 3 level, for development of severe accident management strategies and for emergency planning analysis. The project features possibility to obtain data directly applicable to new designs of NPP with VVER-type reactors providing severe accident management measures.

Scope of Work and Technical Approach

Task 1. Assessment of results of severe accident sequences modeling

Task description and main milestones	Participating Institutions
Assessment of results of severe accident sequences modeling **Task Stages: 1) Assessment of results of severe accident sequences modeling for different NPP designs with PWR or VVER reactors. Justification of initial data for experimental investigations. 2) Justification of applicability to be obtained experimental data for computer codes validation. Preparation of experimental programs.** **Tools to solve the task: 1) Results of severe accidents modeling. 2) Computer codes RATEG/SVECHA/HEFEST, CORCAT, DINCOR, KUPOL-M, SCDAP/RELAP, MELCOR. Assessment of results of numerical modeling.**	1- SPAEP 2- IBRAE

Description of deliverables	
1	Report on initial data for experimental programs for tasks 2, 4, 6 (stage 2)

The goal of the analysis is to determine the parameter ranges within the reactor plant and containment, core melt parameters, FP aerosol characteristics, surface boundary conditions at structures and equipment, chemical content of containment sump solution, dose rate ranges in the equipment and containment, and other parameters, necessary to develop the final test specification for Tasks 2, 4, and 6. Participants will also analyze the capabilities of physical models for aerosol generation and transport for RATEG/SVECHA/GEFEST.

Task 2. Experimental research on FP release from molten pool/core melt catcher

Task description and main milestones	Participating Institutions
Experimental research on FP release from molten pool **Work stages: 1) Experimental investigations of low-volatile fission products release during molten corium oxidation. Melt characteristics and composition of the FP in question are determined from the results of Task 1. 2) Experimental investigations of low-volatile fission products release during water supply onto the melt surface.** **Tools for solving the task: 1) A set of "Rasplav" experimental installations, equipped with aerosol sampling system, for studying high-temperature phenomena in molten corium. 2) A complex of instruments and equipment for tests preparation, conducting posttest analyses and processing experimental results. The complex includes XRF spectrometers, microsizer, mass spectrometer, spectrophotometer, auxiliary equipment (crusher, microgrinder, laboratory balance, etc.)**	1- NITI

	Description of deliverables
1	Report on experimental study of low-volatile fission products release during molten corium oxidation
2	Report on experimental study of low-volatile fission products release from molten corium pool covered by water layer

A calculated prediction of the main radiation safety objectives during a severe accident requires substantiated data, e.g. coefficients of the radiologically significant radionuclides release from molten fuel into the environment. At present such data are available for the majority of volatile radioactive FP (radioactive noble gases, iodine, Cs, Rb, etc.), which evaporate during the core degradation and molten fuel pool formation. The release of such low-volatile FP as Ba, Sr, La, Ce, isotopes of the platinum group elements (Ru), lanthanoids and actinoids form a high-temperature molten core pool still has not been studied sufficiently due to extremely difficult engineering aspects of experimental investigations.

For suppressing the FP release, protecting the superstructures from heat radiation from the melt surface and increasing the efficiency of corium pool cooling, the core melt catcher (CMC) envisages water feeding onto the melt surface after inversion of the oxidic and metallic layers. The resulting decrease in radionuclides release into the containment is mainly achieved owing to:

- capture of a significant part of aerosols by the water layer at bubbling the gas-aerosol flow through it,
- melt surface temperature decrease at the film boiling of water,
- crust formation at the melt surface.

At present, there does not exist a unified theory that would describe the mechanisms of evaporation from oxidic melts. The complexity of oxidic systems evaporation is that evaporation of few oxide follows one chemical pattern (congruously). The majority of data on evaporation have been obtained by the classical Knudsen's method (effusion into vacuum), as well as by high-temperature mass spectrometry (a combination of Knudsen's method with mass spectrometry of the evaporated products) and are available for individual oxides. These data are hardly applicable to the multicomponent oxidic melts and, correspondingly, to the severe accident conditions.

The study FP evaporation from molten corium (Task 2) envisages application of the flow method which belongs to the dynamic methods of steam pressure determination. The essence of the method is in saturation of the carrier gas passing at a constant rate above the melt (water-flooded, too) with vapors of the substance in question. The amount of the transported substance will be determined by means of physicochemical analyses.

The high temperature and chemical activity of the molten ceramic corium place limitations on the application of conventional heating methods and crucible materials. The method of induction melting in the cold crucible (IMCC) in the RF band has been chosen for producing ceramic melts and achieving objectives of the project.

Characteristic features of the method:

- internal power in the melt;
- the presence of a crystallized melt layer (crust) between the melt and the crucible cold wall, which prevents mass transfer of the crucible material to the melt.

This combination of the non-contact heating and the non-contaminating method of oxides melting ensures:

- melt purity as high as that of the initial products;
- melt superheating above T_{liq}, chemically active oxidic materials included;
- melting and long-term maintenance of an oxidic system in molten state in both neutral and oxidizing atmospheres;
- universality and compactness of the melting device.

The level of experimental investigations is determined to a considerable degree by the available material and technical basis. The backbone of the facility are three experimental installations for the induction melting of corium in which the IMCC technology is realized at different frequencies of the heating current. They allow experimenting with a broad range of corium compositions which differ greatly in electrical conductivity when in molten state. The specification of the experimental installations are given in Table 1.

Table 1. Specification of experimental installations.

Specification	Experimental installation		
	Rasplav-2	Rasplav-2/C	Rasplav-3
Molten corium preparation method	Induction melting in the cold crucible (IMCC)		
Installed capacity, kVA	250	250	100
Melt mass in crucible, kg	Up to 5	Up to 10	Up to 2
Melt temperature, °C	Up to 3000		
Above-melt atmosphere	Air, nitrogen, helium, argon	Air	Air, nitrogen, helium, argon
Melt composition	Oxidized corium		Unoxidized corium and steel
Possible manipulations with melt	Ingot production	Spreading	Ingot production
Commissioned, year	1988	1995	2002

The installations are equipped with modern monitoring instruments, including those for measuring the melt temperature, electrical characteristics of melting, calorimetry of heat fluxes and the process video monitoring. Acquisition, processing and storage of the results of measurements is done using the data acquisition and measuring system IIS-R designed and produced by the NITI specialists. IIS-R incorporates modern software controlled by the Lab View 5.5 software package.

The experimental installations are supported by the laboratory equipped with modern instruments for physicochemical analyses.

Table 2 NITI contribution to the EVAN project: suggested experimental. Stage 1.

	Test	Test objective	Specifications	Notes	Time
Stage 1	EVAN–FP1	Study of low-volatile fission products release during molten corium oxidation	Corium composition: $UO_2 – ZrO_2$ - Zr, U/Zr(at)=1.2, C-32 (specified according to the results of Tasks 1 and 2)>C-100, Corium mass: 1-2 kg, Melt temperature: T_{liq}+(50-100)C, FP: Ru, Mo, Ce, La, Sr, Ba	Oxidation in air	1-4 quarter

Notes:

- Determination of the FP release coefficients is carried out using stable FP simulators by the flow method that envisages measurements of FP concentrations in the melt, gas (steam) flow and water layer on the melt surface.

Task 3. Analytical investigation of fission products release from molten pool or core catcher.

Task description and main milestones	**Participating Institutions**
Analytical investigation of fission products release from molten pool. **Task Stages: 1) Review of modern codes capabilities to simulate FP release from molten pool. Justification of applicability to be obtained experimental data for computer codes validation. 2) Pre tests/post tests simulation (in connection with experimental program performance).** **Tools to solve the task: High performance computers, analytical and numerical calculation models**	1- IBRAE
Description of deliverables	
1	Report on modeling results of fission products release from molten pool

By now, many physical models of FP release from the molten pool have been implemented in the computer codes. They are characterized by the various levels of sophistication, from simplest correlation models to mechanistic ones. To do the calculations, it is supposed to use codes RATEG/SVECHA (code RELOS, Germany, if provided by counterparts). Experimental data from EU Framework Programme LPP project provided by collaborators could be used for additional analysis.

Task 4. Experimental study of aerosols transport processes in the primary circuit equipment

Task description and main milestones	Participating Institutions
Experimental study of aerosols transport processes in the primary circuit equipment **Work stages: 1) Final completing and adjustment of experimental facilities. Development of research procedures. 2) Experimental studies of modeling aerosol particles deposition on pipeline surfaces from a gas flow and re-entrainment of particles.** **Tools to solve the task: 1) A test facility for studying aerodynamics of a "dust-laden flow": distributions of velocities, concentrations, and dynamics of deposition of aerosol particles (depending on disperse composition of aerosol) on the channel walls and re-entrainment of particles in the flow, equipped with an online optical monitoring system. A test facility for gas cleaning from aerosol impurity. A test facility for calibration of the measuring system, adjustment of aerosol particle generators and determination of spectral composition of the particles. 2) A complex of instruments and equipment for experiment preparation, performance of post-test analyses and processing of experimental results. The complex includes: lasers, thermoanemometer, signal analyzers, LDA-processor, PC-based workstations.**	1- CKTI

Description of deliverables	
1	Report on results of experimental studies of aerosol particles transport processes in the primary circuit pipelines

Fission products deposited at the initial stage of a severe accident in the primary circuit (including heat-transfer surfaces of steam generators) can in future enter the atmosphere of the containment or the enviontment in case of containment bypass. Account of FP retention in the primary circuit at the initial stage of the accident may influence the evaluation of accidental release, which can be both overestimated (due to possible additional discharge of deposited FP from the primary circuit to the containment atmosphere at a later stage of the accident) and underestimated (in case of reliable FP localization within the primary circuit). To forecast the rates of FP leaving the primary circuit surfaces (due to resuspension and re-evaporation), it is important to know conditions of aerosol deposition on walls of pipelines of different diameters from the steam-gas turbulent flow. Experimental research of local problems of particles deposition and resuspension, and processes of FP re-evaporation from inside surfaces of the primary circuit will allow more precise definition of characteristics of FP entering the containment atmosphere from the primary circuit late in severe accidents.

Initial stages of the experimental research will be carried out using the available installation that was earlier used in experimental study of fluid mechanics and heat transfer in Russian Fissile Material Storage Facility cooling pipes. In particular, there is a steel cylindrical channel of 98 mm inside diameter, 6.2 m long. Optical windows for flow scanning by laser Doppler anemometers are located in four cross-sections along the length. Coordinate devices for flow scanning by wire sensors (thermal anemometers and resistance thermometers) are disposed in five cross-sections along the length. All measurements are computer-controlled.

Optical methods as applied to the task under consideration can be successfully used both for measuring kinematical characteristics of particles and for fractional analysis of a two-phase flow.

Kinematical measurements

The laser Doppler method is used for kinematical measurements. It permits to measure, with sufficient accuracy (of the order of several percent):

- carrying phase velocity profile,

- suspended phase velocity profile (for particle size larger than several microns).
The measuring method is absolute and does not require any calibration.
The measured velocity range is 0.1…100 m/s.
Measurement of both longitudinal and transverse velocity components is possible. Both average and pulsating velocity components are measured. The measurements are performed in an online mode.
The time of traversing the channel diameter is about 1 min. Simultaneous measurements in several (up to four) check cross-sections along the pipe length are possible. The tube is supplied with the protective glasses.
CKTI has main measuring equipment units, which does not exclude the necessity of adapting them for solution of the problem under consideration. At the same time, adaptation of the experimenta; setup for the radial velocity measurements is considered to be unnecessary complex so for the radial flow velocity component distribution and its pulsation characteristics will be measured by three-wire thermoanemometer.
Fractional analysis
Fractional analysis is understood as measurement of an average size (and, sometimes, also the size distribution function) and the volume concentration of particles. Unlike kinematical measurements, there is not any optical method today which enables measurements throughout the entire required range of particle sizes. Information available at present is not sufficient for final selection of a measuring method. As a first approximation, selection of the spectral transparency method (STM) for liquid particles and the particle counter method (PCM) for hard particles seems reasonable. A similar solution was used in experiments on the STORM test facility.
For measurements in flows with particle sizes of up to several microns, optical constants (refraction index) of particles must be known.
STM is absolute method and does not require calibrations, but it is integral (that is, it gives an averaged value along the beam path in the medium under study). The use of the method allows measurement of a certain combination of size and volume concentration. In some cases, both parameters can be measured separately. This depends on particle material and size range.
PCM has a high spatial resolution (fractions of a cubic millimeter) and allows measurement of a size distribution function of droplets. Thus, building of a profile of particle size and concentration over the channel diameter is possible. The main drawback of the method is that it is not absolute and requires provision of a calibrating apparatus. The exception is performance of relative measurements (e.g., piecewise concentration of particles).
The STM is limited by particles concentration at the lower boundary while the PCM at the upper boundary.
The STM allows online measurements, and the PCM requires a certain time (not more than a minute) for measurements at a single point.
All the above considerations are stated for an assumption that particles have a spherical shape. In case the particles have large deviations from spherical form, special calculations of light dissipation and additional experiments on a calibration apparatus will be required.
Engineering implementation of the fractional analysis methods under consideration will not require purchase of any special expensive equipment. All optical methods considered allow creation of a fully automated measurement complex including measurement, traversing and processing of results.
CKTI has considerable experience both in kinematical measurements of one- and two-phase flows and in fractional analysis of two-phase media (in particular, analysis of high-velocity steam flows with water droplets of a size from hundredth parts to hundreds microns).

Task 5. Theoretical and computer modeling of aerosol transport in the primary circuit

Task description and main milestones	**Participating Institutions**
Theoretical and computer modeling of aerosol transport in the primary circuit. **Task Stages: 1) State-of-art review of modeling capabilities of the processes in question by modern computer codes, justification of applicability of the expected experimental results for models validation. 2) Pretest/posttest calculations (according to the test schedule).** **Tools to solve the task: 1) 2D and 3D CFD codes coupled with mechanistic aerosol models,** **RATEG/SVECHA/GEFEST code with integral aerosol models. 2) High-performance computers.**	1- IBRAE 2- SPAEP
Description of deliverables	
1	Short description of model for FP in reactor coolant circuit (PROFIT)**.** Report on modeling results for aerosol particles transport in the primary pipelines

Fission products deposited at the in-vessel stage of severe accident in the primary circuit (including heat transfer surfaces of steam generators) can be released into containment atmosphere at later stages of the accident. Taking into account FP confinement in the primary circuit at the initial stage may both increase (due to possible additional resuspension/revaporization of deposited FP from the primary circuit to the containment atmosphere at ex-vessel stage) and decrease (due to formation of stable chemical compounds with FP at surfaces of primary circuit equipment) FP release. To predict FP release rate from surfaces of primary circuit equipment (due to resuspension and revaporization), it is greatly important to know conditions of aerosol deposition from steam-gas turbulent flow onto reactor plant pipe walls of different diameters. Partly, of the principal interest are the flow characteristics (laminar and turbulent flow), fluid density and temperature gradients in the near-wall space for analysis of aerosol deposition due to diffusionphoretic and thermophoretic forces. Besides experimental investigation of these processes, it is necessary to carry out joint calculations on gas-dynamical and aerosol models. While modeling the aerosol transport in the real geometry of the primary circuit it is necessary to employ such thermal hydraulic models that allow to account for Reynolds number change for changing pipeline geometry (e.g. in elbows, and bends). Numerical and experimental investigations of local problems related to FP species deposition, resuspension and deposited FP revaporization from internal surfaces of the primary circuit will allow better prediction of FP release to the containment atmosphere at severe accident ex-vessel stage.

To model the transport and deposition processes, the hydrodynamics equations with aerosol particle dynamics equations will be solved numerically. By now many effective ways to solve hydrodynamics equations has been developed. The main problem is to correctly model the turbulent transport processes. For this two principally different ways exist. The first approach imply using the Reynolds Averaged Navier-Stokes equations (RANS) with semi-empirical constitutive models for turbulence. Using this approach, it is possible to build the effective numerical algorithm and to perform calculations for complex 3D flows. The main shortcoming of this approach is that the assumption of turbulent folws being proportional to the concentration gradients is used (which is not always correct, especially for near-wall area) along with not sufficiently accurate modeling of the turbulence parameters.

The other approach is the Direct Numerical Simulation (DNS) turbulence modelling. While using this approach, the hydrodynamics equations for turbulent flow are solved at such fine grid so it becomes possible to resolve flows for all scales up to Kolmogorov's turbulence micro-scale. Combined with the particle transport modeling, such approach can allow direct calculation of all deposition processes with the only external data necessary being aerodynamical particle characteristics and Brownian diffusion coefficient. However, this approach is very demanding for the numerical grids used (number of nodes for such grid is about the Re number to the degree of 9/4) which limits is applicability to the relativels low Re-number flows.

The so called Large-Eddy Simulation (LES) approach holds the intermediary position between these two approaches. In this approach only relatively large, energy-retaining eddies are explicitly resolved at eh grid, while flows with smaller scales (sub-grid) are modeled parametrically. This approcah requires significantly less efforts and allows to model the wide range of turbulent flows with minimal requirements for empirical constitutive relations. Advantage of this approach compared to RANS is that it allows to model with more accuracy the impact of turbulence on the particles behaviour and provides more detailed information about turbulence parameters necessary for modeling the particles deposition and resuspension.

SPAEP NPP safety research department and IBRAE have access to the modern high-performance computers allowing to use complex and resource-consuming computer codes for necessary calculations.

In IBRAE the aerosol transport processes are modeled with the baseline models implemented in the RATEG/PROFIT computer code. The PROFIT models are used for evaluating the fission products aerosols and vapours transport within the reactror coolant system and the in-containment source term. The PROFIT models are interfaced with RATEG thermohydraulics code. Within this project the Task 4 experimental data will be analysed with the aid of those models by specialists from SPAEP and IBRAE. The 3D models will be used to estimate the limitations of the baseline models and to gain independent insights into the modeled processes.

Thus, for Task 5 realization the hydrodynamics models coupled with aerosol models will be used. External boundary conditions necessary for calculations will be chosen based on the results of Task 1. Task 5 stages are: (I) analysis of the main processes and the physico-mathematical models for particle transport and deposition; (II) calculation and analysis of results; (III) calculations with aerosol kinetics models coupled with thermal hydraulic codes, and sensitivity study for different parameters on final results. There will be joint work of IBRAE and SPAEP on cross-validation of aerosol transport models implemented in the integral RATEG/SVECHA/GEFEST code with CFD-codes. Also analysis of experimental date for STORM (JRC Ispra) and PSAERO (VTT) installations is proposed based on data provided by collaborators.

Task 6. Experimental investigations of containment parameters impact on volatile iodine content and correlation

Task description and main milestones	Participating Institutions
Experimental investigations of containment parameters impact on volatile iodine content and correlation. **Task stages: 1) Completing and adaptation of the experimental installatios, methodics perfection, experimental researches of sludges effect (Fe-oxyhydrates and silicates) on volatile iodine species content and correlation in gas and water phases.** **Tools to solve the task: Autoclave installations with sampling for researches of same iodine species and the water/gas phase iodine partitioning coefficients in the impurities present and the temperature range 20-150^{0}C, pressure 0,1-0,8 MPa, γ-irradiation-0-5 kGy/h. Gamma-radiation, facility RChM-γ-20. Methods and sorbents for the determination of iodine species ratio in the water and gas phases. Analytical and chromatographic methods and techniques for the impurities radiolysis products and various iodine species detection; ion-selective and red-ox electrodes, ionometer, spectrophotometer, gas-liquid-chromatography, gamma-spectrometry, iodine sensor and other**	1- VNIPIET 2- NITI (Department 5)

Description of deliverables	
1	Reports on experimental tests (Information)
2	Report on experimental researches of sludge effects in water phase on iodine volatility

For assessment of NPP radiation safety under reactor accident conditions and for prediction of volatile radioiodine species release it is necessary to have reliable data on main containment parameters and impurities in water phase influence on iodide-ions oxidation rate, on iodine partition coefficients between water/gas phases, volatile iodine species in gas phase accumulation rate, and on the ratio of inorganic/organic gaseous iodine species, particularly during long-term containment conservation (post-accident period).

Among the main factors providing the iodine safety there are the following: supression of gaseous iodine species generation, stability of processes of volatile iodine species fixation and trapping, accounting for containment parameters and impurities effects on iodine state and volatility.

Effect of containment parameters, such as temperature, pH and red-ox-potential of water phase, dose rate of gamma-irradiation, was researched enough and correctly interpreted. So iodide-ion oxidation to molecular iodine (volatile species) under gamma-irradiation of aqueous low-acidic solutions depends on iodide-ion oxidation by radiolysis water products (mainly OH-radicals), and oxidation rate depends on dose rate, solution pH, temperature and iodide concentration. Essential dependence iodide oxidation rate from pH was stipulated by participation of H^+-ions in competing reaction of radiolytical oxidation of ion I^- and reduction of I_2 by radicals of hydrogen peroxide. Limitation of I_2 formation would lead to reducing of generation organic iodides RI (R-alkyl-, aryl), thus mainly two processes influence the volatile iodine compounds generation and the ratio of iodine volatile/unvolatile species: water radiolysis, molecular iodine and organic iodide generation. Binding or trapping of elemental iodine are more effective processes in comparison with methyliodide where trapping is ineffective.

The interaction with surfaces in the containment can influence the iodine volatility due to its temporary hold-up at the surfaces or due to iodine chemical species change-over owing to reactions with surface material components (polymeric paints, steel, sludges).

In realistic severe accident conditions sludge including ferric oxides and hydroxides, silicates and gels of silicium acid, perhaps boron carbide will be accumulated in the containment sump. These impurities can influence the iodine content in the water phase, as they can adsorb and retain the iodide-ions. So sludges can act as effective iodine “sinks” and reduce iodine concentration in water phase; accordingly, the possibility of iodide-ions oxidation and accumulation of volatile iodine species in the gas phase can decrease. Ferric ions (Fe^{3+}) can oxidized of iodide ions in solution (at low pH), therefore iodine behaviour in present of ferric sludges would be predicted with difficulty.

These processes have hardly been studied, data on iodine adsorption are scarce, data on iodine sorbing behavior are in general not available. It is noteworthy to mention that iodine chemistry and behavior under increased temperature (up to 150-200^{0}C) have not been studied enough and there were problems in predicting iodine behavior in realistic accident condition.

Experimental programme includes the investigations of influence on iodine volatility ferric and silicate sludges, at varied proportions m/V, in temperature interval from 25 to 100 ^{0}C , pH – from 7-8 to 5, iodine concentration – 10^{-5}-10^{-8} gat/l, under γ-irradiation and ohne its.

Ferric oxides sludges impurities are representative for sump water under accident conditions. Ferric ions come into water phase by the various types of steel corrosion (mainly carbon steel) and in a state of aerosols from corium molten pool (core catcher) (sources – "sacrificial" ferric oxide and structure core materials); silicium also can come with aerosols from core catcher (refractory facing) and as impurity from construction materials. It is necessary to determine kinetics and sorption degree of various iodine species for temperature exposure (20-25; 50; 100^{0}C) and gamma-irradiation (0; 3 kGy/h).

Proposing matrix of investigations is given in the Table 3. Experiments are performed in autoclave apparatus for researches of iodine mass transfer. Solutions are prepared with high purity water ("nanopure") and addition of boric acid, KOH and HNO_3 (for pH regulation), CsI (KI). Inner volume of autoclave – up to 2 dm^3.

Table 3. Proposed matrix of tests on EVAN-project, Task 6

Test code	Test purpose	System investigated			Medium parameters				Analyzed parameters	Type of technique	Comment
		Water phase	Sludge mass	CsI concentration	T, °C	pH	γ-dose rate	Atmosph.			
I6-B1	Determination of effect of γ-irradiation on sorption by sludge and on iodine volatility in Ar and air atmosphere; investigation of process kinetics, impact of γ-dose	Water – 10 g/l H_3BO_3	0 2.5 g/l	10^{-5} mole/l	50-60	~5	0 ~1 kGy/h	Argon	pH; E_h; concentration I^-, IO_3^-, I_2, Fe in water phase; I_2 in gas phase	pre-test and post-test	Blank-tests with ^{131}I; ampoule technique
I6-B2			2.5 g/l				~1 kGy/h Σ5-10 kGy	Air			
I6-1	Investigation of process kinetics; determination of sorption by sludge and of iodine volatility depending on pH, sludge mass, T, C_{I^-}	Water – 10 g/l H_3BO_3	0 2.5 g/l	10^{-5} mole/l	50-60	~5	~1 kGy/h	Air	pH; E_h; concentration I^-, IO_3^-, I_2, Fe in water phase; I_2 in gas phase	pre-test and post-test	Kinetics 1-24 h with ^{131}I; ampoule technique
I6-2			0 2.5 g/l	10^{-5} mole/l	25; 95-100; 150	~5					
I6-3			2.5 g/l 5.0 g/l	10^{-7}-10^{-8} mole/l	50-60	4; 5; 6-7; 8					
I6-4	Determination of iodine sorption by sludge depending on water iodine species, pH and T (no γ-irradiation). Comparison of ampoule and autoclave tests	Water – 10 g/l H_3BO_3	2.5 g/l	10^{-4} mole/l (CsI, CsI+I_2)	50-60 95-100	5; 6-7; 8	0	Air	pH; E_h; concentration I^-, IO_3^-, I_2, Fe in water phase; I_2 in gas phase	pre-test and post-test	Ampoule technique
I6-5	Investigation of iodine sorption by sludge and sludge components depending on content and parameters of water phase	Water – 10 g/l H_3BO_3 (+$5\cdot10^{-5}$ mole/l H_2O_2)	0 2.5 g/l 5.0 g/l (H_2SiO_3, FeOOH)	10^{-4} mole/l (CsI, CsI+I_2)	25 50-60 95-100	4; 5; 6-7; 8			pH; E_h; pI-on-line; concentration I^-, IO_3^-, I_2, Fe in water phase; indication of I_2 in gas phase	on-line pre-test and post-test	Autoclave technique

Experiments in presence impurities and under γ-irradiation can be performed with ampoule methodic. VNIPIET is performing experiments without irradiation, NITI – with irradiation. At iodine low concentrations (<10^{-8} mol/l) test are performed with ^{131}I. Solution samples are analyzed on iodine total content and ratio of inorganic/organic species. Iodine partition coefficients are calculated from experimental results. Experimental autoclave apparatus would be reconstructed and adapted to experimental matrix conditions. Techniques and analytical instrumental equipment would be checked and adapted to necessary measurement ranges and increased temperatures. Used experimental methods and equipment are given in the Table 4.
New experimental results on volatility and iodine speciation would be used to iodine behavior model for its approximation to realistic accident regimes, also for the assessment of iodine environmental source terms for selected accident scenarios.

Table 4.- Methods of iodine analysis

Phase	Component	Analytical technique	Equipment	Sensitivity, mole/l
Water	I^-	I-selective electrode Photometry	Ion meter ANION-4110 photocolorimeter KFK-2MP	$3\cdot10^{-7}$ 10^{-6}
	IO_3^-	Photometry	Photocolorimeter	10^{-6}
	I_2	Extraction, photometry	Photocolorimeter, spectrophotometer	10^{-6}
	^{131}I (I^-, IO_3^-, IO_4^-)	Radiochromatography (frontal chromatography at non-organic sorbent) Gamma-spectrometry	Gamma-spectrometer	10^{-8}-10^{-11}
	pH, E_h	Potentiometry	Ion meter ANION-4110	pH=0.01 E_h=±1 mV
	electrical conductance	Conductometry	Conductometers UPK HJ 98309 PWT HJ 98308	0.001 μSm/cm 0.1 μSm/cm
Water	ΣFe, Fe(III)/Fe(II) soluble forms	Analytical techniques, photometry, membrane filtration	Photocolorimeter, spectrophotometer SF-2,6	10^{-6}
Gas	I_2 (RI)	Sorption at filters assembly, extraction, photometry	Spectrophotometer SF-2,6	1-5 μg of I_2 in sample
	I_2 (RI)	Gas chromatography	Gas chromatograph	10^{-9}
	^{131}I ($R^{131}I$)	Collecting at selective sorbents, gamma-spectrometry	Gamma-spectrometer	$1\cdot10^{-5}$ Bq/l
	I_2, HI, CH_3I, HIO_3	Ion Mobility Spectrometry (IMS)	Ion Mobility Spectrometer (prototype)	1 μg in sample

Task 7. Numerical and theoretical modeling of containment parameters impact on volatile iodine species content and correlation

Task description and main milestones	Participating Institutions
Numerical and theoretical modeling of containment parameters impact on volatile iodine species content and correlation. **Task stages: 1) Iodine model analyses and adaptation, choice of parameters and process constants. 2) Pre-test/post-tests calculation (according to test schedule).** **Tools to solve the task: 1) Containment iodine behavior model under accident conditions, developed by VNIPIET/SPAEP. 2) Computer codes for calculations of pH and E_{red-ox} in solution; databases on iodine rate and equilibrium constants; published experimental and calculation data; proprietary unpublished data.**	1- SPAEP 2- VNIPIET

Description of deliverables	
1	Preliminary report on iodine model adaptation
2	Pre-test/post-tests calculation results (information)

The main computer code is based on developed computer model of iodine mass transfer and chemical iodine species (I^-,I_2, IO_3^-, CH_3I) permanent partition in systems of /water phase/steam-gas phase/rooms/equipment surfaces/. Calculations are carried out with the available database on rate and equilibrium constants of radiolytical, chemical reactions and iodine mass transfer.

The uncertainty study of the results on volatile iodine species release into containment atmosphere is usually performed on the base of mathematical statistics and probability theory methods. Uncertainty of results is connected with uncertainty of the values used for constants of processes and medium physico-chemical parameters, and also with incompleteness of processes and contaminating substances accounted for. Completeness of considered processes and contaminating substances in gas/water containment phases is to be estimated. It is necessary to range the processes with iodine participation in the containment by their significance for iodine release into gas phase, to determine the confidence intervals for values used and final calculated results, to carry out the correlation analysis of dependence of volatile iodine species release to the containment atmosphere against radiolytical processes with iodine participation and iodine mass transfer rate in the containment.

For pre- and post-tests calculations of effect of water phase impurities on the iodine volatility and iodine speciation in water/gas phases, it is necessary to update the iodine model. Experimental tests are carried out in steady-state condition without mass transfer in other volumes, and at 25 and 50^0C – without water evaporation and condensation. Types of impurities are also limited. Therefore it is necessary to adapt the iodine model to test conditions. Numerical simulation of reactions and iodine mass transfer under experimental test conditions with database available will be performed. Then the algorithm and computer programme for assessment of iodine concentration and its speciation in water/gas phases and partition coefficients between phases will be developed. Then pre- and post-tests calculations are carried out, from their results the applicability of experimental results for numerical modeling is justified, separate factor sensitivity effect is determied, correctness of iodine model is estimated and degree of uncertainty of used constants is obtained. Then correction of model and computer programme for every tests and for the whole total experimental programme is carried out. Besides the computer model for assessment of radioiodine accident environmental source term is developed and used for model calculation, significance of influence of impurities and containment medium parameters on iodine concentration in gas phase and on iodine accident source term is assessed.

2. Summary of Technical Progress

2.1. Current Technical Status

Task Subtask	Beginning (quarter)	End (quarter)	Status / Comments
Task 1	1.01.2007	31.12.2007	Analysis of calculation results for severe accident scenarios has been accomplished. Determination of boundary conditions for experimental programs has been justified. The pre-test analyses for the planned experiments have been performed. Assessment of aerosols release from the core melt at the final stage of severe accident (LLOCA type) has been accomplished. The boundary conditions of aerosol deposition for the accident with the primary-to-secondary circuit leak have been specified more precisely.
Task 2	1.01.2007	31.12.2007	Supporting calculations of modeled molten core composition and pre-test calculations of the IMCC furnace gas dynamics have been completed. A pre-test has been made to improve the calculation accuracy and choose conditions for the main test performance. Experiment EVAN-FP1 has been made to study the release of Uranium and Zirconium oxides and fission products stimulants from the sub-oxidized corium melt at its oxidation from C-70 to C-100. The results of the post-test analyses have been processed. The annual progress report has been drawn up.
Task 3	01.01.2007	31.12.2007	Theoretical calculation research has been accomplished for the fission products release from the molten pool /core catcher.
Subtask 1	01.01.2007	31.12.2007	A general analysis of the most important factors affecting the flow rate of the fission products' release from the molten pool has been conducted. Two models for the release of fission products from the core melt have been developed: atomic and molecular models. The molecular model has been implemented as MFPR-MELT individual program code.
Subtask 2	01.10.2007	31.12.2007	Predictions of both the models have been compared with the results of EVAN 1 experiment. The comparison results have been analyzed and used for finding a range of modeling parameters.
Task 4	1.01.2007	31.12.2007	Experimental findings have been performed for aerosol transport processes in the model, simulating the primary circuit pipelines. Experimental data have been obtained for deposition both liquid and solid aerosols and transport of solid aerosols.
Task 5	1.01.2007	31.12.2007	Theoretical calculation investigation of aerosols transport in the primary circuit has been fulfilled. Survey of options for modeling the transport processes with up-to-date codes has been performed. Applicability of experimental results for verification of the models has been justified. Pre-test / post-test calculations have been conducted.
Task 6	01.01.2007	31.12.2007	Experimental findings regarding influence of containment parameters on the content and interrelation of volatile Iodine forms have been executed.
Subtask 1	01.01.2007	31.03.2007	Experimental installations have been fully equipped and adjusted. The relevant techniques have been optimized.
Subtask 2	01.04.2007	31.06.2007	Optimization of techniques related to analysis, synthesis and characteristics of slurry has been completed. Primary test

			experiments have been conducted.
Subtask 3	01.07.2007	30.09.2007	Experiments related to the test matrix have been fulfilled.
Subtask 4	01.10.2007	31.12.2007	Test experiments have been completed. Relevant test reports have been drawn-up.
Task 7	01.01.2007	31.12.2007	Experimental calculations modeling regarding influence of containment parameters on the content and interrelation of volatile Iodine forms has been fulfilled.
Subtask 1	01.01.2007	31.03.2007	Analysis and optimization of Iodine model have been accomplished. The process parameters and constants have been selected.
Subtask 2	01.04.2007	31.06.2007	Modification of iodine model has been completed. Pre-test calculations have been accomplished.
Subtask 3	01.07.2007	30.09.2007	Post-test calculations have been done. Iodine model has been improved.
Subtask 4	01.10.2007	31.12.2007	Post-test calculations have been done. Iodine model has been improved. Relevant test reports have been drawn-up.

2.2. Tasks of the work plan

Task 1: (statement) Analysis of calculation results for severe accident scenarios

Subtask 1.1: (statement) Analysis of calculation results for severe accident scenarios applied to various designs of NPP with pressurized water reactors. Determination of boundary conditions for experimental programs.

Subtask 1.2: (statement) Applicability analysis of expected experimental findings to be used for the verification of the calculation codes. Pre-test analyses of the experimental programs. Preparation of test protocols.

1. State / Situation at the beginning of the project duration

By the moment the Project implementation has been started, a work plan has been prepared to study the approaches applicable for performance of the design calculations to identify radiological consequences of severe beyond design basis accidents and justify the radiological acceptance criteria for NPPs with VVER.

Based on the experience available for modeling severe accidents for reactor plants with pressurized water reactors (VVER) a list was prepared and a plan drawn up to conduct both analysis and modeling accident scenarios, required to analyze conditions of aerosols generation and release.

In order to analyze the conditions of aerosols generation and transport in the reactor plant, a matrix of the necessary parameters has been prepared to reflect the transport conditions and velocity of steam-gas mixture and fission products in the reactor plant and dynamics of the melt formation during in-vessel and ex-vessel stages of the severe accident.

Approved and verified calculation codes have been selected for performance of calculation analyses for severe accidents.

2. Fulfilled work

2.1 The report describes approaches to design calculations of radiological consequences of severe beyond-design-basis accidents and to establishing radiological acceptance criteria for nuclear power plants with VVER reactors. The analysis of design approaches is performed to determine the degree of conservatism of design approaches, to define main uncertainties, to minimize them using best estimate codes and to confirm the adequacy of the models by experimental findings.
The report also gives typical values of parameters inside the containment, which are needed to determine parameters for experiments to be carried out for Tasks 2, 4 and 6 of the Project.

2.2 For the design NPP-91 (VVER-1000) the accidental release classification is proposed using scale for operating Russian NPPs and the INES scale. For conditions associated with the efficiency of FP localization inside the containment (LOCA), the results of the accidental release analysis for

reference nuclides xenon-133, iodine-131, and cesium-137 released during the first day of the accident are shown in Diagram 1. For comparison, the Diagram also shows release levels (R0÷R3) for iodine-131 and cesium-137 as their groups by and large account for the predicted level of public exposure. The additional scale shows the probability of formation for these categories of releases, in 1/reactor·year: R0 — 1.2E-05 (conditions contributing less than 1% of the total probability are not shown); R1 — 6.4E-08; R2 — 1.2E-08, R3 and R4 —2.9E-9 (without considering 3-LR conditions).

2.3 Calculations estimating the character of FP behavior inside the containment («in-containment accident source term») and FP releases from the primary containment to the secondary containment and to the environment have been performed.
Content and contribution of main fission products to total activity in the VVER reactor core are given in Table 5.

Table 5 Contribution of main fission products to total activity (VVER)

Element	Mass, %	Activity, $T_{release}$ = 0 day, %	Activity, $T_{release}$ = 30 days, %
Xe	0.44	3.9	0.4
I	0.02	5.2	0.7
Cs	0.2	3.5	1.3
Ru	0.19	1.7	9.7
Sr	0.07	4.2	6.7
Mo	0.27	3.9	0.01
Ba	0.14	4.4	2.9
Ce	0.23	3.3	15.3
La	0.1	4.8	0.0
total	1.7	35	37

2.4 Accident scenario Dnom346+SBO with maximum rate of FP release inside the containment and then to the environment as a result of containment leakiness is adopted for calculations performed to estimate RST and the corresponding accidental releases to the environment (“radiological release to the environment”).

Based on the performed thermal-hydraulic calculations the duration of the initial phase of the accident (“gap release phase”) is taken to be equal to 0.5 h, early in-vessel phase 1.5 h, and ex-vessel phase 1.4 h. In accordance with recommendations the duration of the late in-vessel phase is taken to be equal to 10 h.

According to the adopted approaches, FP release to containment originated at the in-vessel phase of the accident is studied for three periods: failure of FE cladding and initial fuel heating (“gap release”), early in-vessel phase and late in-vessel phase.

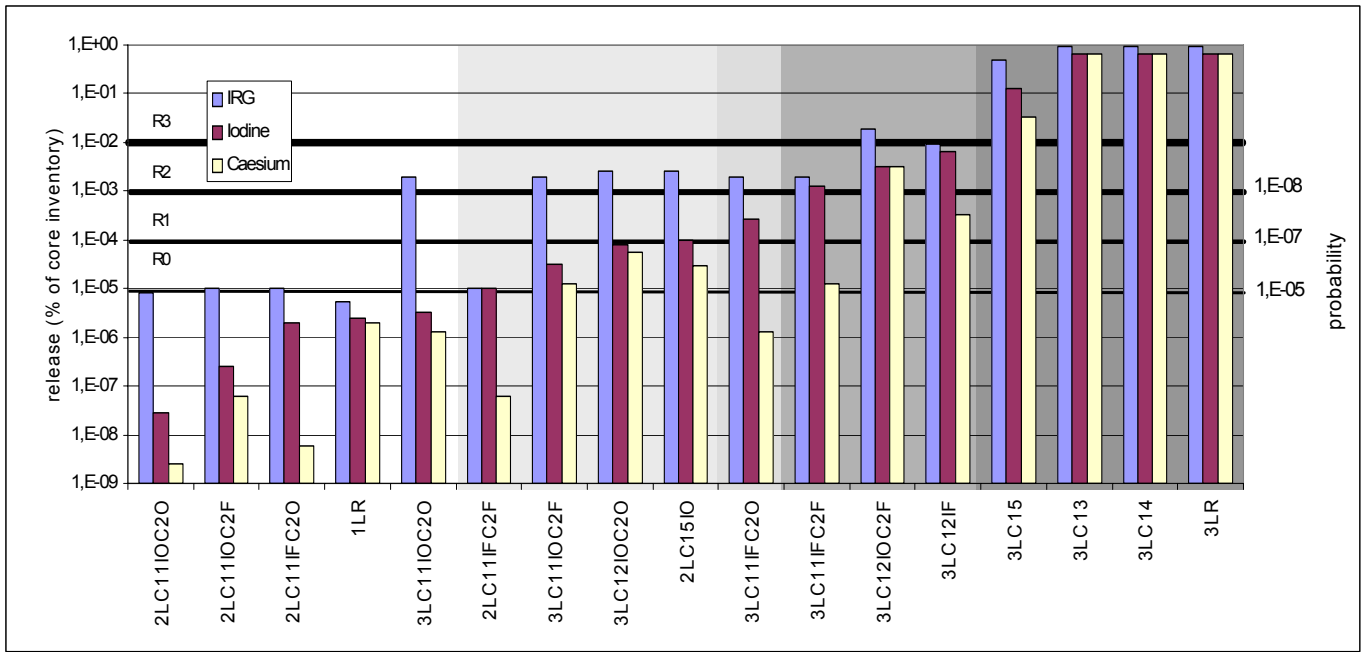

Fig. 1 Point estimate diagram showing accidental releases of reference nuclides for various states of protective barriers/localizing systems

2.5 For the design NPP-91, FP release inside the containment during ex-vessel phase is expected to be very inconsiderable, as the core catcher prevents interaction between melt and concrete and ensures quick melt chill-down. Release of FP and actinoids from melt during the formation of molten pool in the core catcher is limited due to oxidation of zirconium contained in the metal melt and formation of zirconium oxide crust on the metal surface at surface temperatures lower than 2800^0C, which prevents FP evaporation. The layer of water supplied onto the oxide melt surface after melt inversion in the core catcher considerably reduces aerosol and FP release from the corium during ex-vessel stage of the accident. Recommendations NUREG-1465 for corium-concrete interaction conditions are given for comparison in Table 6.

Table 6 – FP release inside containment at various phases of accident

In fractions of content in fuel

Group	Elements	In-vessel phase*/			Ex-vessel phase	
		NPP-91	NUREG-1465 [4]	IAEA-TECDOC-1127 [5]**/	NPP-91	NUREG-1465 [4]****/
I	Inert radioactive gases	0.95	0.95	0.51	-	0
II	iodines, bromes	0.65	0.45	0.51	-	0.25
III	cesium, rubidium	0.65	0.35	0.51	-	0.35
IV	Te, Se, Sb	0.505	0.055	0.51	7. E-3	0.25
V	Sr, Ba	0.02	0.02	0.002	2.E-4	0.1
VI	Ru, Rh, Rd, Mo, Tc	2.5 E-3	2.5 E-3	7.E-7	2.5 E-3***/	2.5 E-3
VII	Zr, Nb, Y, La,	5.0 E-4	5.0 E-4	2.E-7	2.0 E-5	5.0 E-3

	Ce, Pr, Nb, Pm, Sm, Eu, Np, Pu					

Note 1:
*/ Without considering FP release during initial period ("gap release").
**/ Recommended for determining RST as best estimate for PWR.
***/ Adopted according to data NUREG-1465 due to lack of experimental data.
****/ Provided that melt interacts with concrete.

2.6 The adopted rates of FP release from fuel into containment for NPP-91 remain rather conservative as compared with recommendations [5] due to the lack of a representative experimental database both for high-temperature tests with fragments of irradiated fuel elements with fuel UO2 and for melt chill-down. Main uncertainties remain in the estimates for elements of group VI (Ru), for which the experimental findings are rather inconsistent.

2.7 Analysis of the effects produced by radiolysis of aqueous medium on iodide-ion oxidation, I^2/I^- ratio in the aqueous phase and content of volatile forms of iodine in the gaseous phase has revealed that an important factor controlling the formation of I_2 during I^--ion oxidation is pH of the aqueous medium of the containment. When pH falls from 7.5-8.5 to 4-5 (dose rate 0.5-2 kGy/h) I_2 concentration rises tenfold in the aqueous phase, and ten- to hundred-fold in the gaseous phase.

The design NPP-91 solves the "iodine" problem by maintaining and controlling pH level in the containment above the value of 7 during the first day by discharging 2 m3 of 30% NaOH or KOH solution into the emergency sump.

During the subsequent phases of the accident when power supply at the power unit is to be restored, pH level is not expected to become much lower. The value of pH is still controlled at a level not lower than 7, which is ensured by discharging $15m^3$ – $30m^3$ of alkali solution from chemical reagent tanks.

The formation of volatile forms of iodine is strongly influenced by the level of gamma radiation. Variation of gamma-radiation dose rate in the atmosphere and emergency pool during a severe accident is shown in Table 7.

Table 7. Gamma-radiation dose rate in atmosphere and emergency pool during severe accident

Time, h	Dose rate in containment air, kGy/h	Integral dose in containment air, kGy	Dose rate at sump bottom, kGy/h	Integral dose at sump bottom, kGy
0	66.9	-	25.0	-
1	54.7	60.8	20.5	22.7
10	3.85	324	3.53	131
24	1.49	362	2.21	171
72	0.62	417	0.45	235
240	0.26	486	0.27	296
720	0.05	560	0.14	394
1440	0.03	588	0.09	477
3600	0.02	641	0.08	663
7200	0.02	716	0.07	930

According to recommendations, iodine release inside containment under conditions of pH control in the containment above the value of 7 is adopted in the design in the following forms: 95% - aerosols, 4.85% - molecular iodine, 0.15% - organic compounds.

2.8 Activation of spray system (24 h after the initial moment of accident) ensures further effective removal of aerosols from atmosphere of containment rooms reducing their concentrations to levels determined by the presence of aerosol sub-micron fraction suspended in atmosphere.

2.9 Behavior of various forms of iodine-131, aerosols (strontium-90, cesium-137, tellurium-131m, lanthanum-140) and ruthenium-103 (volatile oxides) in the containment atmosphere during the first 24 hours of the accident is shown in Fig. 2, Fig. 3.

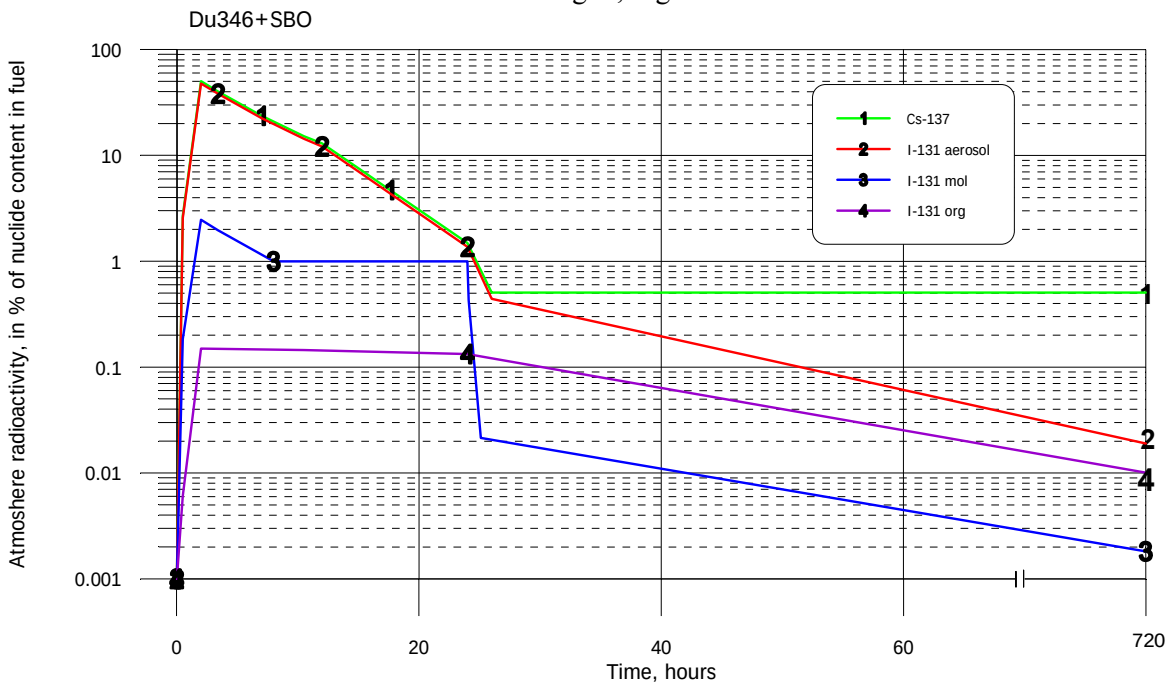

Fig. 2 Behavior of I-131 and Cs-137 in containment atmosphere at various stages of reference accident

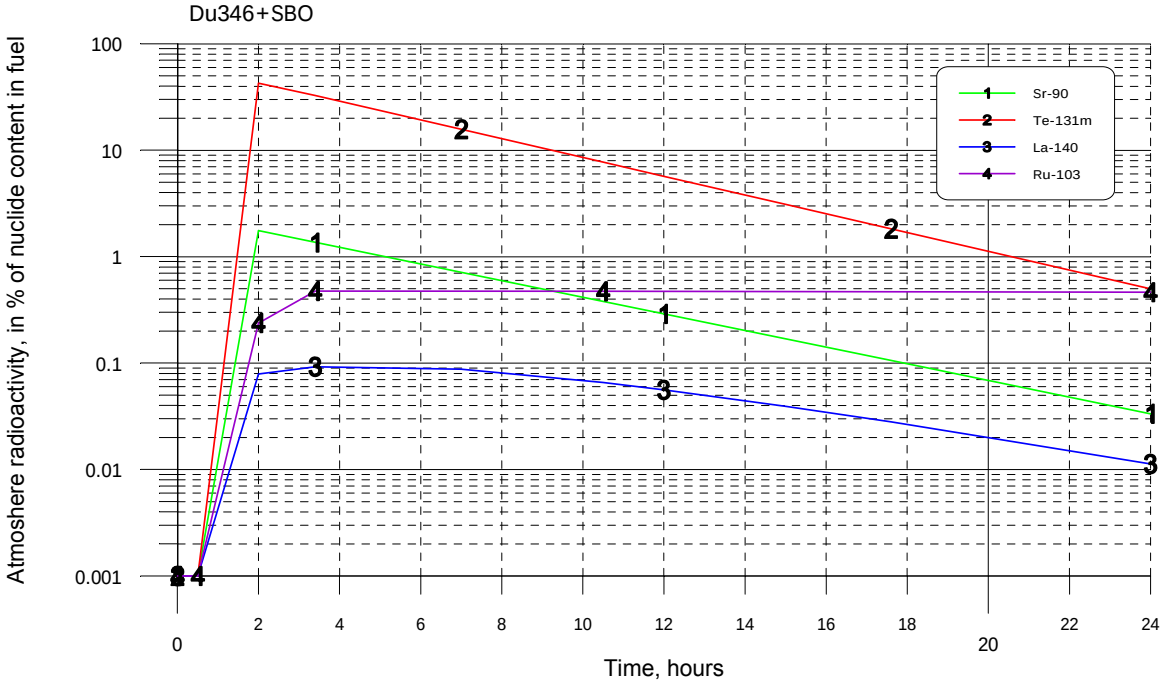

Fig. 3 Behavior Sr-90, Te-131m, La-140 and Ru-103 in containment atmosphere at various stages of reference accident

2.10 Accidental release of long-lived nuclides during the first day of the accident due to containment bypass amounts to 4% for gases (Xe-133, Xe-135, Ru-103) and 16% for aerosols (% of integral release due to double containment leak); during the second stage of the accident 1% for IRG and ~11% for radioactive iodines and aerosols (% of accidental release through system KLC11/41).

According to the requirements EUR this level is acceptable for present-day power units with double containment.

2.11 In works issued within the design NPP-91 it is noted that the calculations of aerosol behavior in containment atmosphere are sensitive to the specific character of the accident scenario, average size and the selected size distribution of aerosols.

Main uncertainties associated with FP release from fuel remain for elements of group VI (Ru, Mo) during both in-vessel and ex-vessel phases of accident due to the ability of these elements to form volatile oxides. Available experimental data are inconsistent.

Maintaining pH value in the containment at a level not lower than 7.5 during all phases of a severe accident allows reducing by much radioactive iodine release to the environment. However, the analysis has shown that the recommended constant content of volatile iodine forms in the containment is a value with a considerable conservative margin and can be reduced taking into consideration specific features of a particular design (chemical composition of aqueous medium, sorption ability of coatings, iron hydroxides etc.).

2.12 Severe accidents accompanied by fuel melting and associated with non-isolable primary coolant leaks outside the containment are among the accidents which may have the most severe radiological consequences at nuclear power plants with VVER reactors.

The most probable scenario for this class of severe accidents accompanied by core melting involves non-isolable primary-to-secondary-circuit coolant leaks.

Analyses have shown that one of the important factors determining the value of accidental release to the environment for the class of severe accidents with SG tube break is taking into account sedimentation of fission products released from melting core in the form of aerosols. At high flow velocities in damaged SG tubes (10-100 m/s and more) there can occur intensive deposition aerosols in SG tubes due to turbulent deposition processes.

In estimating the time during which fission products remain in the primary equipment it is necessary to take into consideration the carry-over of aerosol particles deposited on primary circuit surfaces.

2.13 The FP buildup inside fuel and FP release analysis out of fuel and melt have been performed.

The roadmap for the FP buildup and release analysis and their interrelation with the other EVAN project tasks are given below (Fig. 4).

The accumulated inside fuel FP are released from the fuel into the fuel cladding gap and in case of the cladding failure are release into the reactor coolant circuit (RCS). FP released as gases, volatile species, and aerosols are transported in RCS, are partly deposited on the surfaces, and are transformed and released from RCS into the containment. The relevant models are the basis of the radionuclide block connected with the thermo-hydraulic code (Fig. 5).

2.14 The FP buildup inside fuel.

The activities of the most significant isotopes in fuel calculated by different codes are compared. It can be derived (see Fig. 6) that the fuel FP activities are adequately consistent.

Calculation of the iodine concentrations in the fuel had been performed. The relative fraction of the stable and radioactive iodine isotopes depend on the reactor operation time. In the beginning period of time, the most important contribution will be due to the radioactive isotopes, by the end of three-year campaign the most significant contribution will be due to the stable isotopes.

Main portion of the nuclides is accumulated in the core as stable (or long-lived) nuclides whose concentration increases practically linear with the time. By the time the campaign ends, the radioactive isotopes contribution practically does not affect the total iodine concentration.

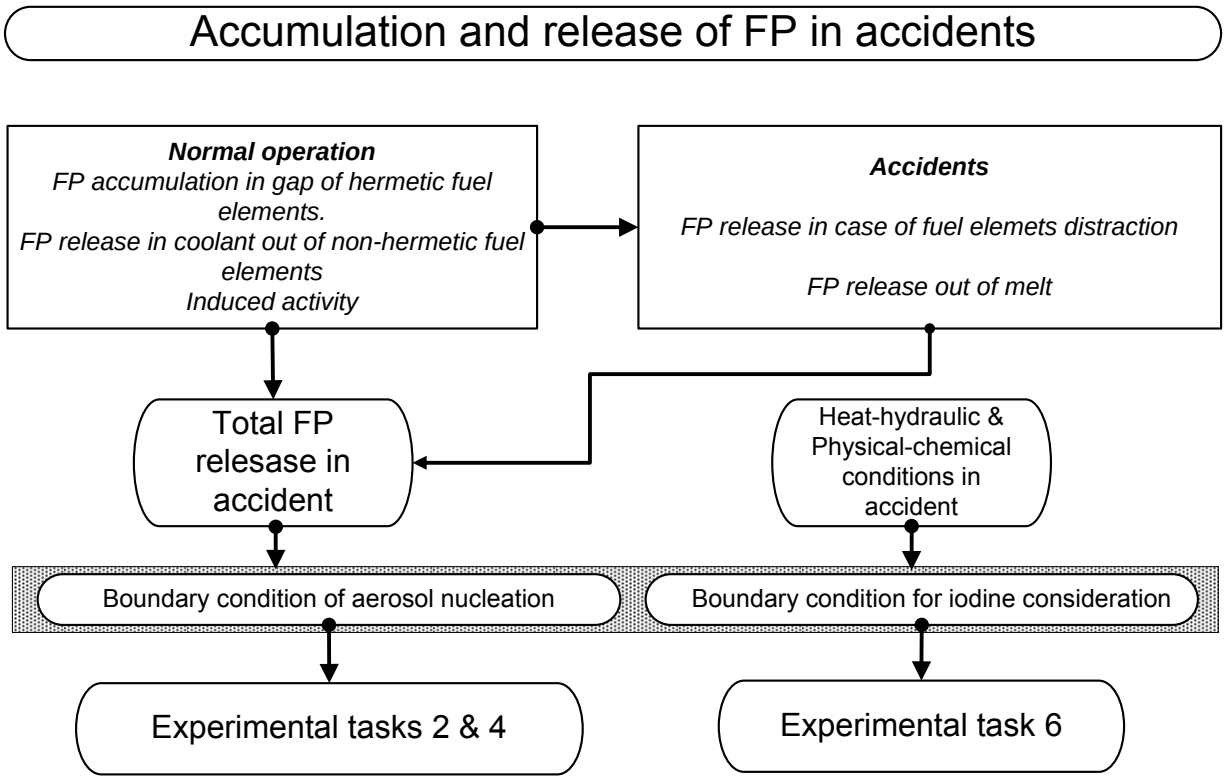

Fig. 4 Roadmap for the FP buildup and release analysis and their interrelation with the other EVAN project tasks.

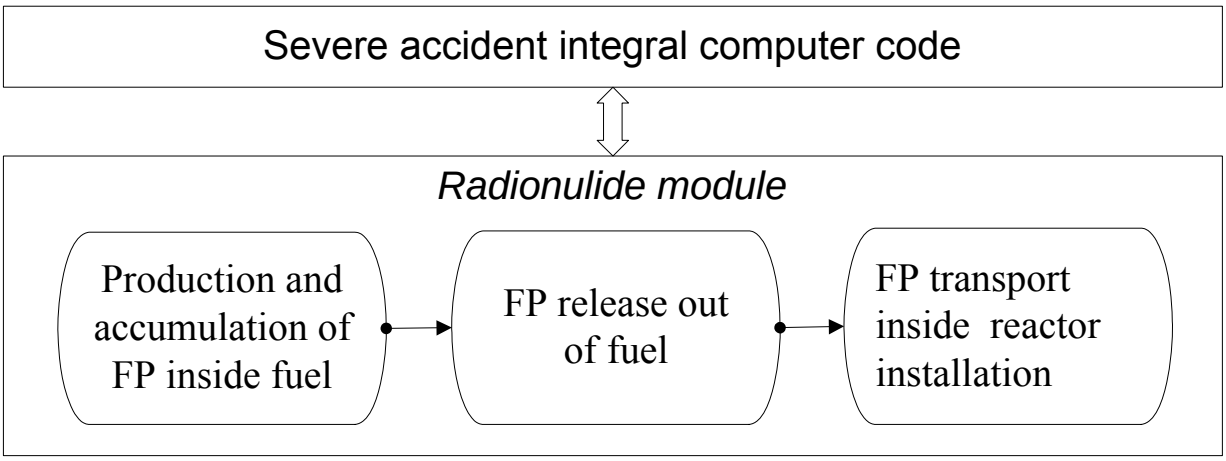

Fig. 5 FP package of the thermal hydraulic code

The FP buildup in the fuel by the moment of three-year campaign end with burnup of 45MW·day/kgU. In the Table 5 the FP buildup (including low-volatile and non-volatile) by the time of reactor shutdown, along with the activity in the different moments of time after VVER and PWR shutdown. First three rows describe the volatile and gaseous FP contributing most into the radioactive release during severe accident. Furthermore, the FP which form the low-volatile oxides and metals are shown, which can also contribute significantly in the late stage radioactivity release.

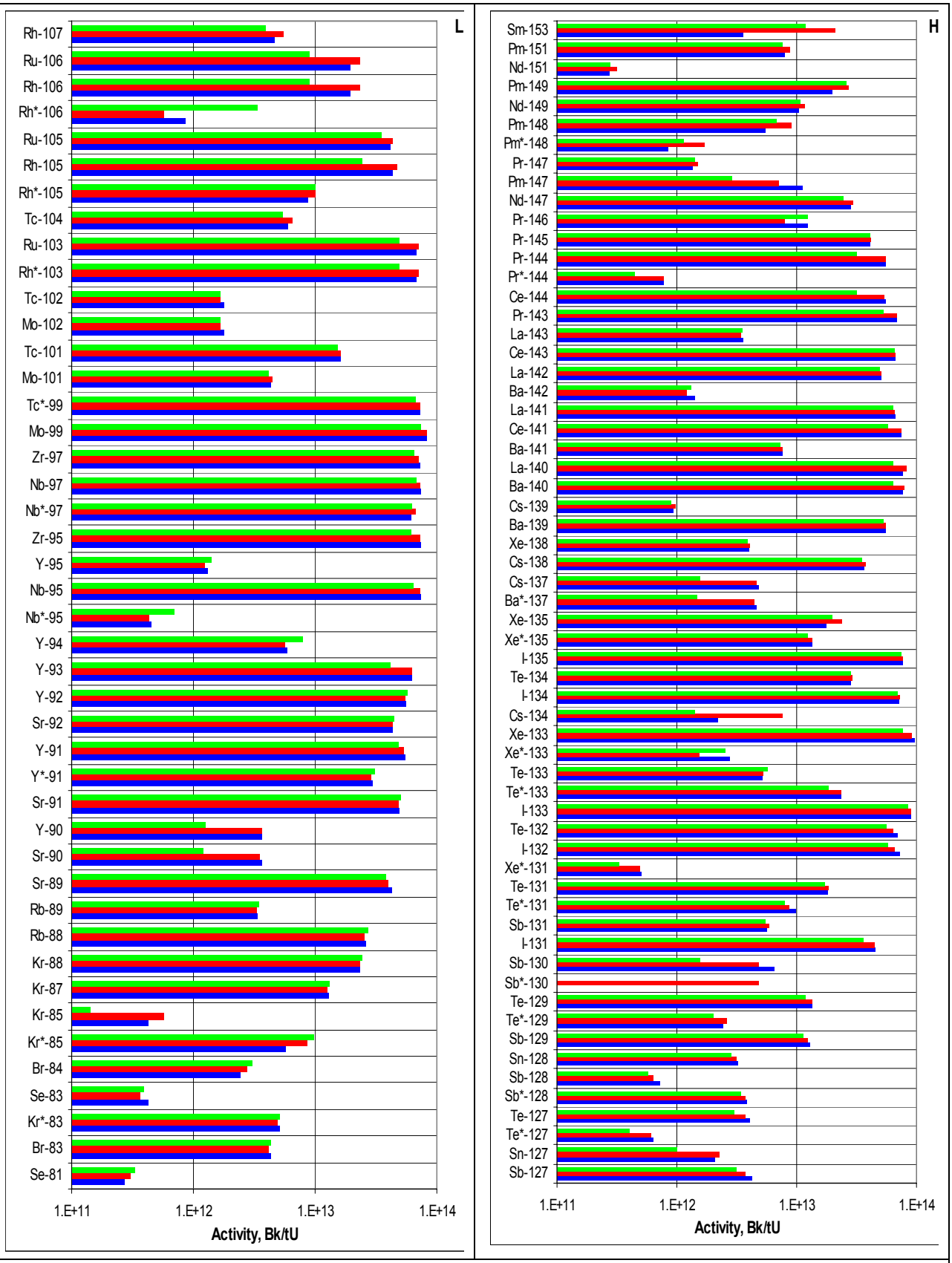

Fig. 6 Activity of the "light" (L) and "heavy" (H) nuclide groups, by 1 hour after VVER-1000 shutdown.

Green- RadioNuclide, blue-BONUS, red-V.M. Kolobashkin at al, Handbook,Moscow,1983

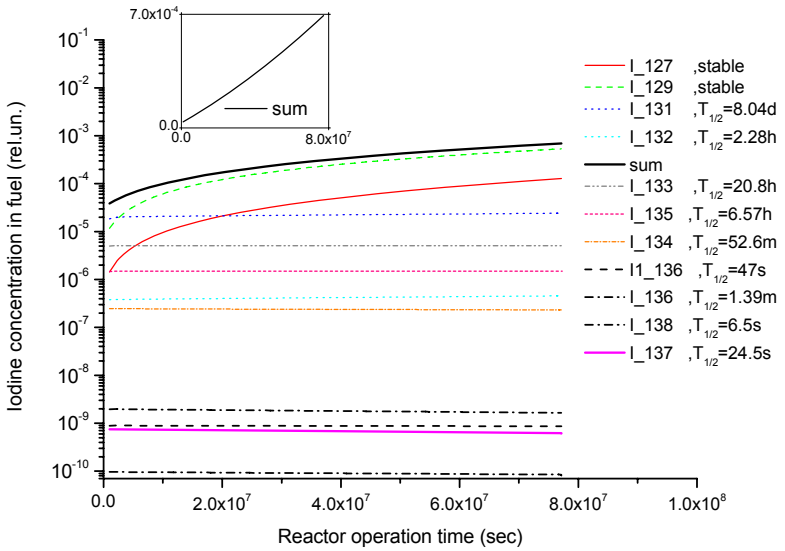

Fig. 7 Iodine buildup in the fuel during reactor power operation

2.15 FP accumulation analysis under the cladding by reactor shutdown and during the accident has been performed. Conditions , important for aerosol formation, were analised.

During the accident the volatile FP and gaseous FP are released completely, then their accumulation under the cladding is negligible for the accident analysis.

Non-volatile FP are accumulated in gap during the normal operation mode in such quantities which significantly exceeds their accidental release. The main quantity of the accumulated FP are remaining in the fuel, while the latter is in the solid phase. The non-volatile FP releases in normal operation, during fuel destruction and from the molten pool.

During fuel cladding failure the volatile and low-volatile FP will be released. Noble gases are released completely. Other volatile FP (I, Br, Cs, Rb, Te) can be retained under the cladding due to high chemical activity. According to the estimations, about one third of those elements will be released. Release of the low-volatile FP (Ba, Sr, Ce, La, Ru, Mo) is significantly lower.

During core structures meltdown the aerosol source mass generation rate increases drastically by two-three orders of magnitude and the aerosol compositions changes. The main component is now the structural materials and fuel aerosols which will carry the fission products.

During ex-vessel stage the FP transport as low-volatiles FP and their oxides becomes important.

FP release during several accident has big uncertainty. The least studied phenomenon is the low-volatile FP release due to challenging experimental conditions at high temperatures (>2400 K) and long test run time (>10 min) needed for generation of the detectable releases.

The most essential factors influencing the aerosol generation during severe accidents, according to the review, are the next.

- FP & their chemical forms accumulated inside fuel.
- FP & their chemical forms accumulated inside gap.
- Dynamics of fuel element (FE) destruction in core during accident.
- Dynamics of constructive material (CM) destruction during accident.
- Dynamics of temperature inside reactor installation.
- Chemical forms of FP & CM inside and above melt.
- Dynamics of oxigen, hydrogen, steam and FP vapor partial pressure in reactor.

2.16 Reactor Aerosols' Morphology

Reactor aerosols' morphology property have been reviewed in accordance with the available literature information. From morphological viewpoint, aerosol properties may categorized as follows:

- Aerosol geometry: isometric particles, fibrae, platelets.
- Aerosol dimensions are characterized by the following parameters: Feret diameter, Martin diameter, aerodynamic diameter, and Stokes diameter.
- Aerosol structure: solid or liquid particles (such as microcrystals, drops, hollow or filled forms) coalesced into agglomerates or flocculi.
- Surface properties: aerosol is characterized by well-developed surface, on which adsorption and chemical reactions may proceed; aerosol surface properties determine its water absorption and interaction with electric charges.
- Material composition: matters of which aerosol consists.

2.17 Selecting aerosols for deposition and transport experiments.

Liquid aerosol has been selected to study the deposition processes. In this case transport processes can be practically ruled out. Particles of the liquid aerosol are of even spherical form. This allows for reliable optimization of measurement techniques and facilitates clear interpretation of the experiment results and application of the acquired results for verification of the calculation programs.

Ammonium chloride (NH_4Cl) has been chosen as a source of aerosol generator for conducting experiments to study solid aerosol deposition, resuspension and transport processes. The main reasons under the selection in question are as follows.

- The generated aerosol particles morphology is approximately equal dimensions along the 3 coordinates, as concluded from the literature data and subsequent experiments. Similar picture is observed for the CsI investigated in a number of ex-vessel experiments. In the reactor plant simulations such particles are also considered as spherical.
- The NH_4Cl crystal has cubic structure, similar to the CsI.
- The aerosol size spectrum generally corresponds to the size spectrum of aerosols generated at the late stage of the severe accidents. The aerosol size varies in the range of 0.05 to 10 μm with the mean value about 1 μm).
- NH_4Cl has good handling characteristics, well-known, and sufficiently available.

2.18 Aerosol formation model in calculations

The nuclides which are actively released from the fuel are grouped into the following groups for the purpose of study of the aerosol behavior in RCS:

- Inert: Xe, Kr.
- Volatile: I, Br; Cs, Rb; Te, Se, Sb.
- Non-volatile: Ba, Sr; Ru, Rh, Pd, Mo, Tc, Nb; La, Nd, Eu, Yb, Pm, Sm; Ce, Np, Pn.
- Structural materials.

To calculate the aerosol behavior, the aerosol size distribution and aerosol concentration distribution along the sizes are input. It is usually assumed that the aerosol size distribution is log-normal and the polydisperse particles are spherical.

The following 6 states are considered:

- steam in the atmosphere;
- aerosols in air;
- steam condensed at surfaces of the wall and aerosols (both at "native" CI aerosols, and at "alien" aerosols);
- aerosols deposited onto surfaces;
- aerosols chemisorbed by the steel surfaces of the pipes and structures of the RCS;

- resuspended aerosols.

Vapor nucleation, phase transitions, sorption/desorption are taken into account.

For refractory elements the mass of those elements is distributed onto solid spherical particles. In general case, the aerosol population characteristics are well described by the log-normal distribution. For refractory aerosols and for aerosols formed upon nucleation of the FP vapors, all the processes relevant for the given spatial volume are taken into account (diffusiophoresis, turbophoresis, gravitational deposition, thermophoresis, etc).

2.19 Calculations for NPP-91 with VVER-1000 with application of SOKRAT severe accident calculation complex have been conducted for relatively wide range of severe accident scenarios. All the considered accidents lead to severe damage of the core followed by formation of molten pools and finally to failure of the reactor pressure vessel with corium melt release in the core catcher. Failure of fuel elements' cladding and formation of molten pools lead to release of aerosol particles into the gas-steam mixture of the reactor plant primary circuit.

2.19.1 Several scenarios have been considered for severe accidents with loss of coolant from the primary circuit into the containment:

- Large-break loss-of-coolant (Dn 346) with rupture of the pressurizer surge line under blackout conditions,
- Large-break loss-of-coolant (Dn 300) from the cold leg of the primary coolant pipeline with failure of the ECCS active part,
- Large-break loss-of-coolant (Dn 179) with rupture of the pressurizer injection line and failure of the ECCS active part,
- Small-break loss-of-coolant (Dn 80) from the cold leg of the primary coolant pipeline with failure of the ECCS active part,
- Small-break loss-of-coolant (Dn 25) from the hot leg of the primary coolant pipeline under blackout conditions.

The modeling calculations provided for operation of the four hydraulic accumulators of the ECCS passive part and inoperable ECCS active systems presupposed by the scenario conditions. In case of blackout accidents an additional failure of steam generators feed water supply system has been superposed.

2.19.2 One scenario of the coolant leak from the primary to the secondary circuit has been studied. Initial event is the rupture of live steam pipeline in the segment from the steam generator (SG) to the motor-driven isolation valve with Dn 600 equivalent leak. This event initiates the double-sided rupture of SG three pipes with Dn 32 equivalent leak. The accident has been superposed by extra failure (blackout conditions).

2.20 Based on the conducted calculations, a progress of molten pool formation on the reactor pressure vessel bottom has been analyzed and data, related to change of the melt surface chemical composition, which is the source of aerosols generation, have been obtained. Data, related to the composition and temperatures of the melt surface and corium for the moment of the reactor pressure vessel meltdown, are given in Table 8. The conducted supporting thermodynamic calculations proved that during the melt stratification at the bottom of the reactor plant under conditions of low and middle degree of Zirconium oxidation, the metallic melt is composed up to 14 mass % of Uranium with admixtures of low volatile fission products, namely – Mo and Ru metals, and up to 7 mass % of Zirconium. This is also confirmed by experimental findings, executed under MASKA project; therefore, these substances have to be accepted as a part of the melt composition when analyzing aerosols generation from the melt surface.

Table 8– Melt characteristics at the moment of the reactor pressure vessel meltdown

Melt parameters	Accidents					
	Dn346	**Dn300**	**Dn179**	**Dn80**	**Dn25**	**Primary-to-secondary circuit leak**
Melt surface, mass %						

Steel Zr	0.93 0.07	0.938 0.063	0.933 0.067	0.984 0.016	0.994 0.006	0.998 0.002
Melt surface temperature, K	2700-3000		2600-2900			3000
Corium, mass % UO2 ZrO2 Zr Steel	0.807 0.094 0.099	0.829 0.078 0.092	0.833 0.079 0.088	0.789 0.184 0.026	0.766 0.221 0.013	0.658 0.286 0.056
Corium temperature, K	2800-3070		2660-2940			3200

2.21 At the stage of severe accident, characterized by formation of molten pools, one-dimensional circuit codes do not allow for correct accounting of convection processes, which determine conditions for aerosols generation and deposition. To specify thermal hydraulic parameters over the melt surface under these conditions, a calculation analysis has been performed with application of 3-D code for the following calculation model: the reactor pressure vessel was taken as a cylinder, filled with hydrogen with temperature distribution as per calculations of SOKRAT code for the moment of molten pool formation at the reactor plant bottom; the containment was accepted as a certain volume filled with steam atmosphere and connected to the reactor vessel by system of pipelines. The calculation results have provided the range of velocities from 0.3 to 0.85 m/s over the melt surface at the average temperature of 1500 °C.

2.22 A severe accident with the primary-to-secondary circuit leak has been chosen to specify the boundary conditions of experimental programs for investigation of aerosols deposition processes on the surfaces of the structural components. In the case of accident in question the emergency gas removal system starts steam-gas mixture release to the containment 7200 s after the accident onset. Long small-diameter tubes in the system co provide the conditions for aerosol deposition when steam-gas mixture being in the intense aerosol release phase moves via these tubes in the case of fuel element failure. Another potentially dangerous place with regard to aerosols deposition includes failed tubes of the steam generator. The emergency gas removal system (EGRS) consists of pipelines and valves installed on these pipelines to remove steam-gas mixture to the bubbler and to the containment:

- from under the reactor head (via pipeline 38x3.5 mm);
- from SG primary circuit collectors via pipelines 18x2.5 mm; the pipelines designed for steam-gas mixture removal from SG are connected by a collector 38x3.5 mm;
- from the pressurizer via pipeline 76x7 mm connected to the steam release pipeline between the pressurizer and the pressurizer pilot-operated safety valve.

The calculation results have revealed that the most favorable conditions for aerosol deposition on the inner surface of the gas removal system pipelines will be created in small-diameter tubes d=13, 31 and 62 mm (see Table 9). In case of further development of the accident, these velocities will do nothing but reduce due to the reduction of differential pressure of the reactor, steam generator and the containment.

Table 9– Calculated values of velocity and pressure for some pipelines of the gas removal system

EGRS pipelines	Diameter, m	Length, m	Location	Velocity (inlet – outlet), m/s	Pressure (inlet – outlet), MPa
Pipelines from the steam generator	0.013	1.0	Vertical	28	5.8
	0.013	15.525	Vertical	57 – 60	5.7 – 4.6
	0.013	16.375	Horizontal	70 - 102	4.4 – 2.9
	0.013	8.4	Vertical	111 - 172	2.7 – 1.6
Pipelines from the reactor	0.031	13.075	Vertical	53 - 56	1.6 – 1.5
	0.031	13.375	Horizontal	57 -60	1.48 – 1.4
	0.031	0.9	vertical	60	1.38
Pipelines from	0.062	10.0	Horizontal	47 - 44	1.36

the pressurizer and the pilot-operated safety valve	0.062	5.0725	Vertical	42	1.35
	0.187	5.0	Vertical	152 - 157	1.24 – 1.22
	0.187	1.0	Horizontal	157	1.22
	0.207	3.2	Horizontal	222	1.45
	0.207	1.8	Vertical	230	1.42
EGRS connecting pipes	0.062	3.0	Vertical	41	1.36
	0.062	14.0	Horizontal	40 - 80	1.35 – 1.2

Table 10 – Calculated values for velocity and flowrate change along the length of SG tube versus differential pressure

Distance from the tube origin, m	**Differential pressure of SG tube**		
	14 atm – 1 atm	**8 atm – 1 atm**	**3 atm – 1 atm**
	Velocity, m/s		
1.0	107	100	83
3.0	117	11	90
5.0	133	125	99
7.0	157	147	112
9.0	204	189	132
11.0	369	315	172
	Steam flowrate in SG tube. kg/s		
---	0.0973	0.0541	0.0175

Simulation of the accident in question provides for different variants of SG tubes rupture, but the most interesting one from the viewpoint of aerosol deposition is the tube rupture at the shortest distance from the cold collector. The period of intense aerosol deposition lasts since the 21 200th s till the 24 500th s. The calculated values for velocity change along the length of SG tube versus differential pressure are given in Table 10. Hence, favorable conditions for aerosol deposition on the inner surfaces of SG tubes will be created in the inlet segment with a length of nearly 1 m from the hot collector.

2.23 A calculation has been performed to identify fission products behavior for large loss-of-coolant accident (LLOCA) in case of the pressurizer surge line rupture under blackout conditions. Time dependence has been obtained for fission products, which have been accumulated, released and deposited in the primary circuit. The major mass quantity of released aerosols is made up of $CsMoO_4$, Cs, Te, CsI, Cs_2I_2, Cs_2 and Cs_2O.

2.24 Assessment of aerosol deposition on the inside surface of the SG damaged tube has been made for the severe accident associated with primary-to-secondary circuit leak.

With SG tube inlet and outlet differential pressure prescribed according to the severe accident calculation results the velocity distribution and aerosol accumulation along the tube length have been obtained. It should be noted that in the below-given calculations the hydraulic diameter of the channel doesn't change under conditions of aerosol accumulation on the wall and equals the diameter of heat-exchange tube without any depositions. When comparing the aerosol mass growth rate in the first volume with maximum possible mass of aerosol in this segment of the tube, it could be predicted that aerosol flowrate via the tube will be completely blocked. At that, turbophoresis has proven to be the major deposition mechanism, intensified under conditions when aerosols are coagulated inside the tubes.

2.25 Possibility of aerosol detachment and relocation in the SG tube with allowance for the initial data given above and in the distribution spectrum of particles, which correspond to deposition simulation, has been investigated using module "ROCK'NROLL". When making calculations for this model, the hydraulic diameter of the channel doesn't change as well under conditions of aerosol accumulation on the wall. The assessments performed have shown that under the realized conditions of coolant flow in the SG damaged tubes (for the primary-to-secondary leak accident) and at realized aerosol velocities the repeated relocation will not exert a significant influence on the increase of aerosol depositions on the tube walls.

2.26 As for the severe accident with Dn346, the fission products release from the molten pool, that corresponds to the time period since the moment of reactor vessel meltdown and metallic melt layer release to the core catcher till the moment of final melt release to the core catcher, has been calculated. Melt composition and temperature versus time are given in Table 11. Steel has been assumed to have the following composition: Fe 76.4%, Cr 17.6% and Ni 5.9%. Melt FP concentration is given in Table 5 (with regard to UO_2–Zr–ZrO_2, this is the same composition as in experiment EVAN 1). Area of the melt surface has been set equal to 3.8 m^2, atmosphere composition – pure water steam, above-melt pressure – 2.5 atm. Above-melt steam-gas mixture velocity has been adopted equal to 1 m/s, based on the calculating assessments with calculation code 3-D CFD being used. Calculation results for melt component release in the period since the 9 000th s till the 11 000th s are given in Tables 12 and 13. Total mass of aerosol release from the melt at above-melt velocity of 1 m/s has been equal to 20.6 kg.

Table 11 – Temperature and mass % of the molten pool surface.

Time, s	Melt surface temperature, K	UO_2, mass %	ZrO_2 mass %	Zr mass %	Steel mass %
9 000	3 005	71.1	10.7	5.1	13.0
9 400	3 000	63.8	9.6	4.6	22.0
9 800	2 930	58.3	8.7	4.2	28.8
10 200	2 900	54.5	8.2	3.9	33.3
10 600	2 840	49.9	7.5	3.6	39.1
11 000	2 620	48.6	7.3	3.5	40.5

Table 12– Concentration of fission products within the melt, mass %

FP	SrO	BaO	CeO_2	La_2O_3	Ru	Mo
Mass %	0.1218	0.2001	0.3915	0.174	0.3045	0.4002

Table 13 – Integral release of the melt components

U, kg	Zr, kg	Fe, kg	Ni, kg	Cr, kg	Mo, kg	Ru, kg	Ba, kg	Sr, kg	La, kg	Ce, kg
1.53E+00	1.96E-03	1.37E+01	3.03E+00	2.30E+00	2.57E-02	3.52E-03	6.05E-03	1.53E-02	1.01E-03	1.47E-03

2.27 To provide a basis for selecting boundary conditions for experimental programs, the calculations related to melt formation dynamics in the core catcher have been made using under-development calculation code GEFEST-ULR for severe accident with Dn346. Melt from the failed reactor pressure vessel enters the core catcher portionwise. At that, two periods can be distinguished, which can be considered as different boundary conditions with regard to aerosols generation from the melt surface. The initial period when metallic melt leaves the reactor vessel takes about several hundred seconds. The source of aerosols in this time period will be the surface of steel melt consisting of non-oxidized zirconium, uranium and steel sacrificial material at a temperature of 1730 - 2130 °C, to be oxidized in the steam-air mixture. The second period, which lasts approximately 3000 s, is characterized by portions of melt (consisting mainly of uranium, zirconium oxides with metallic zirconium and vessel steel additives) entering the core catcher. Portions of entering oxide melt interact with the remaining steel sacrificial material and oxide sacrificial material. At this stage of melt entering the dynamics of molten pool formation is determined not only by the thermal processes, but also by physicochemical processes of oxide melt – oxide sacrificial materials interaction, accompanied by heat release due to reduction-oxidation reaction between Zr and Fe_2O_3 (being a part of oxide sacrificial material), as well as by processes of corium natural convection and various component stratification due to buoyancy forces.

The calculation analysis has assumed that the molten pool formed in the core catcher is homogenous (it contains UO_2, ZrO_2, Al_2O_3, Fe_2O_3, ZrO_2, Fe and Zr) in the period of melt

entering from the reactor vessel. As UO_2 enters, melt temperature starts going up, that leads to gradual meltdown of sacrificial materials and melt dilution. As the melt composition changes, gradual temperature change takes place. Comparing with melt contained at the bottom of the reactor vessel, the core catcher melt has the lower temperature, as well as the lower concentration of fission products. Therefore, the expected aerosol release from the melt is assumed to be smaller. Composition changes for the upper melt layer until the moment of water supply are given in Table 14. The results show, that melt temperature goes down as the oxide sacrificial material blocks melt.

Table 14– Upper layer composition in the core catcher

Time, s	UO2 mass %	ZrO2 mass %	Zr mass %	Fe2O3 mass %	Al2O3 mass %	Fe mass %	T, K mass %
8 600	0.1	---	4.8	15.2	5.1	74.8	2400 - 2000
9 100	0.8	0.1	4.2	14.9	5.0	75.0	2400 - 2000
9 600	30.2	4.5	4.3	10.4	3.5	47.2	2680 - 2430
10 000	31.2	4.7	4.1	11.6	3.9	44.5	2400 - 2100
10 400	31.5	4.4	4.0	11.9	4.1	43.8	2360 - 2030

After water supply onto the melt surface, a high-melting-point crust is formed on the surface. This crust together with the steam layer above the crust surface will significantly hinder aerosol relocation from the melt.

When considering core catcher process, not only aerosols release from the molten pool surface due to materials evaporation, but also a possibility of their generation during gases release from the melt depth should be considered.

The core catcher release of gases (oxygen) in the melt is possible due to reaction of ferrous oxide recovery, which is a part of sacrificial material. At that, interaction of the melt oxides with oxide sacrificial material leads to degradation of Fe2O3 in endothermal reactions:

$2Fe_2O_3=4FeO+O_2$,

$6Fe_2O_3=4Fe_3O_4+O_2$,

A series of experiments to justify NPP-91 core catcher application have been conducted to study physicochemical processes that take place during interaction between corium melt and sacrificial material. The experiments showed that for the corium melt, which has Zirconium, the oxygen emerged as a result of these reactions, is consumed for Zirconium oxidation. At that, gas release from the melt is insignificant. The similar result is obtained when corium melt has steel and /or FeO. At that, further oxidation of the melt corresponding component is achieved.

For low concentration of Zr, Fe and FeO, corium experiments have been conducted with corium containing Zirconium oxide and no free Zirconium and Ferrum. In this case oxygen precipitation from the melt would occur after some time period, during which it will be absorbed in the melt due to formation of Uranium oxides with different degree of oxidation (UO_{2+x} type compound). At that, emerging Uranium oxides have a higher, when compared with UO2, degree of oxidation and lower liquidus temperature, which leads to their predominant release into atmosphere in the form of vapors over the melt and formation of aerosols. Thus, in case of sub-oxidized corium, it is probable that aerosols release would be intensified due to evaporation of uranium oxides UO_{2+x} despite lower oxygen release caused by oxygen absorption in the corium. This process has to be further investigated by setting additional experiments.

2.28 During project implementation the code for numerical simulation of aerosol dynamics was used. Code based on numerical solution of kinetic condensation/coagulation equations and allows to simulate condensation, coagulation and deposition of multicomponent aerosols. Code was verified on known analytical and numerical solutions of condensation/coagulation equations. Cross-verification on code MELCOR was carried out. Fig. 8 & Fig. 9 present some results obtained during these simulations. Coagulation and deposition of CsI particles were considered in this case.

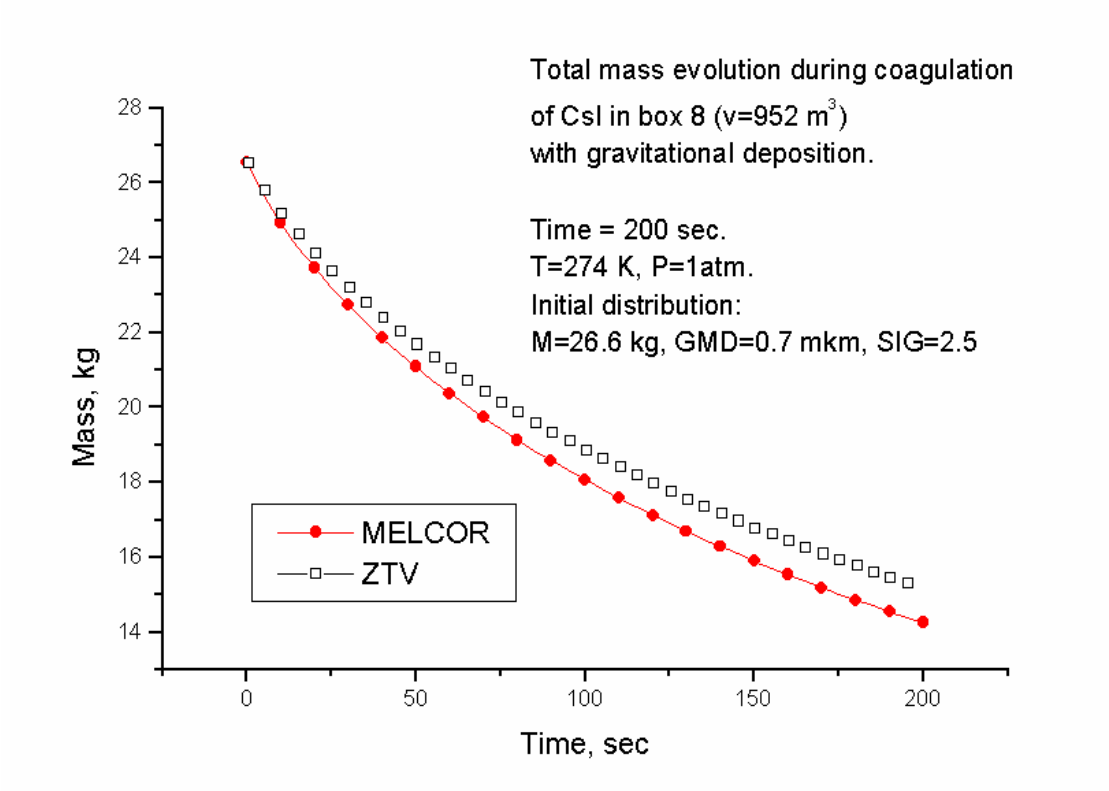

Fig. 8 Aerosol mass in box evolution

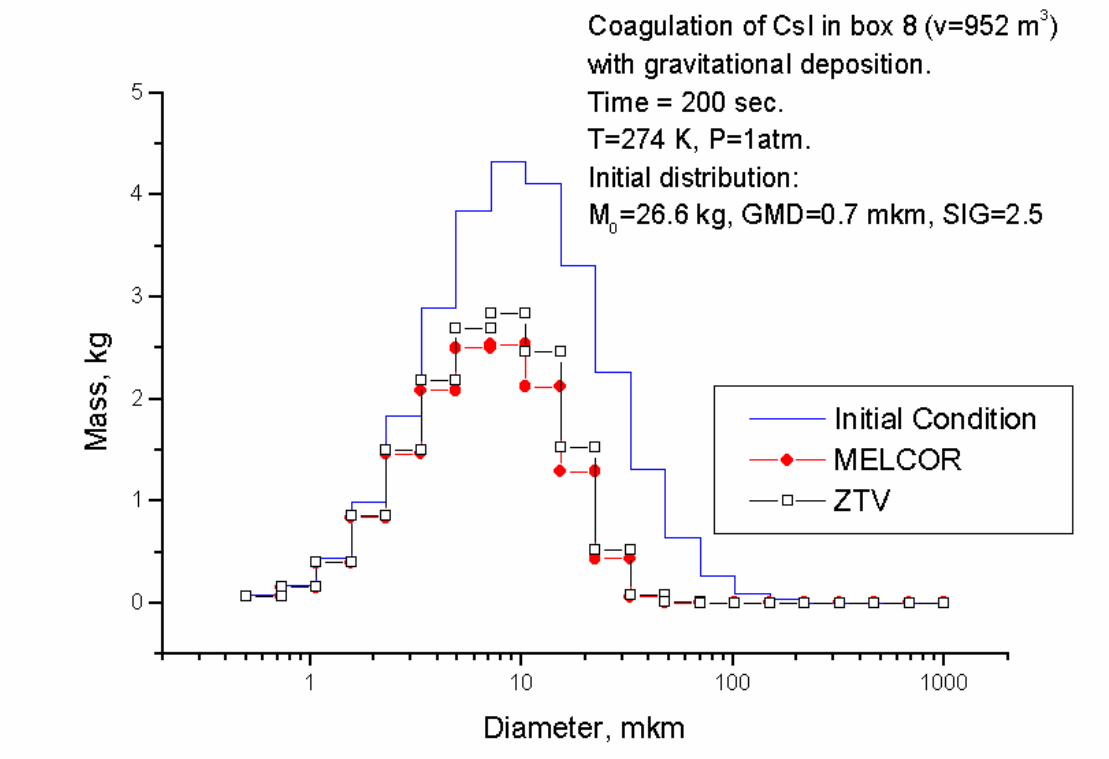

Fig. 9 Aerosol mass distribution.

2.29 The code was integrated with thermohydraulic code KUPOL-M. The data obtained with integrated code demonstrate considerable discrepancy between calculated results and project estimations which give the understated amount of aerosols in containment atmosphere during first hours after emission (up to 2 times), however by the end of the first day they exceed calculated result up to the order. Slow aerosol output at the beginning stage is caused by

relatively small size of aerosol particles and absence of water vapor condensation due to superheated media (coagulation process occurs only).

3. Results by the end of the project duration

Approaches and models for assessment of emergency emissions used for NPP-91 project with VVER-1000 reactor have been reviewed as well as EUR, NRC and IAEA recommendations for LWR.
The conducted analysis has revealed the following main factors, which considerably affect the expected volume of emergency emissions, namely:

- Significant uncertainty in estimates of Ru group fission products from the fuel both at in-vessel and ex-vessel stages of accidents.
- Accounting for aerosols deposition and transport to reactor plant equipment proves to be an essential factor for severe accidents, related to non-isolated leaks from the primary to secondary circuit, which lead to «global emission» under INES scale of accidents. Percentage of aerosols retained in the primary circuit equipment could amount up to 70%.
- Accounting for Iodine persorption with polymeric coatings, steel corrosion products and core catcher materials may decrease the expected emission of radioactive Iodine, which is one of the main dose forming fission products, as much as 3 to 10 times in case fission products are localized within the containment.
- Proper modeling of aerosols behavior inside the containment facilities and the containment annulus determines the volume of expected emission of radioactive aerosols.

Buildup of fission products in the fuel under normal operating conditions and their release from the fuel under normal operating conditions and in case of accidents has been analyzed in the cause of work. Calculation results for buildup and release of fission products have been acquired. Analysis of morphological properties of reactor aerosols has been performed. Selection of ammonia chloride has been justified for doing experiments with solid aerosols.

Calculations have been performed for a wide range of severe accidents, including loss-of-coolant accidents with coolant leak from the primary circuit to the containment and primary-to-secondary circuit leak.

Initial data for UO2–Zr–ZrO2 melt composition required for molten pool aerosol release under EVAN1 experiment have been compiled following the results of calculations for molten pool formation dynamics at the reactor vessel bottom.

Initial data for CKTI experiments related to aerosols deposition and analysis of Iodine isotopes behavior in the containment have been complied based on results of assessment of steam-gas medium relocation velocities at different stages of severe accidents, changing media properties in the containment and calculations of fission products release from the fuel as well as their behavior in the primary circuit.

As a result of the calculations conducted for melt formation dynamics in the core catcher, conclusions have been made regarding mechanisms and conditions of aerosols release with conditions suggested for performance of experiments to analyze aerosols release from the core catcher.

The performed analysis allows for defining boundary conditions required for experimental tasks of the Project, namely:

- Task 2 – composition and quantities of low-volatile fission products in the molten pool, composition of materials, thermohydraulic and thermophysical conditions of the molten pool.
- Task 4 – aerodynamic conditions for conducting experiments and justification of ammonium chloride, selected for experiments performance.
- Task 6 – Iodine release into containment, thermohydraulic, material and radiation conditions in the containment.

Personnel Commitments

Name	Category	Days
Bezlepkin Vladimir	1	**76**

Name	Category	Days
Zatevakhin Mikhail	1	**55**
Blinova Lidia	1	**96**
Leontyev Yury	2	**41**
Semashko Sergey	2	**76**
Ivkov Igor	2	**115**
Frolov Andrey	2	**115**
Astafyeva Vera	2	**40**
Lebedev Leonid	2	**29**
Ryabova Anastasia	2	**26**
Ignatyev Alexey	2	**105**
Potapov Igor	2	**90**
Sidorov Valery	2	**87**
Alexeev Sergey	2	**60**
Krylov Yury	2	**58**
Fomina Yulia	3	**22**
Buzharov Nikolay	4	**10**
Azaryeva Nadezda	3	**45**
Kiselev Arkady	1	**58**
Vasilyev Alexandr	1	**50**
Filippov Alexandr	1	**52**
Kobelev Gennady	1	**44**
Zaichik Leonid	2	**44**
Tkachenko Alexandr	2	**46**
Alipchenkov Vladimir	2	**12**
Zagryazkin Valery	1	**19**
Mosunova Anastsia	2	**27**
Stepnov Vladimir	2	**18**
Tomashchik Dmitry	2	**92**
Tarasov Oleg	2	**13**
Karyukina Tatyana	3	**64**

Task 2: (description) Experimental studies of the low-volatile fission products release at the oxidation of suboxidized molten corium.

1. State / Situation at the beginning of the project duration

In accordance with the Work plant the Project was started by the preparation and discussion of the experimental matrix to be implemented by the Alexandrov RIT (NITI) within the EVAN Project - Stage 1, which is presented in Table 15.

Table 15. Experimental matrix of NITI with the EVAN project. Stage 1.

	Test	Experimental objective	Specifications	Note	Deadline
Stage 1	EVAN–FP1	To study the release of low-volatile FP at the oxidation of molten corium	Corium composition – UO_2 – ZrO_2 - Zr, U/Zr(at)=1.2, C-32 (specified after completion of tasks 1,2)→C-100, Corium mass – 1-2 kg, Melt temperature - T_{liq}+(50÷100) ^oC, FP: Ru, Mo, Ce,La,Sr,Ba	Ar/O_2 oxidation by mixture	1-4 q.

Input data have been prepared to specify the boundary conditions in the experimental program.

2. Fulfilled work

2.30 Activities within Task 2 are aimed at getting an insight into the local effects influencing the volatilization of FP and melt components and at extending the verification basis on the FP release in the high-temperature region of liquid corium. The work included the determination of the melt temperature and oxidation degree influence on the FP release rate. The melt composition and temperature were chosen to approximately correspond to a certain transient condition of the top melt layer inside the reactor vessel at scenarios with small or large loss of coolant (SLOCA and LLOCA).

The experimental program was divided into two stages. The first stage had methodological objectives: to determine the reachable superheating of a melt having different oxidation degrees; test the availability of the whole gas-aerosol system and its components (F1 and F2 filters); identify the optimal accident-free flow rate of coolant; possibilities for the numerical control of the melt oxidation rate – a preliminary scoping experiment Pr1-EV1 was conducted. The Pr1-EV1 melt did not contain FP simulants. In the subsequent Pr2-EV1 the liquid-phase synthesis of corium charge was performed. After the availability analysis of all systems and experimental data on the melt component release the aerosol sampling line was improved and a procedure for the main test was developed.

At the second stage the main test EVAN-1FP with FP simulants in the molten pool was conducted.

Table 16 gives the matrix of experiments conducted within Task 2.

Table 16. Task 2 experimental matrix

Experimental parameters	Test		
	Pr1-EV1	**Pr2-EV1**	**EVAN-1FP**
Melt composition, mass.%	UO_2=74.1 ZrO_2=19.7 Zr=6.2	UO_2=75.5 ZrO_2=18.1 Zr=6.4	UO_2=72.64 ZrO_2=19.38 Zr=6.15
Melt oxidation degree, C_n	70÷100	70	70÷100
Temperature range, C	2538÷2697	2600÷2640	2535÷2696
Atmosphere	Ar÷Ar/O_2	Ar	Ar÷Ar/O_2
Fission product simulants, mass.%	-	-	SrO=0.14 BaO=0.23 CeO_2=0.45 La_2O_3=0.20 Ru=0.35 Mo=0.46

The following oxides were used as simulants of low-volatile fission products: SrO, BaO, CeO_2, La_2O_3, also metallic Mo and Ru. Concentrations of FP simulants in corium were chosen in accordance with their content in the fuel taking into account the sensitivity of their mass-spectrometry determination in the samples. Sr and Ba oxides were introduced as metazirconates to exclude their interaction with moisture and carbonic acid of air.

2.31 Specifications of EVAN-FP1

The experimental setup included a HF generator having the oscillating power of 60 kW and 0.13 MHz frequency of the current. The melt was prepared by induction melting in a cold crucible at the “Rasplav-2” test facility.

The schematics of gas supply and aerosol collection system was optimized using the experience of Pre1-EVAN.

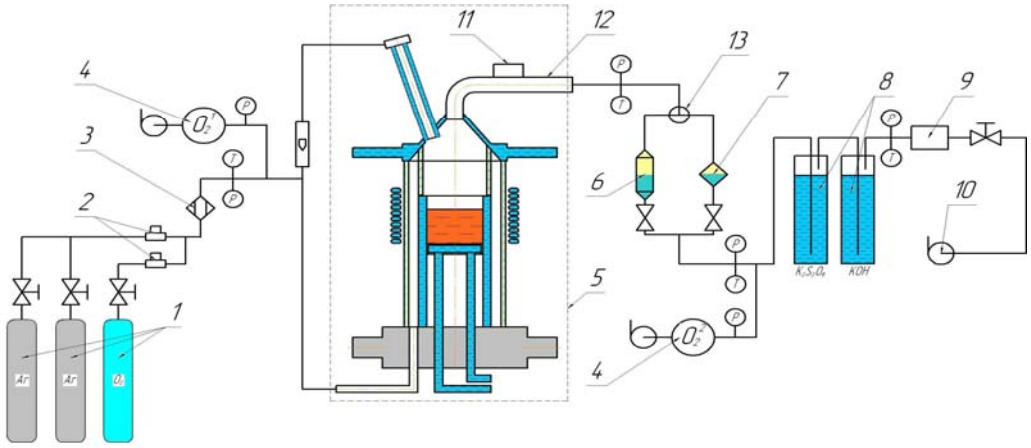

1. Ar and O tanks; 2. Gas flow-rate regulators and meters; 3. Gas mixing unit; 4. Electrochemical oxygen sensors; 5. Induction furnace; 6. F2 filter; 7. F1 filter; 8. Spargers; 9. Gas flowmeter; 10. Ventilator; 11. Vibrator; 12.Copper line.

Fig. 10. Gas supply and aerosol collection system schematics

2.32 EVAN-FP1 experimental procedure

After the molten pool was produced in the inert atmosphere the aerosol release rates were measured by collecting aerosol samples to the F1 filters at different temperatures and oxidation degrees of corium (2 – 3 steady temperature conditions for C-70, C-85 and C-100). The melt oxidation degree was raised in stages, by supplying the argon-oxygen mixture (oxygen - 20% vol.) to the surface.

Fig. 11. shows the registered experimental parameters: operational modes of HF-generator, melt temperatures.

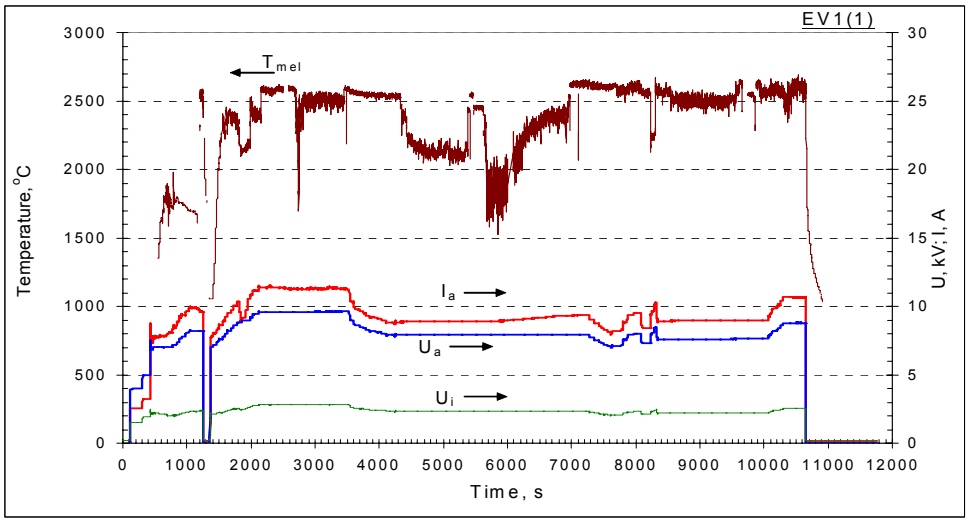

Fig. 11. values of anode current (I_a), voltage (U_a), inductor voltage (U_i) and pyrometer readings (T_{mel})

2.33 Posttest analysis

Just like in pretest Pr1-EV1, after the furnace was disassembled aerosol depositions were observed on the walls of crucible sections, lid and quartz ring located between the crucible sections and the lid. The ingot was broken during its extraction from the crucible. Differently from the pretest, a metallic inclusion having the mass of 5.11 g was found during the ingot

crushing approx 5 mm below the ingot edge. All fragments were subjected to the physicochemical analysis.

The following methods of analysis were used: X-ray fluorescence (XRF), chemical (ChA), mass-spectrometry with induction-coupled plasma (ICP MS), scanning-electron microscopy and energy dispersion X-ray analysis(SEM/EDX), laser small-angle light dispersion for determining the dispersion composition of aerosols, high-temperature mass-spectrometry (HT MS).

Sample preparation for the physicochemical analysis

Oxidic ingots and melt samples, as well as above-melt crusts resulting from Pr1-EV1 and EV1 were crushed to the particle size ≤2 mm. After that average samples were produced by quartering, and they were crushed to get the particle size of ≤ 250 μm.

The Pr1-EV1 and EV1 spillages were quartered to get average samples, which were crushed to the particle size of ≤ 50 μm.

The Pr2-EV1 oxidic ingot was crushed to the grain size of ≤ 2 mm. The average sample was produced by quartering, which was crushed to the particle size of ≤ 50 μm for the purposes of physicochemical analysis. After that 1390 g of crushed corium ingot was used as a charge material in the EV1 test.

2.34 The posttest analyses determined the releaser rates of melt components, elemental, phase composition and morphological characteristics of aerosols depending on the experimental conditions.

Mass balance

During and after experiments, also in the course of posttest analyses a careful collection and accounting of aerosol deposits and experimental materials was made. Imbalance, i.e. the difference between the initial mass of charge materials and those collected after Pr1-EV1 and EV1, was +50.40g (Table 17) and +37.42 g (Table 17) respectively. The imbalance was caused by the interaction between melt components and aerosols with the oxygen supplied by doses, which led to the change of ratio between the oxygen and total metal content in the melt, that is, to the oxidation of metallic zirconium and final oxidation of uranium oxide to a higher degree. The evaluated imbalance practically coincides with calculated volume of oxygen absorbed during the test. The mass balance data were used to determine coefficients taking aerosol losses into account for calculating uranium oxide and FP simulants' release rates.

Influence of corium temperature and oxidation degree on the component release rates

Table 17 gives the summarized measurements of oxide volatilization rates from corium using the flow method. We should note that it is difficult to interpret oxidation rates during the transition regimes, at which the melt was oxidized, because the melt surface temperature was not determined at those regimes. It is evident that it changed at the oxidation, the inductor voltage being the same, due to the heat of chemical reactions and changes of power deposition in the melt caused by the changes of melt electric conductivity. It is not possible to evaluate the input of these phenomena.

Using the data of Table 17 temperature curves of elemental release rates were constructed in the Arrhenius coordinates for the melt components and FP simulants. In order to evaluate the influence of corium oxidation degree on the release rates of elements the latter were considered in the same temperature conditions. To minimize the extrapolation region the temperature of 2652 C was chosen, i.e. the data for C-70 and C-85 were linearly extrapolated in the Arrhenius coordinates into the high-temperature and low-temperature regions respectively. In this way the release rates from suboxidized corium were produced for the temperature, at which C-100 corium release rates were measured, and curves of release rates versus the oxidation index were constructed.

Table 17 . Volatilization rates of oxides in Pr1-EV1 и EV1

Test	Melt oxidation degree	Above-melt atmosphere (carrier gas)	Carrier gas flowrate G, l/ min	Melt surface temperature, T^0C	Release rate V[1], $mg/cm^2 \cdot h$
Pr1-EV1 **Pr1-EV1** **EV1(1)** **EV1(1)**	70	Ar	10	2562 2538 2595 2535	156.94 115.04 249.29 136.64
Pr1-EV1 **EV1(1)**	72÷85	Ar/O_2 (80/20)		2538 - 2626	127.90 152.71
Pr1-EV1 **Pr1-EV1** **EV1(1)** **EV1(2)** **EV1(2)**	85	Ar		2628 2648 2639 2696 2655	236.58 320.23 154.01 533.24 373.25
Pr1-EV1 **EV1(2)**	85÷100	Ar/O_2 (80/20)		2648 - 2697	152.23 299.41
Pr1-EV1 **EV1(2)**	100	Ar		2697 2652	546.46 333.64

[1] – average rate only for F1 filters taking transport losses into account.

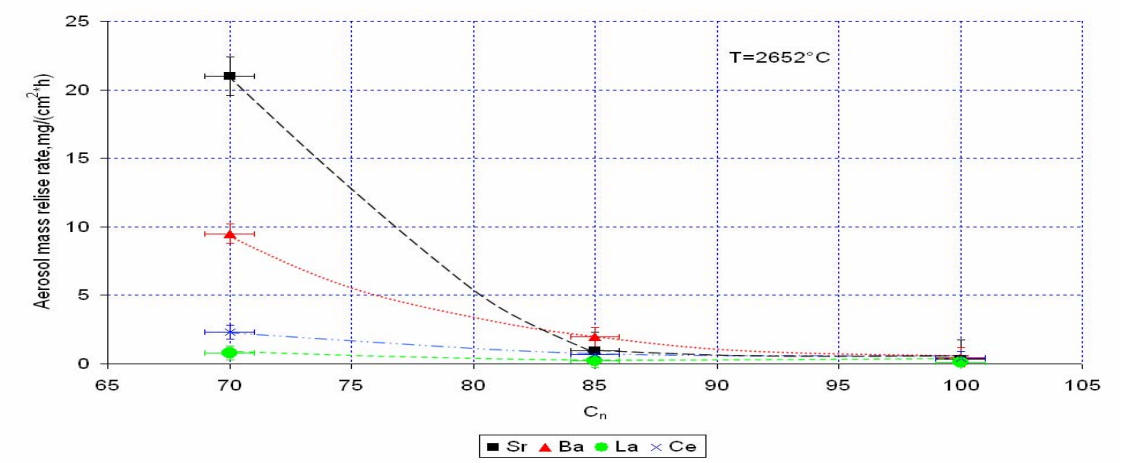

Fig. 12. Release rate of Sr, Ba, Ce, La versus the melt oxidation index at 2652 C

It was found that the increase of melt oxidation degree from C-70 to C-100 causes a substantial decrease of Ba and Sr release, approximately by 20 and 10 times. At this the Mo release rate has an approx. 3 times acceleration. The total aerosol mass release rate drops by approx. 5 times.

Size distribution of aerosol particles and their morphology

Samples prepared for analysis by the laser analyzer Microsizer-201A were the mixture of particles (primary aerosol particles produced at the steam condensation above the melt, particles formed during the volumetric coagulation at the aerosol flow progression in the gas lines, and agglomerate particles shaped as lumps and flakes). It was determined that size distribution of aerosols depends on the sampling place (F1 filters, furnace components), melt temperature and composition, and above-melt atmosphere.

Four typical sizes of particles prevail in the gas-aerosol mixture. The first maximum (peak) of the distribution curves corresponds to the small primary particles having sizes up to 1 μm, the second maximum has small particle agglomerates of 1.59-3.63 μm. The third maximum corresponds to agglomerates of 3.63-5.49 μm, and the fourth – large agglomerates of 9.54-12.6 μm. A certain amount of primary aerosol particles of 0.2 μm and smaller should be noted.

The melt temperature is likely not to produce substantial influence on the characteristic sizes of aerosol particles. The changed melt temperature influences only the ratio between the number of primary particles and agglomerates. A higher melt temperature causes the increase in the share of small primary particles and decrease of agglomerates.

The melt oxidation degree also produces a certain influence on the aerosol distribution. After the melt oxidation from C-70 to C-100 a share of heavy particles (11-12.6 μm diameter) noticeably grows.

Introduction of oxygen into the above-melt atmosphere produces a cardinal change in the size distribution pattern. Aerosols show a substantial increase in the number of primary particles (sizes up to 1 μm), and the share of other particles is very small, i.e. the melt oxidation in the argon/oxygen atmosphere does not support coagulation processes. This phenomenon should be taken into account when determining the source term of a severe accident with the core meltdown.

3. Results by the end of the project duration

The release rates of FPS and SrO, BaO, La_2O_3, CeO_2, Ru, Mo, UO_x, ZrO_2 from the melt have been determined at its oxidation from Cn 70 to C 100 at different melt temperatures.

The largest influence on the FPS and melt components release is caused by the Zrfree temperature and amount. The increase of Cn produces a considerable Sr and Ba release rate reduction (20 and 10 times) and an approx. 3-fold increase of Mo release rate. The mass aerosol release rate drops approx. 5 times. The formation of gaseous RuO4 has not been detected before the total oxidation of Zrfree.

It was shown that at the prototypic concentrations of Ru and Mo in the suboxidized melt it stratifies; Ru and Mo concentrate in the metallic liquid.

It was determined that primary-condensation aerosol particles have a characteristic size smaller than 1 μm. The influence of Tmelt, Cn and above-melt atmosphere on the aerosol particle size distribution has been determined. An important aspect to be taken into account in justifying such safety systems, as SPOT GO/PG and hydrogen catalytic recombinators, is the tendency of aerosol particles to form dense deposits, which have a good adhesion with cold surfaces and substantial thermal and diffusion resistance.

The XRF has shown that U oxides condense above the melt to form the UO_2 phase. U_3O_8 is the prevailing phase, which condenses in the oxidizing atmosphere.

Oxygen absorption rate (oxidation rate) does not depend on Zr concentration in the melt; it is determined by the O content and the pattern of hydrodynamical flow in the above-melt atmosphere.

The melt sample examination by the high-temperature mass-spectrometry determined that a decreased amount of Zrfree in the melt samples is accompanied by a lower volatility of uranium oxides.

The resulting experimental data can be used for updating databases on FP release from molten corium and for the validation of corresponding severe accident codes.

Methodologies, specifications, experimental procedures and results have a full description in the Report on Task 2.

Personnel Commitments

Name	Category	Days
Aniskevich Yuri	1	**52**
Beshta Sevostyan	1	**79**
Blizniuk Valentina	1	**79**
Granovskaja Nadezhda	1	**47**
Granovsky Vladimir	1	**79**
Gusarov Victor	1	**79**
Kalyago Elena	1	**79**
Kamensky Nikolay	1	**75**
Khabensky Vladimir	1	**79**
Kirin Gennady	1	**26**

Name	Category	Days
Krushinov Evgeny	1	**79**
Kulagin Igor	1	**79**
Lyssenko Anatoli	1	**79**
Martynov Valery	1	**55**
Sabinin Vladimir	1	**79**
Smirnov Sergey	1	**80**
Sulatsky Andrey	1	**79**
Vitol Sergey	1	**79**
Almyashev Vyacheslav	2	**77**
Belyaeva Elena	2	**54**
Bezlepkin Pavel	2	**77**
Bulygin Valentin	2	**67**
Chemeriskin Vladimir	2	**78**
Chertkov Alexander	2	**69**
Gromov Vadim	2	**76**
Kalyago Alexander	2	**78**
Kosarevsky Roman	2	**73**
Kotova Svetlana	2	**83**
Kucherov Yuri	2	**77**
Lopatin Sergey	2	**39**
Peregud Sergey	2	**76**
Shevchenko Evgeny	2	**78**
Fadeev Andrey	3	**31**
Ignatov Alexander	3	**31**
Shuvalov Sergey	3	**46**
Talalaeva Tatiana	3	**46**
Poldyaeva Inessa	3	**27**

Task 3: (statement) Analytical investigation of fission products release from molten pool or core catcher .
Subtask 3.1: (statement) Review of capabilities to model the fission products release from molten pool, using the modern computer codes; justification of applicability of the expected experimental results for models verification.

1. State / Situation at the beginning of the project duration

It was evident that there were two independent cases: fission products release from the molten corium pool and release from core-catcher. In the case of corium in the core-catcher, it can interact with concrete which leads to the possibility of release in gas bubbles or in droplets. In case of in-vessel retention the open surface of the melt is expected to be quiet. This case was to be simulated in the EVAN experiment. Hence only evaporation of FP and CM from the reactor was considered.

2. Fulfilled work

Two models of FP and CM release have been developed: atomic model and molecular model. Molecular model is realized as a stand-alone FORTRAN code.

A) Atomic model:

Estimate of release of low-volatile FPs and CMs is based on the description of the corium as atomic regular solution. This model allows to describe thermodynamic properties of the melt using minimum number of adjustable parameters.

The partial pressure of k-th component of the gas phase, P_k, over the melt $U–Zr–O–FP_k$ has the form:

$$\begin{aligned} RT\ln P_k &= RT\ln P_k^0 + RT\ln x_k + L_{k-U}x_U(1-x_k) \\ &+ L_{k-Zr}x_{Zr}(1-x_k) + L_{k-O}x_O(1-x_k) - L_{U-Zr}x_U x_{Zr} \\ &- L_{U-O}x_U x_O - L_{Zr-O}x_{Zr}x_O \end{aligned} \quad (1)$$

Here R = 8,31696 J/(mol·K) is the universal gas constant; x_k is the concentration of *k*-th element in the melt (k = *O*, *U*, *Mo*, *Ba*, …); $L_{ij} = L_{ji}$ is the coefficient of binary interaction of i-th and j-th component in the melt; P_k^o is the pressure (in atm) over the pure melt of atoms «*k*» which can be taken from pure material databases and T is temerature. The rate of evaporation from the open surface into vacuum is calculated according to Langmuir equation

$$V_k = 44.44 P_k \beta_k (M_k/T)^{0.5}, \quad g/(cm^2 \cdot s), \quad (2)$$

where β_k is the Langmuir coefficient and M_k is the atom mass.

In order to use these equations it is necessary to know the excess parameters L_{ij}. For O-U-Zr they were fitted to the results of MASCA STFM experiments. The parameters between FPs and oxygen were fitted to results of STFM-FP experiments. Parameters FP-U,Zr were obtained as follows. For non-soluble in the O-U-Zr melt FPs (Mo,Ru) they were fitted to known phase diagrams. The parameters for La, Ce, Ba, Sr were chosen using the Miedema method based on the Pauling's conception of electronegativity.

The most vague parameters are Langmuir coefficients β_k.All of them were set equal to β_{Fe} and β_{Fe} was obtained from the rate of Fe release in STFM experiments.

B) Molecular model

The melt is considered as a regular molecular solution. Chemical potentials of the model are given by the formulae (3, 4)

$$\mu_i = \mu_i^{(id)} + \mu_i^{(ex1)}, \quad (3)$$

$$\mu_i^{(id)} = \mu_i^{(0)} + RT\ln x_i, \quad \mu_i^{(ex1)} = \sum_{j(\neq i)} L_{ij}x_j - \sum_{j<k} L_{jk}x_j x_k, \quad (4)$$

where i = U, UO_2, Zr, ZrO_2, …, L_{ij} are excess interaction parameters and $\mu_i^0(T)$ is potential of pure liquid taken from IVTANTHERMO and other databases. In the model a simplified approach has been used: for fission products μ_{ex} were constants.

Gas phase is considered as an ideal molecular gas. It's composition near the melt surface is equilibrium, i.e. chemical potentials of each element in gas phase and in the melt are equal. It allows to obtain equilibrium partial pressures p_{eq} of all elements in the gas phase near the melt surface. Evaporated FPs and CMs diffuse in the gase phase according to diffusion equation. The vapors over the melt are blown away by an air flux *W'* (L/s). The rate of release of each element is given by a simplified formula

$$J_i = p_i^{eq} \frac{W' AD/hRT}{W' + p_{tot} AD/hRT}, \quad (5)$$

where *A* is the area of the open surface of the melt, *D* is the diffusion coefficient, *h* is the thickness of diffusion gas layer, p_{tot} is total pressure in the gas phase.

In order to describe the release correctly it is necessary to take into account the melt oxidation under oxygen-containing atmosphere. According to the model, the oxygen in the atmosphere interacts with the melt until the chemical potentials of oxygen become equal.

3. Results by the end of the project duration

A) Atomic model

For the melt main components the values of the excess parameters are:

$L_{U\text{-}Zr} = 19.075;\ L_{U\text{-}O} = -9.180;\ L_{Zr\text{-}O} = -42.470.$ (6)

Parameters for FPs are shown in the Table 18:

Table 18. Excess energy parameters for atomic model.

	Excess interaction parameter L_{ij}, kJ/mol					
	Sr	Ba	La	Ce	Mo	Ru
U	190.2	204.3	60.6	54.4	1.9	8.2
Zr	188.9	204.8	51.4	46.5	5.8	20.0
O	-207.6	-22 5.4	-149.5	-127.05	98.7	91.1

Saturated vapor pressures over pure substances are obtained using the formula

$$\ln p_k^0(atm) = A + BT^{-1} + C\ln T \quad (7)$$

Parameters A, B, C are given in the Table 19.

Table 19. Parameters for saturated vapor pressures of *Mo*, *Ru*, *Sr*, *Ba*, *Ce* and *La*.

Element	A	B	C	Temperature interval, K
Mo	6.112	- 30324	-	2896-4000
Ru	9.755	- 34154	- 0.4723	298-2523
Sr	4.523	- 7423	-	1041-1641
Ba	4.007	- 8163	-	1002-1200
Ce	5.611	- 21200	-	1071-2450
La	5.911	- 21855	-	1193-2450

B) Molecular model

The excess potentials for FPs were chosen in such a way as to describe the results of EVAN experiment (task 2). They are shown in Table 20.

The molecular model is realized as a stand-alone code. Its input data are :
- Initial corium composition
- Time grid
- Atmosphere composition (time-dependent)
- Gas flow rate *W'* (time-dependent)
- area of of the melt surface *A*
- thickness of the diffusion gas layer *h*
- diffusion coefficient in the gas phase *D*

The output data are time-dependent corium composition, gas phase composition and FP release.

Table 20. Excess potentials and activities of FPs in the melt.

Species	γ_i	$\mu_i^{(ex1)}$, kJ/mol
Mo	5.00E+02	144.7
Ru	3.00E+01	79.2
BaO	5.00E-02	–69.7
SrO	5.00E-02	–69.7
La2O3	5.00E-02	–69.7

CeO2	5.00E-02	–69.7
Ce2O3	5.00E-02	–69.7

Subtask 3.2: (statement) Pretest assessments of fission products release for the EVAN–FP1 experiment conditions.

1. State / Situation at the beginning of the project duration

At the beginning of the project duration there was not enough experimental data about FP release from the melt. But some information about release of CMs from the melt was available from the results of MASCA project. They were used during modeling the rate of release until EVAN experimental results became available.

2. Fulfilled work

Both models predicted the rates of FP release under conditions of EVAN experiment. The predictions of the models were compared to the experimental results. The comparison was useful for parametrization of the models.

3. Results by the end of the project duration

A) Atomic model:

Initial corium composition shown in Table21 was set as follows: *Zr* oxidation degree C-70, *U*/*Zr* atomic ratio is approximately 1.2, FP simulants were added as oxides *SrO*, *BaO*, CeO_2, La_2O_3 and metals *Mo* and *Ru*.

Table21. Composition of the furnace charge in EV1 experiment.

Component	Mass %	Mass, g
UO_2	72.64	1234.88
ZrO_2	19.38	329.46
Zr	6.15	104.55
SrO	0.14	2.38
BaO	0.23	3.91
CeO_2	0.45	7.65
La_2O_3	0.20	3.4
Ru	0.35	5.95
Mo	0.46	7.82

During the experiment corium was oxidized by oxygen-containing atmosphere and finally reached oxidization degree C-100. During this process aerosol and corium samples have been taken at different moments. Table 22 shows compositions of the corium probes (* - melting after crystallization).

Table 22. Corium probes composition

Probe	Corium oxidation	Element concentration, mass %

number	degree	U	Zr	Sr	Ba	La	Ce	Mo	Ru
№1	C-70	64.6	19.9	0.11	0.26	0.14	0.21	0.40	0.06
№2	C-85	64.1	20.4	0.05	0.21	0.14	0.05	0.44	0.08
№3*	C-85*	64.2	20.7	0.05	0.06	0.14	0.39	0.72	0.07
№4	C-100	63.2	20.6	0.05	0.11	0.14	0.31	0.56	0.08

Aerosols were blown away from the melt surface by an air flux. Its composition was pure argon or 80% argon and 20% oxygen; its rate was 600 L/h. The rates of FP release with aerosol loses in lines taken into account are presented in Table 23.

Table 23. FP release rates in EV1 experiment

Probe	Temperature, °C	Evaporation rate $V_{exp.}$, mg/cm^2·h					
		Sr	Ba	La	Ce	Mo	Ru
№1	2535	10.960	5.665	0.326	0.114	0.961	0.161
	2595	14.273	6.817	0.469	0.505	2.452	0.326
№2	2639	0.962	1.627	0.190	0.385	1.874	0.249
№3	2655	0.962	1.954	0.253	0.650	2.099	0.825
	2696	1.584	2.682	0.549	0.495	4.373	0.912
№4	2652	0.363	0.521	0.136	0.433	27.310	0.319

The release rates predicted by the atomic model is shown in the Table 24.

Table 24. Fission products release rates as predicted by regular solution model of corium

Probe	Temperature, °C	Release rate V_{reg}, mg/(cm^2·h)					
		Sr	Ba	La	Ce	Mo	Ru
№1	2535	68.5	16.5	0.015	0.010	0.018	0.011
	2595	81.3	20.0	0.023	0.015	0.028	0.017
№2	2639	40.1	17.6	0.030	0.045	0.043	0.034
№3	2655	65.4	7.27	0.038	0.047	0.075	0.033
	2696	62.6	8.17	0.050	0.061	0.100	0.045
№4	2652	36.4	8.34	0.030	0.029	0.060	0.037

B) Molecular model

In Table 25 the comparison of the rates of total release at different stages of the EV-1 experiment is shown.

Table 25. Comparison of calculated and measured total FP release rates

Time, s	Corium	T, K	V_{exp}, mg/sm^2/h	V_{mod}, mg/sm^2/h
2840–3400	C70	2868	249.24	232.11
4500–5350	C70	2808	136.22	151.52
6000–6936	C70...C85	~2900	152.51	189.08
8620–9540	C85	2912	154.43	131.61

4140–4610	C85	2969	532.95	472.45
5260–5850	C85	2928	373.33	293.30
7150–8250	C85…C100	~2950	314.84	271.62
9210–9770	C100	2925	333.98	311.05

In Fig. 13 the rate of total release as function of time is shown: model predictions and experimental results.

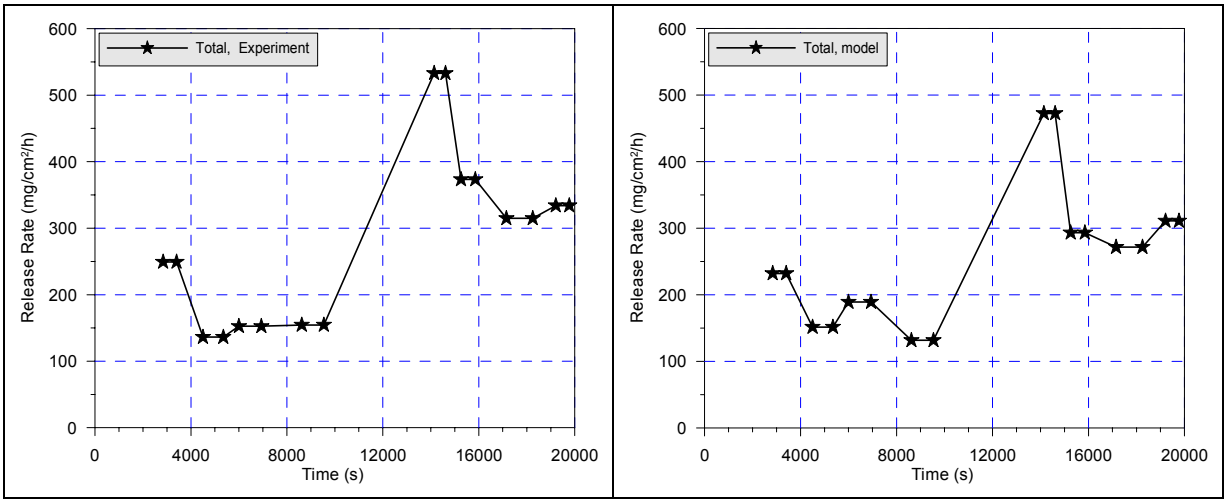

Fig. 13. Comparison of the molecular model and experimental total release rates

In the Fig. 14- Fig. 17 the rates of release of all FPs are shown. Predictions of the molecular model and results of the EVAN experiment are compared.

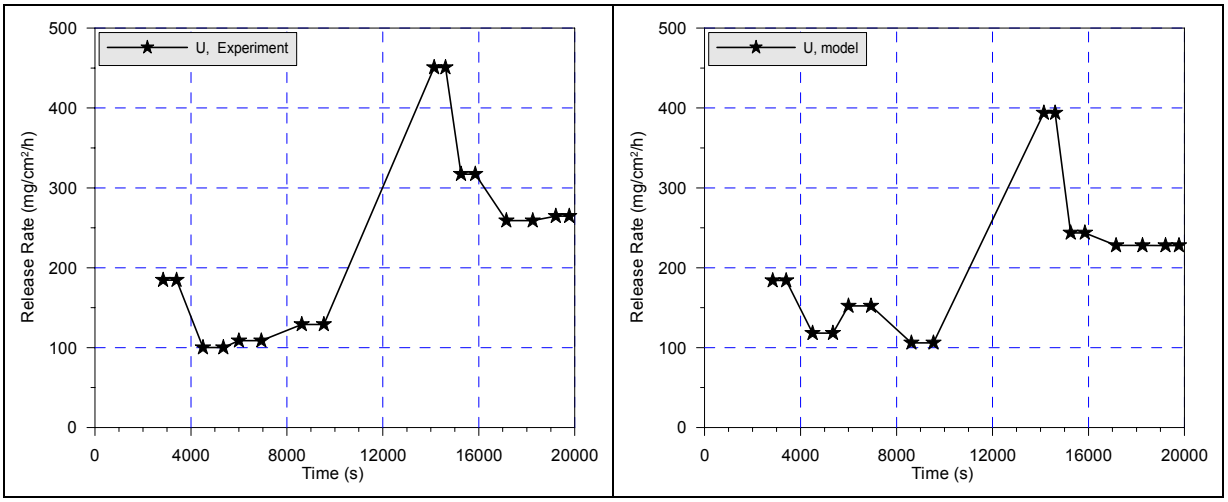

Fig. 14. Comparison of the model and experimental release rates of Uranium

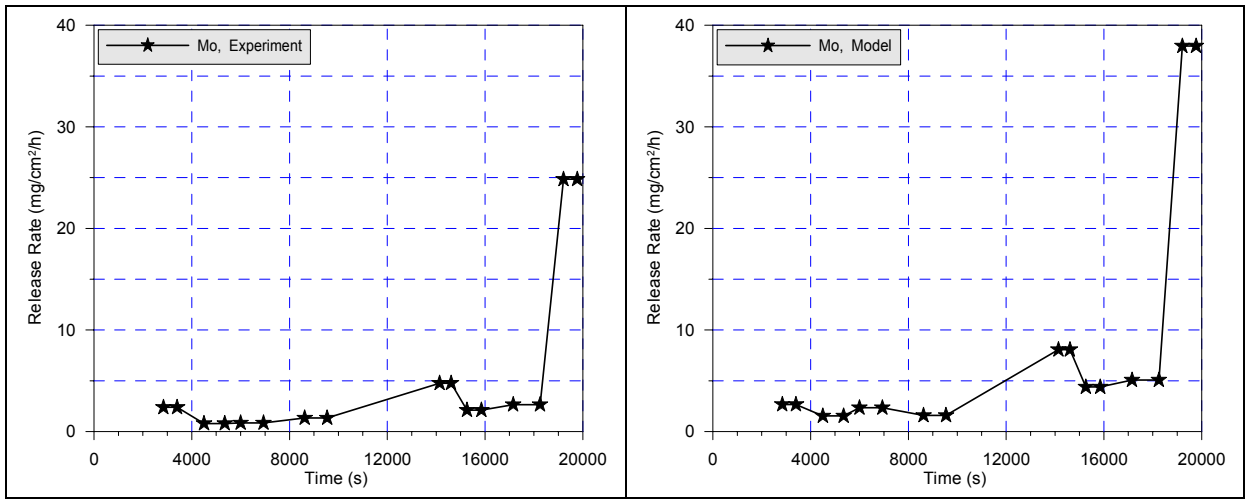

Fig. 15. Comparison of the model and experimental release rates of Molybdenum

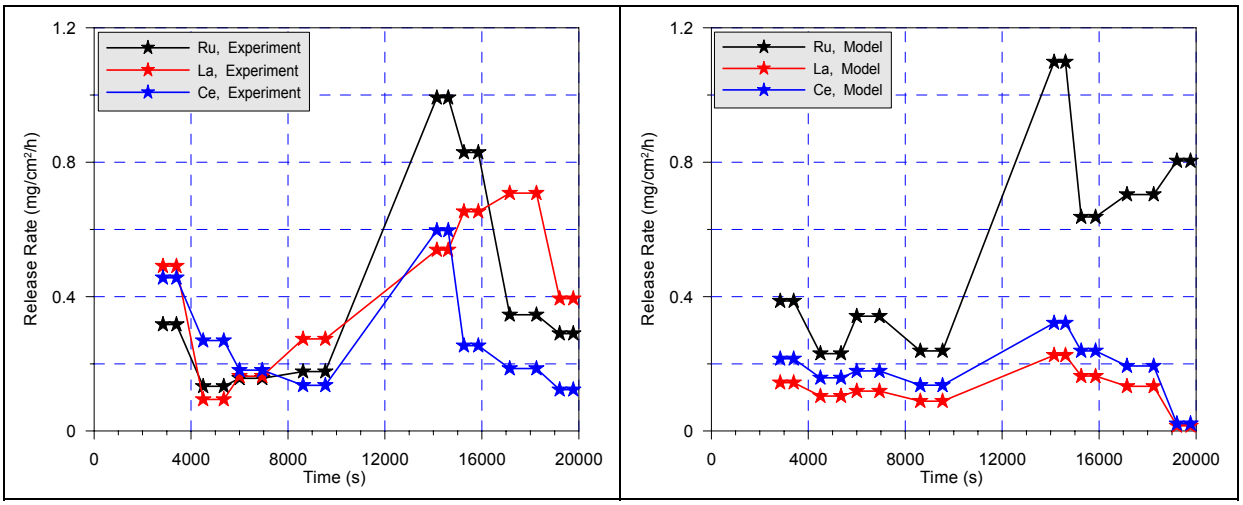

Fig. 16. Comparison of the model and experimental release rates of *Ru*, *La* and *Ce*

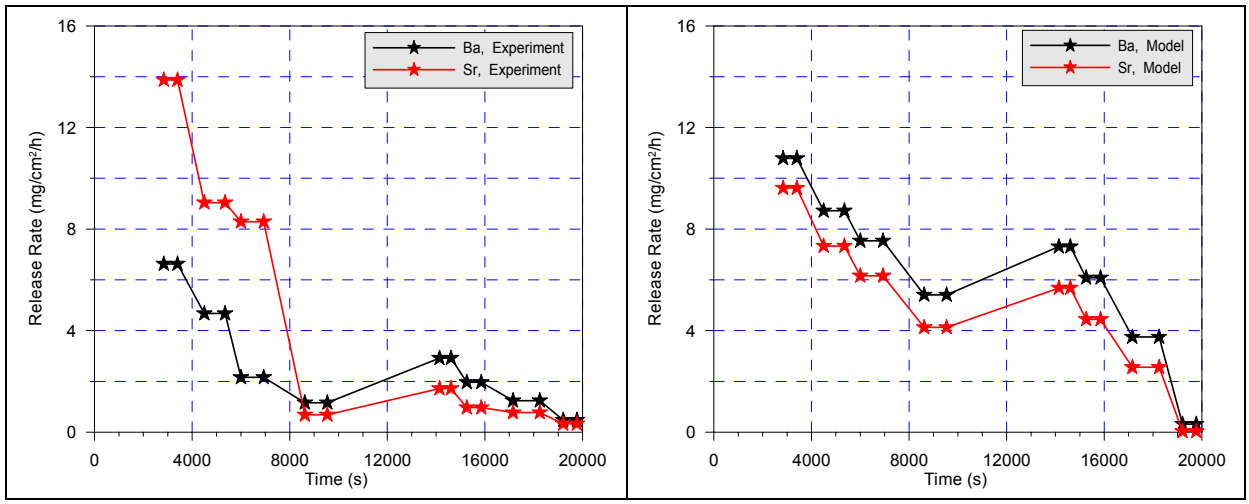

Fig. 17. Comparison of the model and experimental release rates of Ba and Sr

Personnel Commitments

Name	Category	Days

Name	Category	Days
Kiselev Arkady	1	**23**
Vasilyev Alexandr	1	**0**
Filippov Alexandr	1	**37**
Kobelev Gennady	1	**21**
Zaichik Leonid	2	**0**
Tkachenko Alexandr	2	**64**
Alipchenkov Vladimir	2	**0**
Zagryazkin Valery	1	**81**
Mosunova Anastsia	2	**9**
Stepnov Vladimir	2	**65**
Tomashchik Dmitry	2	**32**
Tarasov Oleg	2	**15**
Karyukina Tatyana	3	**36**

Task 4.(description) Experimental study of aerosols transport processes in the primary circuit equipment

1. State / Situation at the beginning of the project duration

At the beginning of the project duration the objectives, including experiment Matrix, have been formulated. There were some experimental equipment and some experience in measurement of kinematic and dispersed aerosol characteristics.

2. Fulfilled work

2.35 The necessary missing equipment were obtained: gaging and electronic equipment, large liquid drops generator (with the particle size up to 10 microns) and the powerful fan for obtaining experiment parametres, declared in the experiment Matrix.

2.36 Experimental setup and test tube revision has been done to adapt them for investigation of liquid aerosol transport. The following works have been fulfilled:

- Upgrading of the test tube for optical measurements;
- Creating ventilation system;
- Creating the system for removing exhaust gases;
- Creating the system for aerosol generation and distribution;
- Creating the system for data collection and treatment.

The design of the liquid aerosol experimental setup changed according to different regime parametres. As a result, three configurations of the liquid aerosol setup (ATF1, ATF2 and ATF3) have been used.

2.37 Optical measurement techniques of dispersed characteristics have been developed in details. Laser Doppler anemometers technique (LDA) has been developed for measurement of high speed flows.

2.38 The tuning of test tube configuration has been done on the basis of heat-loss anemometer measurement. These measurements were made:

- for obtaining of symmetric and developed flow;
- for tuning of test tube configuration;
- for calibrating of air flowmeters;
- for detailed investigation of turbulent fluctuations;

2.39 Adjustment of velocity measurement system (LDA) have been done and plan of experiments was optimized.
During experiments it has been found out that liquid fog particles as well trace air stream, as well as the smoke particles do. Therefore further experiments with use LDA the fog generator was used (instead of smoke which is usually used in LDA).

It has been found out also that the difference between large particles velocity and flow velocity in one point was rather small, so that they may be considered the same in flow velocity measurements. However, for turbulent fluctuations measurements this difference was too big.

2.40 Flow velocities have beed measured with LDA. The velocity range corresponded to Reynolds numbers 10000 - 260000 according to the Matrix of experiments.
For measurement of tangential velocity some modifications of measurement techniques was needed. As a restlt, small swirl flow has been eliminated.
In experiments axial velocities and turbulent intensities were measured. For some cases with high flow velocity specral power of turbulent fluctuations has been obtained.
It should be noted tn some cases maximum velocity turbulent fluctuation was rather high (2/3 of average flow velocity).

2.41 Disperesed composition measurements of gas-particle flow have been carried out. These measurements were done at two levels of test tube, at various air velocity (from 6,5 m/s up to 39,6 m/s) and various particle concentrations (from 0,73 g/m^3 до 6,5 g/m^3). All liquid particles we conditionally distinguish as “large” and “small”. Measuremets showed that concentration of “small” particles decresed between two levels for 5÷15% and average particle size slightly increased. As a result, numeric particle concentration was decresed also. For example, in one case average particle size increased for 5%, mass concentration decresed for 14% and numeric particle concentration decresed for 25%.

2.42 In experiments we found out that size particle distribution was close to log-normal law for both “large” and “small” particles. Measurements of mass particle concentrations were also done in different locations in one cross section of the tube. It has been found out that particle concentration increased towards the wall and irregularity of concentration profile increased down the flow.

2.43 Particle deposition rate was calculated based on concentrations at two levels. Satisfactory agreement between experimental and theoretical data has been obtained.
Visual examination showed that particle deposition led to liquid film formation on the inner tube wall. High air velocity caused small waves on the film surface but did not lead to liquid drop resuspension.

2.44 After investigations with liquid particles a number of experiments with solid particles according to Matrix of experiments have been carried out. For this some arrangements have been done:

- as a substance for solid particles ammonium chloride NH_4Cl was used. For that new aerosol generator has been developed, made and tuned. Principle of its operation is based on reversible chemical reaction dissociation-recombination of ammonium chloride;
- ventilation system was reconstructed;
- system for removing exhaust gases was reconstructed;
- new measurement techniques were introduced: quantitative chemical analysis, triers, impactors, filters and precipitators, usage of electronic microscope and high-accuracy weighing machine and so on. Optical methods were improved. New test tube have been developed and made;

2.45 The channel for solid aerosol experiments was a vertical tube in diameter of 50 mm and length 5140 mm made of stainless steel (12X18H10T). Roughness of inner wall was 0,02÷0,03 mm. The channel consisted of six part of different length and included: stabilization section in length of 1,6 m, two sections in length of 0.23 m, optical equipment, two ring precipitators in length of 0,03 m, and test section in length of 3 m.

2.46 Depending on the case one of two configurations of the setup were used: ATF4 or ATF5. Configuration ATF4 was used for investigation of deposition process and ATF5 - for resuspension. Ventilation system in ATF4 setup was combined with exhaust gas clearance system with help of two industrial vacuum cleaners DELVIR GRAND which created air flow

and cleared air simultaneously. ATF4 setup could produce air flow 38 m/s.
In experiments on resuspension (ATF5 setup) for creating high speed flow industrial powerful air supply system (gas blower TH-200, 200 kW) was used. In order to decrease hydraulic resistance gas exhaust in these experiments realized directly into laboratory room since amount of resuspected particles were negligible. This blower could give air velocity up to 105 m/s.
Before experiments some tuning of flow regimes was carried out. Measurements of velocity profiles using heat-loss anemometers and Pitot tube were made. Pressure drop within test section was measured with use of differential manometer.

2.47 During solid particle experiments it was found out that our optical methods could not resolve whole size spectrum of particles created generator, so that optical measurements were used only for the inquiry in this case. For this reason in order to determine deposited mass indirect method based on high dissolubility of ammonium chloride in the water have been developed. After experiment test section was disassembled into parts, and each part was washed off with distilled water. Then, using chemical analysis of obtained samples, masses of deposited ammonium chloride were determined.

2.48 For dispersed analysis of solid particles six cascades impactor was used. Obtained impactor samples were analized using high-accuracy weighing machine. This allowed to get size spectrum histograms with six size ranges. Measurements were done by weighing of impactor substrates before and after deposition.
In order to obtain sufficient amount of deposited aerosol exposition times were chosen rather long (more than 100 min). Using short exposition times and special substrates the samples of multi-layer deposits were obtained and investigated with electronic microscope.
Impactor measurements were duplicated by sampling with special filters. Agreement between results of these two measurements was satisfactory.

2.49 In experiments on deposition of solid aerosol air velocities were 20 – 38 m/s and aerosol concentrations were 0,5-2,25 g/m^3. Particle sizes were 0,3÷10 mkm.
In experiments on resuspension of solid aerosol air velocities were 65 – 105 m/s and duration of each test was 10 min.
As a result, the following experimental data have been obtained:
- aerosol concentrations (including time dependences);
- particle size and mass distributions;
- ammonium chloride mass deposited at test section;
These data were compared with theoretical predictions.
Basing on these results it is possible to draw the general conclusion, that rather small part of ammonium chloride deposits at the tube walls, and simultaneously marked resuspension process occurs especially at high gas velocities.

3. Results by the end of the project duration

Matrix of experiments for phase №1 and phase №2

Test	Velocity for deposition phase, m/s	Velocity for resuspension phase, m/s	Particle size d, mkm	Temperature, K	Test Purpose	Aerosol particles parameters	Orientation and surface parameters of working section
EVAN–№3345 AT 1.1	33,8	None	0.2 – 5	300	Investigation of transport and deposition rate of liquid aerosol	Liquid JEM PRO-SMOKE high density (SP MIX)	Vertical pipe with 98 mm diameter, height ~6 m
EVAN–	39,6	None	0.2 – 28	300			

№3345 AT 1.2.1					particles from gas flow towards the wall		(upwards flow), steel 10ХСНД
EVAN– №3345 AT 1.2.2	33,8						
EVAN– №3345 AT 1.2.3	24,8						
EVAN– №3345 AT 1.2.4	6,5						
EVAN– №3345 AT 2.1	20	65	0.3 – 10	320	Investigation of deposition and resuspension of solid aerosol particles (prototype and preliminary tests)	Solid aerosol particles of NH4Cl	Vetrtical pipe from stainless steel with diameter ~50mm, height ~5 m,
		105					
EVAN– №3345 AT 2.2	30	75					
		105					
EVAN– №3345 AT 2.3	38	75					
		105					

Deposition velocities of liquid aerosol size of 0,2 … 14 microns in the cylindrical vertical channel in a range of Reynolds numbers from 10000 to 240000 have been investigated.

Parameters of carrier gas flow (average velocity, velocity fluctuations and fluctuation frequencies) in the cylindrical vertical channel in diameter of 98 mm have been measured.

Particle size spectra and particle concentrations along the channel (B=98 мм) are obtained.

A novel experimental setup for investigation of aerosol deposition and resuspension has been constructed.

The design of the ammonium chloride aerosol generator based on use of reversible chemical reaction (dissociation - recombination) has been developed.

Deposition intensities of ammonium chloride aerosol in size of 0,2 to 10 microns in the vertical channel in diameter of 50 mm have been obtained under air velocity from 20 to 38 m/s. It has been found out that deposition intensities depend on two simultaneous processes – deposition and resuspension.

Resuspension velocities of ammonium chloride aerosol in the vertical channel in diameter of 50 mm have been obtained under air velocities from 65 to 105 m/s

Obtained experimental results can be used for numerical codes verification.

Personnel Commitments

Name	Category	Days
Krektunov Oleg	1	**145**
Lebedev Mikhail	1	**140**
Fokin Boris	1	**90**
Belenkiy Mikhail	1	**90**

Name	Category	Days
Gotovskiy Mikhail	1	**90**
Arefiev Valentin	1	**200**
Zavelskaya Elena	1	**25**
Salnikov Vjacheslav	1	**25**
Kiseleva Elvira	1	**65**
Danilova Galina	1	**25**
Blinov Mikhail	2	**120**
Mukhin Vjacheslav	2	**124**
Alexandrov Sergey	2	**145**
Grekov Fedor	2	**157**
Gorbachev Yuriy	2	**35**
Feldberg Lev	2	**170**
Semidetnov Nikolay	2	**160**
Juras Stanislav	2	**150**
Terentev Aleksey	2	**150**
Gudkov Eduard	2	**25**
Senkin Boris	2	**45**
Zotov Andrey	2	**145**
Chumakov Yuriy	2	**75**
Filippov Aleksander	3	**131**
Salnikov Evgeny	3	**55**
Volukhova Tatiana	3	**56**
Tchernovets Boris	3	**130**
Rozanov Sergey	3	**77**
Maleva Irina	3	**49**
Getman Sofya	2	**69**
Agafonova Natalia	2	**100**
Ivlev Lev	2	**32**

Task 5: (statement) Theoretical and computer modeling of aerosol transport in the primary circuit

Subtask 5.1: (statement) Review of capabilities to model the processes in question by modern computer codes, justification of applicability of the expected experimental results for models verification

Subtask 5.2: (statement) Pretest/posttest calculations (according to the test schedule)

1. State / Situation at the beginning of the project duration

To the beginning of the project already there was a number of the theoretical developments executed at the Nuclear Safety Institute of the RAS, for the description of aerosol behavior in a turbulent flows. Also to the beginning of the project at the SPAEP was available 3D a code indented for calculation of a viscous incompressible turbulent flows using large eddy simulation model (LES).

2. Fulfilled work

For project period the following works have been fulfilled:

- theoretical model of aerosol particles deposition from the turbulent flow taking into account for various mechanisms has been developed.

- the theoretical particle resuspension model has been developed.

- 3D a code for modelling turbulent flows with particles based on of LES the models, allowing to predict particles behaviour under action of drag force, lift force and Brownian force (causing particles diffusion) has been developed.

3. Results by the end of the project duration

On the basis of the statistical description of aerosol dynamics with use PDF (probability distribution function) the simplified analytical expressions for aerosol velocity deposition from a gas flow in view of various mechanisms have been received.
So, dimensionless deposition velocity (deposition coefficient), caused by mechanisms of turbophoresis and Brownian diffusion has a simple form:

$$j_+ = \frac{0.115\,\mathrm{Sc}_B^{-3/4} + 2.5\cdot 10^{-4}\,\tau_+^{\,2.5}}{1+10^{-3}\,\tau_+^{\,2.5}}$$

The following figure shows the good agreement of the analytical formula (1) with empirical correlations (2), experiment (4) and DNS calculations (3,5,6).

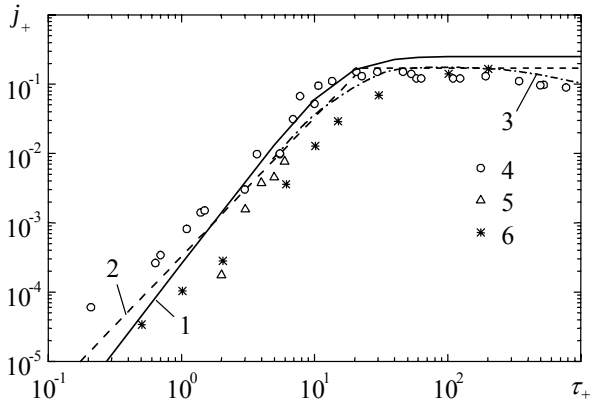

Fig. 18

The generalized expression for velocity deposition, caused by combined mechanisms of convection and fluctuation types, has been received in the form:

$$j_+ = \frac{V_+}{1-\exp(-V_+/j_{+0})},$$

where V_+ is the deposition coefficient, caused by convection–force mechanisms (gravity force, convection, thermophoresis, centrifugal force) and j_{+0} is the deposition coefficient, caused by diffusion migration mechanisms (turbulent and Brownian diffusion).

On the basis of known dependences for fixed size particle velocity deposition and resuspension the dynamic model has been developed, allowing to calculate combine action of turbulent particle deposition and resuspension for arbitrary size distribution and taking into account multilayered deposition character.
The comparison between theoretic and experimental results, concerning solid aerosol deposition, has shown, that, unlike a case of liquid particles, it is essentially necessary to consider combine action of deposition and resuspension processes.
Comparison of experimental and numerical results showed that the aerosol surface density, calculated without taking into account resuspension process, exceeds the corresponding experimental data approximately on the one order of magnitude. Calculation results with use of combine model of deposition and resuspension satisfactory agree with the experiment (see picture below).

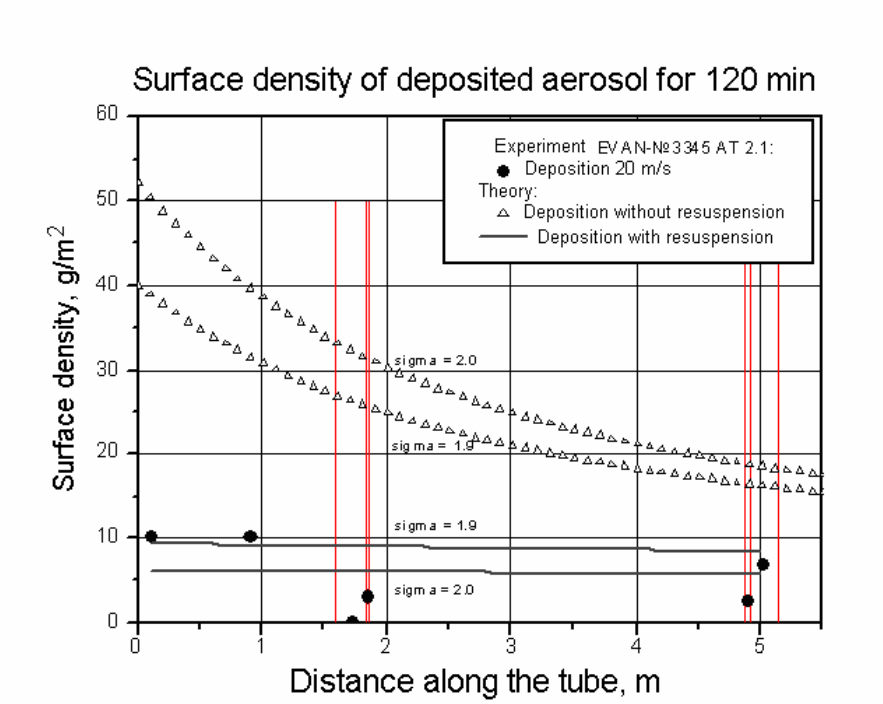

Fig. 19

The 3D code for calculation of incompressible turbulent flows based on LES model with particles moving under action of drag force, lift force and Brownian force has been developed.
Comparison numerical results with experimental data shows satisfactory agreement and confirm code ability to calculate turbulent flows with particles in channels for rather high Reynolds.
Next picture demonstrates numerical field with particles moving in turbulent flow (color flood is the vertical velocity component).

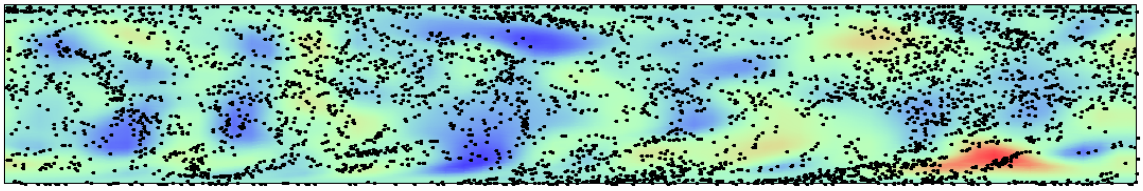

Fig. 20

Our calculations showed also that the developed dynamical particle model witn hydrodynamic code give good agreement with other LES calculation as well as with theoretic formulae (presented above).
Essential influence of lift and Brownian forces has been shown (see picture below).

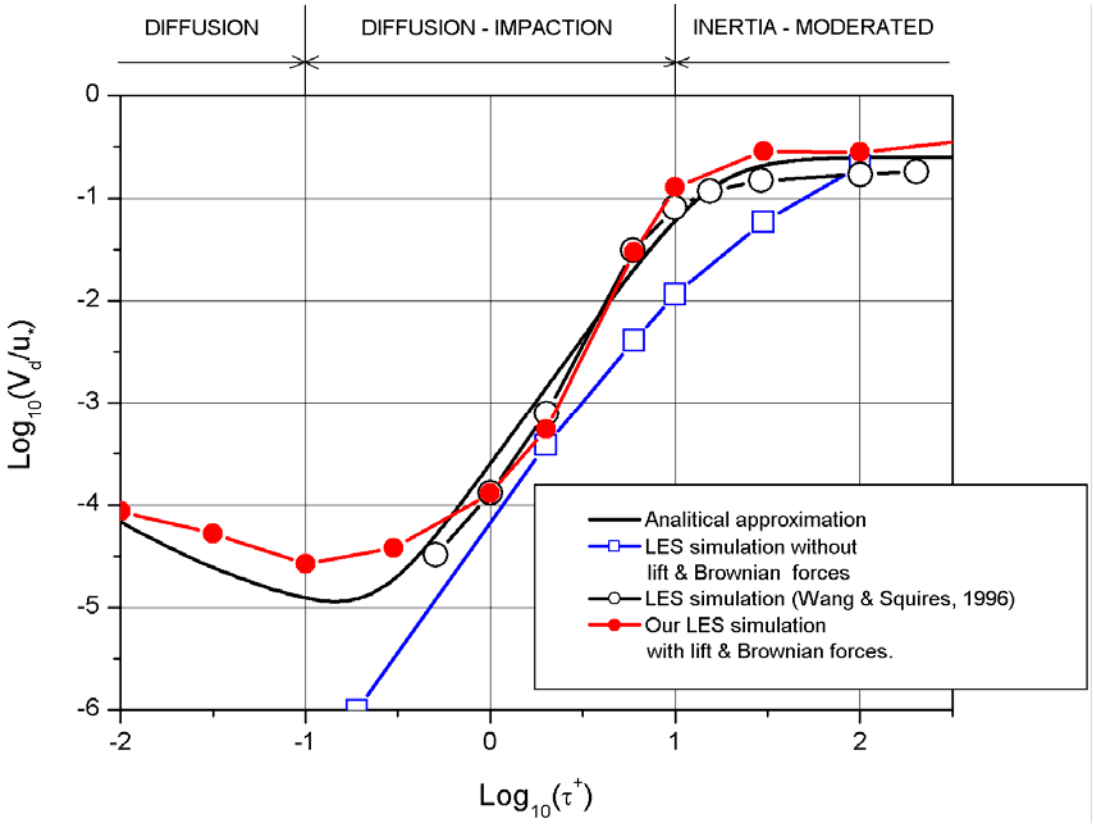

Fig. 21

Unfortunately, due to small time step (10^{-5} s) caused by strong grid stretching near the wall total number of time iterations required for achievement of stationary turbulence may reach one million and such calculation may take time about a month on PC P4 3 GHz. Parallel supercomputers appears to be attractive for such calculations.

Personnel Commitments

Name	Category	Days
Bezlepkin Vladimir	1	**68**
Zatevakhin Mikhail	1	**59**
Blinova Lidia	1	**14**
Leontyev Yury	2	**29**
Semashko Sergey	2	**55**
Ivkov Igor	2	**45**
Frolov Andrey	2	**0**
Astafyeva Vera	2	**60**
Lebedev Leonid	2	**25**
Ryabova Anastasia	2	**0**
Ignatyev Alexey	2	**30**
Potapov Igor	2	**62**
Sidorov Valery	2	**63**
Alexeev Sergey	2	**40**
Krylov Yury	2	**42**
Fomina Yulia	3	**17**
Buzharov Nikolay	4	**4**
Azaryeva Nadezda	3	**40**
Kiselev Arkady	1	**27**
Vasilyev Alexandr	1	**30**
Filippov Alexandr	1	**21**

Name	Category	Days
Kobelev Gennady	1	**25**
Zaichik Leonid	2	**66**
Tkachenko Alexandr	2	**0**
Alipchenkov Vladimir	2	**143**
Zagryazkin Valery	1	**0**
Mosunova Anastsia	2	**14**
Stepnov Vladimir	2	**27**
Tomashchik Dmitry	2	**32**
Tarasov Oleg	2	**22**
Karyukina Tatyana	3	**50**

Task 6: (description) Experimental investigation of containment parameters impact on volatile iodine species content and correlation

Subtask 6.1.: (description) Complection and adaptation of experimental installations, analytical methods perfection

1. State / Situation at the beginning of the project duration

At the beginning of project duration there are inspected in according with passed work plan: the readiness of gamma-radiation facility; the necessity manufacture of needle valves and special ampoules for the experiments at temperature 150^{o}C and so the device for ampoules heating under irradiation.

2. Fulfilled work

In course of first stage there are developed the following works on Task 6.

2.50 The repairs works were performed on gamma-facility RChM-γ-20; facility was prepared for experiments carrying out.

2.51 The rough-drafts were worked out and thermostat was manufactured for maintenance of ampoules assigned temperature under irradiation.

2.52 Set of components was prepared for the experiments performance: steel ampoules with inlet and outlet pipes and locked armature; the needle valves and other.

2.53 Procedure of experiments performance under irradiation was worked out including following stages:

- introduction into ampoule the appointed volume of boric acid solution containing assigned concentration CsI and pH; the measuring of pH, E_h initial values;
- in course of the carrying out of blank-test(I6-B1) in argon atmosphere the ampoule contents is blowing by argon(after FeOOH introduction into ampoule there is performing repeated blowing by argon);
- weighed sludge sample is introduced, in a 5 min pH и E_h is determinate in a solution sample; ampoule is shake, hermetically close, place in thermostat, heating up to assigned temperature and γ-irradiated ;
- irradiated ampoule is extracted and after 30-40 min gas phase and then water phase are sampling.
- water phase samples are analyzed on I_2, $I^-(I_3^-)$, IO_3^- content, pH и E_h are determinate; gas phase samples are analyzed on I_2 and other volatile iodine forms.

2.54 Apparatus calibrating method for chemical iodine forms determination by measuring ionic mobility specrometry is on finishing stage .

2.55 2 ferric hydroxides sludge types are synthesized: by deposition ferric hydroxide from $FeCl_3$ or $Fe(NO_3)_3$ solution. Hydroxides is washed by water up to neutral reaction, some their characteristics are determinate: Fe^{2+}, Fe^{3+}-ions concentrations in aqueous solution in presence of FeOOH, sizes of weighing particles.

2.56 For performing of on-line iodide-ions concentration method of determination with iodine-selective electrode there are researched pH, E_h, Fe^{3+}-ions, I_2, boric acid, Fe-hydroxide influence on reproducible indicates of iodide-selective electrode in range iodide-ions concentrations in

water 10^{-6}-10^{-3} mol/dm^3 . There are ascertained that I_2 influence on electrode potential is registries at concentration $I_2 \geq 10^{-5}$ mol/dm^3 on 10^{-4}-10^{-3} mol/dm^3 KI in the absence of other admixture. There is determinate pH influence - with changing pH from 4 to 7 potential is changing on 25 mV. In the presence of Fe^{3+}-ions (10^{-5}-10^{-4} mol/dm^3) potential is changing on ~10 mV. Introduction into KI solution ferric hydroxide is caused of pH increase from 5 to 8, in the boric acid presence – from 5 to 6.

3. Results by the end of the project duration

To the end of subtask 6.1 duration experiments EVAN-I6 were prepared technical on 65%.

Subtask 6.2.: (description) Finishing of analytical methods perfection. Synthesis and characteristics of sludge's. Initial tests fulfillment.

1. State / Situation at the beginning of the project duration

At the beginning of 2^d stage γ-irradiation facility was prepared to work. Ampoules and device for the assigned temperature maintenance under irradiation were prepared. Procedure of the experiments carrying out was fulfilled. FeOOH sludge's were prepared, analytical methodic were perfected partly.

2. Fulfilled work

2.57 Two set of the dehydrating ferric hydroxide sludge were prepared; its characteristics were determinate with perfected method (Table 26).

Table 26. Characteristics of ferric hydroxides sludge's samples

Sample	Summary Fe content in sludge, mass.%	Concentration of soluble forms Fe(II), Fe(III) in water, mol/dm^3	Sludge solubility in 1% H_3BO_3 solution, mol/dm^3		Specific surface, m^2/g	Particle size, mass.%
			Soluble forms	Dispersed forms		
Ferric gel	64.9 (FeOOH+ admixture of FeO)	Fe(II) $1.7\cdot10^{-6}$ Fe(III)$\leq 3\cdot10^{-7}$ disper.$\leq 4.5\cdot10^{-6}$	$<1.2\cdot10^{-6}$ <66 μg/dm^3	$8\cdot10^{-6}$ 450 μg/dm^3	-	-
FeOOH	64.0 (95%FeOOH +6.15%Fe_2O_3)	Fe(II) $3.3\cdot10^{-6}$ Fe(III) $4.3\cdot10^{-6}$ disper. $1.25\cdot10^{-5}$	$1.2\cdot10^{-6}$ 66.7 μg/dm^3	$7\cdot10^{-6}$ 392 μg/dm^3	96.4	>10μ - 80-88 1-10 μ - 6-8 <1 μ ~ 12 ≤0.15 μ -<1

FeOOH samples pass on for experiments carrying out.. Silica acid gel was prepared.

2.58 The following analytical methods were perfected for determination of iodine forms content in aqueous and steam-gas phases:

2.58.1 Methods of chromatography, titrimetry with oxidation of I^- to I^+, kinetics methods determination of iodide micro quantitatives and method with using of selective iodine electrode were perfected for the determination of I^- and IO_3^- -ions in water phase.

- Chromatography method perfection was indicated that iodate and iodide-ions are well dividing and have acceptable times of keeping on column Transgenomic AN2 SC. Sensitivity of iodate- and iodide-ions determination about 20-30 μg/dm^3 was achieved on column Transgenomic AN2 SC with alkaline eluent. Interval of iodide- and iodate-ions concentrations determinates by this method – from 20 μg/dm^3 to 5-10 mg/dm^3.
- Iodide-ion determination by KIO_3 titration with oxidation I^- to I^+ is used within range of iodide-ion content in sample from 200-300 mg to 1 mg. Method is selective in chloride-ions presence.
- Iodide-ions determination in boric acid solution with use of iodide-selective electrode may be fulfill within concentration interval 10^{-1}- 10^{-7} mol/dm^3 (12.7 g/dm^3 – 12.7 μg/dm^3). Method sensitivity – $0.5\cdot10^{-7}$ mol/dm^3, but impurities presence is influence

appreciably on determination precision. Therefore this method was recommended for measurements on-line with periodical control by other methods of analyze.

- Kinetic method of iodide-ion micro quantitative determination consist in determination of ferrorodanide complex decoloration rate during its oxidation by nitrite-ion, catalyzed by iodide-ions. Iodide-ions detection limit – 10^{-3} μg/cm^3. Decoloration is fixed photometry. Iodide determinate concentrations interval – 0.06-0.1 μg/cm^3. Method is demanded of fresh reagents solutions and daily calibration.

2.58.2 For determination of volatile iodine forms content in gas phase sampling is carried out on filter-adsorbents. Carbon-fibrous material (CFM) is used as absorbing filtering material. Conditions of I_2 absorbtion by this material were perfected in static and dynamic conditions. Iodine absorbtion in static conditions achieves 85-100% (~ 10 mg I_2 on 1 sm^2). In dynamic conditions ≥ 85-95% I_2 is absorbing from gas and steam-gas phase provided that rate of gas flow ensures the time of contact with CFM ≥ 1-2c. I_2 desorption from CFM by n-buthanol, KOH solution with hydroxylamine extracts ≤ 35-45% iodine. Twofold iodine desorption by 15% solution KOH at 80-90^{0}C during 0.5 h extracts 91-100% iodine. Iodine content in solution are determinate by methods stated in p. 2.58.1. Iodine gaseous forms are analyzed by method spectrometry of ions mobility.

2.59 Initial experimental tests fulfillment according experiments matrix.

Following tests are carrying out: I6-2 (150^{0}C), I6-5 (impact of H_2SiO_3 presence, 25^{0}C).

Table 27. Experiments matrix on Task 6, project EVAN-3345. Phase 1.

Test	Experiment goal	Specification	Analysis	Period
I6-2	Determination impact of γ-irradiation, FeOOH sludge presence, temperature on iodine volatility	Medium – aqueous solution 10g/dm^3 H_3BO_3, pH=5, I^-ion concentration-10^{-4}-10^{-5} M, temperature 150^{0}C, dose rate ~ 1 κGy/h, sludge mass 0-1 g/dm^3, gas atmosphere - air	pH, E_h, iodide, iodate, ferrum concentrations in water phase, I_2 in gas phase.	2-4 quart.
I6-5	Determination iodide-ion sorption by sludge and sludge components depending on composition and parameters of water phase	Medium – aqueous solution 10g/dm^3 H_3BO_3, pH=4-5, I^-ion concentration - 10^{-4}M, temperature 25^{0}C, sludge mass H_2SiO_3 -0-0.1 g/dm^3, gas atmosphere - air	pH, E_h, , iodide, iodate, concentrations in water phase	2-4 quart.

Initial experiments parameters are given in Table 28, medium parameters and data of aqueous and gas phase analysis at experiments finishing are given in Table 29.

Table 28. Initial parameters of tests I6-2 и I6-5.

№ test	CsI concentration, mol/dm^3 (mg/dm^3)	Solution volume, cm^3	pH	E_h, mV	Dose rate, κGy/h	Irradiation time	T, ^{0}C	Gas volume, cm^3
I6-2-1	$0.8\cdot10^{-5}$ (1.016)	100	5.49	+490	-	-	149±4	260
I6-2-2	$0.9\cdot10^{-4}$ (11.43)	100	5.53	+368	0.924	2h 09min	149±4	260
I6-2-3	$0.9\cdot10^{-4}$ (11.43)	100	4.88	+367	0.924	2h 09min	149±4	260
I6-5-1	$0.8\cdot10^{-5}$ (1.016)	200	4.87	+490	-	-	22±2	-

Table 29. Solution parameters and iodine content in gas phase at experiment finishing

№ test	Solution volume, cm^3	Water solution parameters				Iodine content in gas phase, μg			
		pH	E_h, mV	C_I,mg/dm^3	C_{Fe},mg/dm^3	1^t filter	2^d filter	Washing out+KOH*	Total
I6-2-	90	5.66	+466	1.016	-	4,1	2,9	-	7

1									
I6-2-2	40	5.63	+368	2.67	24	66±13	858±172	275	1200
I6-2-3**	43	3.83	+363	7.40	-	9	6	6	21
I6-5-1	200	4.79	-	1.3	-	-	-	-	-

* Washing out from filter system walls
** 0.1 g FeOOH was lead into solution before experiment

Steam and condensate leakage from ampoule and filtering system was observed in tests under irradiation at 150 ^{0}C. Collected condensate had the following parameters: volume – 57 cm^3, pH=3.9; E_h=+358 mV; iodide content – 4.4 μg; content of iron– 2.52 mg (44.2 mg/dm^3). In solution rest after test ferric hydroxide precipitation was present. These data are indicated on high velocity corrosion of stainless steel in experiment conditions. On the preliminary assessment corrosion velocity equal 80-90 mg/m^2·κGy.h. In test I6-2-2 iodine yield into steam-gas phase is achieved ~10%. Balance of iodine amount introduced and observed was achieved within the limit of 20% error. In test I6-2-3, in which 0.1 g FeOOH was present in solution, volatile iodine forms yield is reducing appreciable – up to 1-2%, steel corrosion is reducing too. Obtained results are for the present qualitative assessment of observed processes.

Silica acid gel isn't adsorbed iodide-ion from boric acid solution at room temperature.

3. Results by the end of the project duration

Methodic of iodine forms analysis were perfected for water and gas phases. Tests carrying out are started according to experiments matrix. High corrosion rate of stainless steel under irradiation at 150^{0}C was discovered. Correction of parameters some tests is necessary in experiments matrix.

Subtask 6.3.: (description) Tests fulfillment in according with tests matrix

1. State / Situation at the beginning of the project duration

At the start of 3^d quarter there were prepared γ-irradiation facility, ampoules and device for the assigned temperature maintenance, so autoclave and sampling device. Procedure of tests fulfillment was perfected. FeOOH sludge's were prepared, analytical methodic of iodine forms determination in aqueous and gaseous phases were perfected. Tests fulfillment are began.

2. Fulfilled work

2.60 The following analytical methods were perfected for determination of iodine forms content in aqueous phases: method of ionic chromatography, kinetic method determination of iodide micro quantitatives and method with using of selective iodide electrode. For determination of volatile iodine forms content in gas phase following methods were perfected: spectrometry of ionic mobility (in air); iodine forms trapping from steam-gas phase by carbon fibrous filter-adsorbent and iodine desorption from adsorbent by hot alkaline solution, then iodine content in alkaline solution is determinate with kinetic method. Procedure of steam-gas sampling on the ending of test for volatile iodine forms content analysis was corrected.

2.61 Experimental tests fulfillment according with experiments matrix.
Experimental results at temperature 150 ^{0}C carrying out during 2 quarter are shown necessity of water solution starting parameters correction to receive of more simple and reliable data. It is supposed for this test following conditions: pH=6-7; iodide-ions concentrations - 10^{-5} mol/dm^3; temperature 120 ^{0}C (test I6-2).
In course of 3^d quarter following tests are carrying out: I6-2-2,3 (120^{0}C), I6-2-1 (20 ^{0}C), I6-1, I6-b1, I6-B2, partly I6-4, I6-5 according with experiments matrix on Task 6.

Table 30. Experiments matrix on Task 6, project EVAN-3345. Phase 1.

Test	Experiment goal	Specification	Analysis	Period

Test	Experiment goal	Specification	Analysis	Period
I6-B1, I6-B2	Determination impact of γ-irradiation on adsorption by sludge and iodine volatility in atmosphere of argon and air	Medium – aqueous solution 10g/dm^3 H_3BO_3, pH=5, I^-ion concentration-10^{-4}-10^{-5} mol/dm^3, temperature 50-60^{0}C, sludge mass 0-1 g/dm^3, gas atmosphere -argon, air	pH, E_h, iodide, iodate, concentrations in water phase, I_2 in gas phase.	2-4 quart.
I6-1,2	Determination iodide-ion sorption by sludge FeOOH depending on pH, iodide concentration in water phase, temperature	Medium – aqueous solution 10g/dm^3 H_3BO_3, pH=4-8, I^-ion concentration -10^{-5}-10^{-4}mol/dm^3, temperature 25-120^{0}C, sludge mass 0-1 g/dm^3, gas atmosphere - air, dose rate ~1 kGy/h	pH, E_h, , iodide, iodate, iron concentrations in water phase, I_2 in gas phase	2-4 quart.
I6-4	Determination iodide-ion sorption by sludge FeOOH depending on iodine form in water medium, temperature, pH (without radiation). Comparison of ampoule and autoclave tests	Medium – aqueous solution 10g/dm^3 H_3BO_3, pH=5-8,I^-ion-concentration-10^{-5}-10^{-4}mol/dm^3, temperature 50-120^{0}C, sludge mass 0-1g/dm^3, gas atmosphere - air.	pH, E_h, , iodide, iodate, iron concentrations in water phase, I_2 in gas phase	2-4 quart.
I6-5	Determination iodide-ion sorption by sludge FeOOH and sludge's components and iodine volatility depending on composition and parameters of water medium	Medium – aqueous solution 10g/dm^3 H_3BO_3, pH=4-8, I^-ion-concentration-10^{-5}-10^{-4}mol/dm^3, temperature 25-120^{0}C, sludge mass 0-2g/dm^3, gas atmosphere - air.	pH, E_h, , iodide, iodate, iron concentrations in water phase, I_2 in gas phase	2-4 quart.

Initial experiments parameters are given in Table 31, medium parameters and data of aqueous and gas phase analysis at experiments finishing are given in Table 32.

Table 31. Initial parameters of tests I6-2 и I6-5.

№ test	CsI concentration, mol/dm^3 (mg/dm^3)	Solution/gas phase volumes, cm^3	pH	E_h, mV	Total dose, кGy	Sludge mass, g/dm^3	T, ^{0}C	Gas atmosphere
I6-B-1,2-1	$1.2\cdot10^{-4}$ (15.14)	25/50	4.91	+446	3	1	60	Argon
I6-B-1,2-2	$1.2\cdot10^{-4}$ (15.14)	25/50	4.93	+446	3	-	60	Argon
I6-B-1,2-3	$1.2\cdot10^{-4}$ (15.14)	25/50	4.89	+442	3	**1**	60	Air
I6-1	$1.2\cdot10^{-4}$ (15.14)	25/50	4.94	+446	3	-	60	Air -
I6-2-1	$1.2\cdot10^{-4}$ (15.14)	25/50	4.92	+446	3	1	20±2	Air
I6-2-2	2.10^{-5} (2.54)	100/260	6.20	+562	2	-	120±4	Air
I6-2-3	2.10^{-5} (2.54)	100/260	6.45	+558	2	1	120±4	Air

Table 32. Solution parameters and iodine content in gas phase at the ending of experiment

№ test	Water solution parameters				Iodine content in gas phase,			
	pH	E_h, mV	C_I,mg/dm^3	Time of test, h	I_2 mass,* μg(ppb)	Iodine concentr., mol/dm^3 (μg/dm^3)	Iodine yield,%	Iodine partition coefficient
I6-B-1,2-1	4.80	+650	12.08	4	0.0565(100)	$4.4.10^{-9}$ (1.13)	0.017	$1.2.10^4$
I6-B-	4.89	+630	12.24	4	0.085 (150)	$6.58.10^{-9}$	0.0255	$8.1.10^3$

1,2-2						(1.7)		
I6-B-2-3	4.84	+660	12.60	4	0.102 (180)	$8.0.10^{-9}$ (2.04)	0.0307	$6.5.10^{3}$
I6-1	4.81	+650	13.30	4	0.113 (200)	$8.9.10^{-9}$ (2.26)	0.0356	$5.6.10^{3}$
I6-2-1	4.86	+610	12.00	4	0.017 (30)	$1.3.10^{-9}$ (0.34)	0.0050	$4.0.10^{4}$
I6-2-2	5.35	+475	2.47	2	12.55	$1.9.10^{-7}$ (48.27)	4.94	51.3
I6-2-3	5.65	+513	2.16	2	5.62	$8.5.10^{-8}$ (21.62)	2.21	100

* Total mass of volatile iodine forms trapping on 2 filters, and walls of filter-holding.

On the whole in the presence of ferric hydroxide sludge's volatile iodine forms yield into gas phase is reduced on 10-55% depending on gas atmosphere, temperature, iodide-ion concentration in water phase and water quality (the level and type impurities containing in it). In inert atmosphere (argon) volatile iodine compounds yield is below than in air atmosphere in 1.3-1.8 times. Temperature decrease from 60 to 20 ^{0}C under irradiation in the presence of sludge is lead to decrease of iodine volatility in 6 time. Increase of volatile iodine forms release in 10-20 time at temperature increase from 60 to 120 ^{0}C can be connect not only with temperature rise but and with influence of quality used water. So in tests at 60 ^{0}C water refined for ionic chromatography with electro conductivity 0.1 μSm/sm was used, and at 120 ^{0}C – deionized water with conductivity 0.45-0.60 μSm/sm. Besides it is known that reduction in 10 times of iodide-ion concentration in irradiated water solutions reduced noticeable total iodine partition coefficience between phases.

Essential influence of temperature on iodine volatility, specially in the presence of FeOOH sludge, is stipulated by decrease of molecular iodine partition coefficient with temperature rise. It is shown on possibility intensifining of chemical interaction of ionic iodine forms (possible and molecular iodine) in water medium with ferric hydroxide.

Chromatographic analysis of water for chromatography and deionized water was ascertained the presence in water set of inorganic and organic anions. So in water for chromatography anions content (μg/dm^{3}) is on the average: fluoride – 5; chloride – 20; nitrate – 25; sulphate – 18; so acetate is presences. In water solution after irradiation content of fluorides and nitrates is raised ~ in 10 times, chlorides – in 2 times. In deionized water the level of inorganic anions content is more in 5-8 times, organic anions – in 10 times. The presence of impurities specially organic origin lead to iodine volatility rise because iodide-ions oxidation increase and formation of iodine organic compounds.

3. Results by the end of the project duration

Method of iodine forms analysis were perfected for water and gas phases. Set of tests was carried out according to experiments matrix. It is discovered the influence temperature, sludge's of ferric hydroxide presence and water quality on iodine volatility.

Subtask 6.4 (description): Experimental tests fulfillment. Preparation of Reports.

1. State / Situation at the beginning of the project duration

At the beginning of 4^{h} quarter there were prepared and approved apparatus, and procedure was perfected for the experiments fulfillment. Analytical methods of determination of iodine forms in water and gas phases were perfected. The sludge's of ferric hydroxide were prepared. Tests was fulfilled partly.

2. Fulfilled work

2.62 50 tests have been fulfilled in according with experiments matrix. Generalized results of experimental investigation of iodide hydrothermal oxidation as function of temperature, pH, the presence of sludge are presented in Table 33.

Table 33 Iodide thermal oxidation in water medium with volatile iodine species formation

T, °C	pH	$[I^-]_{aq} \cdot 10^4$ (init.) mol/dm^3	Iodine yield In gas phase, % (5h/24h)	$[I_2]_g \cdot 10^7$ mol/dm^3 (5h/24h)	Iodine PC (5h/24h)	Note
30	4.9	1.2	0.17/0.55	0.7/2.2	870/270	
30	4.8	0.95	0.38/0.65	1.3/2.2	370/210	1 g/dm^3 FeOOH
60	4.8-5.1	1.1	0.45/0.26	1.9/1.0	285/480	
60	4.8	1.25	0.10/0.23	0.5/1.0	1300/540	1 g/dm^3 FeOOH
60	4.8	1.0	0.12/<0.09	0.37/<0.3	1200/$\geq 3.10^3$	2 g/dm^3 FeOOH
60	5.2	1.6 I^- + 0.1 I_2	0.97/0.30	7.0/2.2	120/400	
60	4.8	1.45 I^- + 0.124 I_2	0.82/0.38	4.6/2.2	180/400	1 g/dm^3 FeOOH
60	6.8	1.15	<0.09/0.09	- /0.40	$\geq 3.10^3$/1300	
60	6.7	1.1	0.12/0.66	0.44/2.4	1200/220	1 g/dm^3 FeOOH
90	4.8	1.3	0.34/0.52	1.5/2.2	450/290	
90	4.8	1.1	1.65/0.76	5.5/2.65	89/177	1 g/dm^3 FeOOH
90	6.8	1.1	0.37/0.40	1.6/1.8	340/300	
90	6.85	1.0	1.10/0.52	3.8/1.8	130/280	1 g/dm^3 FeOOH

At iodide ion thermal oxidation in solution with concentration 10^{-4} mol/dm^3 and pH 5 (in the presence of boric acid, 10g/dm^3) the formation of volatile iodine compounds is observed with yield in gas phase 0.1-1.7% iodine at 30-90 °C. Iodine release is the greatest in time interval 2-5 h and it is decreased to 24 h exposition (in the presence of FeOOH and in its absence).

The raise of pH from 5 to 7 is decreased iodine volatility in 1.5-2 times. At temperature increase from 60 to 90 °C volatile iodine forms release is raised in 2-3 times. Iodine partition coefficients (PC) in these conditions are within the bounds 200-1300. At introduction into iodide solution 10-15 mass..% I_2 in 5 h of exposition 0.8-1% of introduced iodine is transferred in gas phase, then iodine release is decreased, striving for the stationary magnitude. Molecular iodine is not extracted from solution after experiment finishing. It is supposed, that iodine hydrolyze is the main cause of its release lowering.

In the presence of sludge FeOOH in solution with pH 5 at 60° short lowering of volatile iodine forms yield is observed; mass FeOOH increase in 2 times is lead to stable in the time lowering of iodine release up to level its concentration less the limit of determination. The temperature rise to 90° and pH to 7 in the presence sludge FeOOH it is lead to volatile iodine forms release increase in 2-5 times that is result of iodide oxidation.

At decrease of iodide concentration to 10^{-5} mol/dm^3 volatile iodine forms yield is raised to 7-11%, increase of iodide concentration to 10^{-3} mol/dm^3 is decreased of iodine yield to 0.04-0.14%.

The impact of water quality (salts content, electric conductivity and other) on iodide thermal oxidation and iodine release in gas phase has been researched and shown that probable catalizators of thermal oxidation are the impurities of chlorides and organic matter. It is discovered the presence in deionized water 30-100 μg/l alkyl chlorides which can be the source alkyl iodides owing to substitution of chloride by iodide.

2.63 At irradiation of iodide solution in stainless steel ampoule I_2 yield in gas phase at 60-95 °C is lower on the one order of magnitude in the comparison with iodide thermal oxidation, the PC magnitudes are higher on 1-2 order of magnitude (Table 34).

Table 34 Volatile iodine species formation at iodide irradiation in solution of boric acid

№	T, °C	pH	$[I^-]_{aq} \cdot 10^4$ (init.) mol/dm^3	Iodine yield in gas phase, %	$[I_2]_g \cdot 10^7$ mol/dm^3	Iodine PC	Note
1-2*	60	4.9	1.2	0.015	0.045	$1.3 \cdot 10^4$	Argon atmosphere, with FeOOH and without it
3*	60	4.9	1.2	0.03	0.09	$5.7 \cdot 10^3$	Air

4*	60	4.9	1.2	0.027	0·08	$6{\cdot}4{\cdot}10^3$	Air; 1 g/dm^3 FeOOH
5*	60	4.9	1.2	l.l.d.	l.l.d.	$\geq 8{\cdot}10^4$	Irradiation 15 h, air
6*	60	4.9	1.65	l.l.d.	l.l.d.	$\geq 8{\cdot}10^4$	Irradiation 15 h, air, 1 g/dm^3 FeOOH
7*	95	4.9	1.2	0.15	0.45	$1.3{\cdot}10^3$	Air
8*	95	4.9	1.2	0.015	0.045	$1.3{\cdot}10^4$	Air; 1 g/dm^3 FeOOH
9*	18	4.9	1.2	0.0045	0.014	$4.4{\cdot}10^4$	Air; 1 g/dm^3 FeOOH
10**	120	5.5	0.145	13.0	3.3	28	Air
11**	120	5.65	0.11	7.6	1.5	53	Air; 1 g/dm^3 FeOOH
12**	120	6.4	0.115	8.4	1.9	34	Air; without irradiation
13**	150	5.5	0.09	~ 90	160	2.3	Air
14**	150	4.9	0.09	2.1	3.6	103	Air; 1 g/dm^3 FeOOH

* Experiments - 4 h, dose rate 0,928 kGy/h, volume of autoclave 75 cm^3;
** Experiments - 2 h, dose rate 0,98 kGy/h, volume of autoclave 360 cm^3;
l.l.d. - lower the limit of determination.

With the temperature raise iodine release is increased in 5-100 times. In the presence of sludge FeOOH iodine release at 60-120^o is decreased in 1,1-10 times. The essential raise of iodine release at 120-150^{o}C may be the result of the initial iodide concentration lowering on one order of magnitude, and so of the employment of different methods of gas phase sampling and I_2 content analysis. It appeared that at analysis by IMS method it was probable the appreciable iodine loss, therefore the obtained results are understated in principal. Methyliodide (CH_3I) in gas phase was not discovered.

At temperature higher 100 ^{o}C the rates of iodide thermal and radiolytical oxidation are compared. Under prolonged irradiation (15 h) and/or temperature raise to 150^{o}C it is probable the incidents with sharp lowering of iodide concentration in water phase, the increase of iodine release and autoclave surfaces corrosion; in addition it is impossible to eliminate of probability of gas medium leakage.

The lack of co-ordination of I_2 yield magnitudes in gas phase and iodine PC at iodide thermal and radiolytical oxidation may be the result of different content of chlorides, alkyl chlorides and organic matter in used water, increasing under irradiation, and the probability of I_2 loss from gas phase at the ampoule cooling after experiment, sampling and analysis by IMS method.

3. Results by the end of the project duration

It was been fulfilled more 50 experiments in according to matrix of experiments on task 6.

It was been ascertained that the extent of sludge ferric hydroxide, FeOOH, impact on iodine volatility is depended from solution pH and medium temperature. It is probable two processes: the reverse adsorption on FeOOH and slow, probably heterogeneous, iodide ions oxidation; in thermal experiments at 30-90^{o}C both processes are occurred, under irradiation – adsorption is predominated: volatile iodine forms release in the presence of FeOOH at 60^{o}C is decreased on 10%, with temperature raise to 95-120^{o}C iodine release is decreased in 2-10 times. It is supposed that it is occurred the chemical interaction of iodide-ion with ferric hydroxide.

Personnel Commitments

Name	Category	Days
Kritsky Vladimir	1	**58**
Ampelogova Natalia	1	**133**
Korchomkina Irina	1	**60**
Chetverikov Viktor	1	**156**
Epimakhov Vitali	1	**74**
Matsaev Vladimir	1	**85**
Pankina Elena	1	**82**
Korablev Nicolai	1	**88**
Leontiev Gennadi	1	**38**
Alemaskina Elena	2	**33.5**

Bashilov Sergei	2	**105**
Yudin Igor	2	**113**
Epimakhov Timofey	3	**54**
Surkova Marina	3	**70**

Task 7.: (description) Numerical and theoretical modeling of containment parameters impact on volatile iodine species content and correlation

Subtask 7.1.: (description) Analysis and adaptation of iodine model, selection of parameters and processes constants

1. State / Situation at the beginning of the project duration

At the beginning of the project in according with Work Plan there were proposed the parameters of iodine model adaptation to experimental matrix and experiments conditions, accepting in task 6 of project EVAN.

2. Fulfilled work

During of the first stage of project the following works have been fulfilled on Task 7.

2.64 For iodine model adaptation to experiments conditions according experiments matrix on Task 6 of project EVAN the following conditions have been accepted: the experiments are carried out in static equilibrical conditions at iodide concentration in water phase 10^{-5} and 10^{-7} mol/dm^3; temperature 25, 50 and 100^{o}C; pH = 4; 6,5; 8; dose rate of γ-radiation 1,0 kGy/h; adsorbent (FeOOH) concentration - 0 and 1-2,5 g/dm^3.

2.65 It is accepted, that the equilibrium is achieved in 30-40 min.; adsorption is not depended from temperature; CH_3I is not formatted. Adsorption of I^--ion on FeOOH in according with data published in the literature is presented in Table 35.

Table 35. Iodide ion adsorption on FeOOH, % mas.

I^--ion concentration in water solution, mol/dm^3	**pH**		
	4	**6-7**	**8**
10^{-5}	70	60	15
10^{-7}	80-90	80-90	25

2.66 Iodine model adaptation was carried out to conditions, accepted in p. 2.1, 2.2. The magnitudes of the rate and equilibrium constants have been selected for describing of processes radiolytical oxidation $2I^- \rightarrow I_2$ in water, I^--ion adsorption on FeOOH and I_2 partition between water and gas phases. The verification of adapted iodine model and calculating programme was carried out with published experimental data and the magnitudes of constants were corrected.

2.67 Pre-test calculations were fulfilled for the estimation of the presence of sludge FeOOH in water phase impact on volatile iodine species (I_2) content in gas phase according to experimental condition in matrix of experiments on Task 6. Calculations were fulfilled with the application on licensed Mat Lab Version 7.0.1 (Table 36).

Table 36. Results of pre-test calculations

I^--ion initial concentration in water phase, mol/dm^3	**pH**	**In the absence of sludge**		**In the presence of FeOOH, 2,5 g/dm^3**	
		I_2 release in gas phase, %	**I_2 partition coefficient between water and gas phases, KP_{I_2}**	**I_2 release in gas phase, %**	**I_2 partition coefficient between water and gas phases, KP_{I_2}**
10^{-5}	4	26→14*	3,85→5,7*	14→0,85	7,1→37,6

	6,5	8→8	12,5→7,9	11→1,50	9,1→33,3
	8	1,45→2,0	69→45	1,7→1,45	59→57
10^{-7}	4	6,2→1,35	16→74	4,0→0,5	25→96
	6,5	6,4→1,5	15,6→67	4,5→0,7	22→73,5
	8	6,3→1,5	16→67	5,0→1,1	20→72,7

* The first number – in 20 min., the second – in 10 h from experiment beginning.

2.68 The volatile iodine forms release in gas phase was higher at pH=4 and I^--ion concentration 10^{-5} mol/dm^3.In the presence of sludge I_2 yield in gas phase is reduced at pH=6 in 2,7-16 times; at pH=6,5 - in 2-5 times; at pH=8 - in 1,4 times.

3. Results by the end of the project duration

To the end of subtask fulfillment iodine model adaptation and pre-test calculations are prepared on 75%.

Subtask 7.2.: (description) Iodine model modification completing, fulfillment of pre-test and post-test calculations

1. State / Situation at the beginning of the project duration

At the beginning of second subtask duration iodine model was adapted according work plan to experiment conditions on Task 6. Pre-test calculations were carrying out on base of published data on iodide-ions sorption by hydroxides adsorbents.

2. Fulfilled work

2.69 Adaptation, addition and verification iodine model have been completed on the base of available experimental data on hydrolyse, radiolyse and sorption of various iodine forms in water solutions; the magnitudes of rate and equilibrium constants of iodine reactions made more precise.

2.70 Iodine model was supplemented the consideration of probable processes of iodine forms adsorption/desorption by stainless steel surfaces and hydroxide sorbents (corrosion product).

2.71 Additional mathematic analysis was carried out of included in iodine model processes of various iodine forms adsorption/desorption by stainless steel surfaces and hydroxide sludge's with the purpose make more precise the magnitudes of rate constants of processes.

2.72 Pre-test calculations, carried out in 1^t quarter, were corrected on results of additional mathematic analysis with use the more precise magnitudes of iodine forms adsorption/desorption constants.

2.73 Report was prepared on pre-test calculations results.

3. Results by the end of the project duration

Adaptation of iodine model and performance of pre-test calculations are fulfilled by the end of current subtask. But experimental results received at the end of second subtask are demanded of calculation and correction of rate constant processes of iodine interaction with stainless steel under irradiation at elevated temperature (100-150^{0}C) led to appreciable steel corrosion and appearance of ferric iodide and ferric hydroxide sludge's in solution.

Subtask 7.3.: (description) Iodine model correction, fulfillment of post-test calculations

- **1. Works state at the beginning of the current subtask duration** .

At the beginning of third subtask iodine model was adapted according work plan to experiment conditions on Task 6. Pre-test and post-test calculations were carrying out on base of published data about iodide-ions sorption on hydroxides adsorbents and experimental data obtained on Task 6.

2. Fulfilled work

2.74 It is formulated the task – calculation should be fulfilled kinetics of achievement of iodine equilibrical partition in system "water solution – atmosphere" in the condition of experimental tests on Task 6 project 3345.

2.75 For fulfillment of this task some parameters of adapted iodine model (α,κ,λ), selected in course of pretest calculation, were varied with goal maximal approximation calculation results to experimental tests data.

2.76 Calculations of iodine total content in water and gas phases and in hydroxide adsorbent were carried out in function of time. Comparison of experimental and calculated data was produced on time moment according the test completing (2 h.). Calculations were fulfilled for limited set of experiments. Calculations would be continued in 4 quarter according with accumulation of experimental data.

2.77 Comparison of calculation results with experimental results make it possible the following conclusions about the current version of developed iodine model:

- model yields contented results at calculation of total iodine concentration changing in water phase and understates the iodine total concentration in gas phase (in 10 to 10^3 times);
- model yields qualitative right assessment of influence γ-irradiation on iodine yield in gas phase in tests conditions (iodine concentration rise ~ in 10^3 time);
- calculated data make it possible the conclusion about insignificant changing of iodine yield in gas phase in the presence of ferric hydroxide adsorbent in water phase;
- parameters (α,κ,λ), induced in model for accounting iodine adsorption by hydroxide adsorbent, are distinguished from parameters used in pre-test calculations.

2.78 Iodine model is needed in additional perfection questions formation of volatile iodine compounds in water phase and its partition between water and gas phases.

2.79 Results of fulfilled work were stated into whole in report presented on EVAN ISTC Project Progress Meeting (St. Petersburg, September 9-10, 2007) and in Progress Report on Task 7.

3. Results by the end of the project duration

To the end of third subtask duration the preliminary post-test calculation were fulfilled. Comparison of calculated data with results of some experimental tests was carried out. It was shown that adaptation iodine model give qualitative right assessment of iodine behavior dynamics but understates iodine volatile forms concentration in gas phase. Iodine model is needed in additional perfection of description processes formation of volatile iodine compounds in water phase and its transference between water and gas phases.

Subtask 7.4: (description) Fulfillment of post-test calculations, updating of iodine model, reports preparation

1. State / Situation at the beginning of the project duration

At the beginning of 4-th subtask the iodine model is adapted for conditions of experiment. Pre-test calculations are fulfilled on the basis of the data published in the literature. The calculation program for the given version of the iodine module is developed. Verification of a calculation code by the experimental results received on a problem 6 present projects is partially carried out.

2. Fulfilled work

Results of the experiments on a problem 6 are used for verification of the developed calculation code (post-test calculations). Initial parameters of each experiment were entered into an input file of the program: volumes of liquid and gas phases, area surfaces of a water mirror and wall an autoclave; temperature; dose rate of γ-radiation; FeOOH-sludge mass in water solution; initial pH values and concentrations of components of water and gas phases; time of an irradiation.

Magnitudes of α, K_d, λ – parameters in model equations are accepted the same, as in corrected pre-test calculations.
A result of calculations are determined as time function: total concentration of all iodine forms in water and gas phases; iodine concentration on autoclave walls surface; iodide-ion concentration adsorbed on a mass unit of hydroxide sludge; iodine partition coefficient.
The received dependences for experiment number 5 are given on Fig. 22. Dependences for other experiments have a similar view.

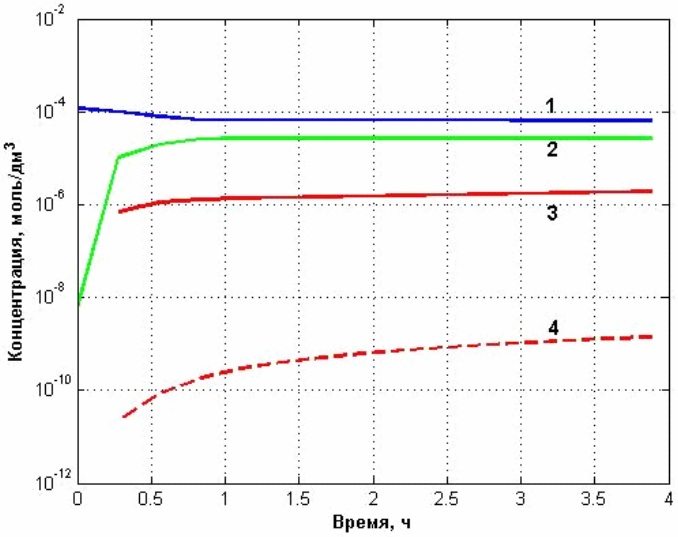

Fig. 22 - Total concentration iodine forms in experiment №5 (95 °C, at presence FeOOH):
1 - in water, 2 - in gas, 3 - on hydroxide sludge, 4 - on a wall

Calculated magnitudes were compared with the experimental data presented in Table 37. Results of comparison are given in columns 10 and 11.

Table 37. The release of volatile iodine forms in gas phase under irradiation (experiment and calculation)

№№ experi-ment	T°, C	Mass FeOOH g/dm³	pH (init.)	Dose rate , kGy/h	Time of experi-ment h	Concentration I^- - ion in water, mol/dm³		Final I_2-concentration in gas, mol/dm³	Iodine partition coefficient (PC)	
						initial	final		exp.	calc.
1	120	0	5,50	0,98	2,1	$1,45\cdot10^{-5}$	$1,26\cdot10^{-5}$	$3,3\cdot10^{-7}$	28	256
2	120	1,0	5,70	0,98	2,1	$1,13\cdot10^{-5}$	$1,02\cdot10^{-5}$	$1,5\cdot10^{-7}$	52,5	191
3	120	0	6,40	0	5,0	$1,15\cdot10^{-5}$	$1,05\cdot10^{-5}$	$1,9\cdot10^{-}7$	34	$5,2310^3$
4	95	0	4,95	0,928	4,0	$1,20\cdot10^{-4}$	$1,1410^{-4}$	$1,85\cdot10^{-6}$ $4,5\cdot10^{-8}$	32/ $1,3\cdot10^3$	103/ $8,5\cdot10^3$
5	95	1,0	5,00	0,928	4,0	$1,20\cdot10^{-4}$	$0,93\cdot10^{-4}$	$4,5\cdot10^{-9}$	$8/1,3\cdot10^4$	118/ $8,1\cdot10^3$
6	60	0	4,90	0,928	4,0	$1,20\cdot10^{-4}$	$1,02\cdot10^{-4}$	$4,2\cdot10^{-9}$ $9\cdot10^{-9}$	12/ $5,7\cdot10^3$	$22/3,3\cdot10^3$
7	60	1,0	4,90	0,928	4,0	$1,20\cdot10^{-4}$	$1,03\cdot10^{-4}$	$4,2\cdot10^{-6}$ $8,0\cdot10^{-9}$	13/ $6,4\cdot10^3$	20,6/ $2,8\cdot10^3$
8	60	0	4,90	0,928	15,0	$1,17\cdot10^{-4}$	$3,00\cdot10^{-5}$	$2,2\cdot10^{-5}$ $<9\cdot10^{-10}$	20/ $> 8\cdot10^4$	$1,8\cdot10^4$/ $1,8\cdot10^4$
9	60	1,0	5,00	0,928	15,0	$1,65\cdot10^{-4}$	$1,26\cdot10^{-4}$	$9,7\cdot10^{-6}$ $<9\cdot10^{-10}$	7,5/ $> 8\cdot10^4$	$3,5\cdot10^4$/ $3,5\cdot10^4$
10	60	1,0	5,0	0,928	10-12	$0,16\cdot10^{-4}$	$0,13\cdot10^{-4}$	$6\cdot10^{-7}$ $<9\cdot10^{-10}$	12/ $> 5\cdot10^4$	$666/1,8\cdot10^3$

11	60	2,5	5,0	0,928	10-12	$0{,}13\cdot10^{-4}$	$0{,}08\cdot10^{-4}$	$1{,}2\cdot10^{-6}$ <$9\cdot10^{-10}$	4,2/ > $5\cdot10^{4}$	537/$1\cdot10^{3}$

Calculated magnitudes of partition coefficient (PC) strongly differ among themselves depending on the moment of determination of iodine in gas phase. The calculated values given in numerator, are received for the moment of time corresponding the duration of experiment. The calculated magnitudes given in denominator, correspond to time of equilibrium iodine partition. The experimental magnitudes received under irradiation, unfortunately, are incommensureable. Short time of an exposition does not guarantee achievement of eqilibrium, and in prolonged experiments collateral processes are possible. I_2 concentration in gas was defined as a difference of concentration of I^-ion in water phase before and after experiment (1-st method)or after cooling an ampoule, by method of ions mobility spectrometry (IMS). The experimental values received on the first method (numerator) agree within the limits of the order of madnitude with calculated PC values at the moment of the end of experiment (excepting experiment # 3 in the absence of irradiation). The values received by IMS method (denominator) are closer to calculated equilibrium PC. According to calculation, equilibrium is reached only in experiments 8, 9.

Calculation predicts PC growth in absence of irradiation, but experimental magnitudes in the given series of experiments have not confirmed this because of data insufficiency. The second series of experiments is lead in the absence of an irradiation (Table 38).

Table 38- The release of volatile iodine forms in gas phase in the absence of irradiation (experiment and calculation)

№№ expe-ri-ment	T °, C	Mass FeOOH, g/dm^3	pH (init.)	Time expe-riment, h	Concentration I^--ion in water, mol/dm^3		Final I_2 concentration in gas, mol/dm^3	Iodine partition coefficient (PC)	
					initial	final.		exp.	calc.
1	30	0	4,85	24	$1{,}22\cdot10^{-4}$	$1{,}17\cdot10^{-4}$	$2{,}26\cdot10^{-7}$	270	320
2	30	0	6,25	5	$1{,}2\cdot10^{-4}$	$1{,}1\cdot10^{-4}$	$7{,}64\cdot10^{-8}$	760	319
3	30	0	7,24	24	$1{,}1\cdot10^{-5}$	$1{,}05\cdot10^{-5}$	$4{,}51\cdot0^{-8}$	115	515
4	60	0	4,83	24	$1{,}14\cdot10^{-4}$	$1{,}0510^{-4}$	$1{,}12\cdot10^{-7}$	470	321
5	60	1	4,83	5	$1{,}25\cdot10^{-4}$	$1{,}06\cdot10^{-4}$	$4{,}55\cdot10^{-8}$	$1{,}3\cdot10^{3}$	326
			4,83	24	$1{,}2510^{-4}$	$1{,}05\cdot10^{-4}$	$9{,}84\cdot10^{-8}$	540	326
6	60	0	5,08	24	$1{,}08\cdot10^{-4}$	$1{,}0\cdot1\cdot0^{-4}$	$1{,}02\cdot10^{-7}$	490	318
7	60	0	5,42	24	$1{,}61\cdot10^{-4}$	$1{,}535\cdot10^{-4}$	$2{,}08\cdot10^{-7}$	370	325
8	60	1	6,73	5	$1{,}1\cdot10^{-4}$	$1{,}06\cdot10^{-4}$	$4{,}38\cdot10^{-8}$	$1{,}23\cdot10^{3}$	252
			6,73	24	$1{,}1\cdot10^{-4}$	$1{,}05\cdot10^{-4}$	$2{,}4\cdot10^{-7}$	220	104
9	60	0	6,86	5	$1{,}3\cdot10^{-4}$		$1{,}2\cdot10^{-7}$	555	319
				24		$1{,}2\cdot10^{-4}$	$1{,}5\cdot10^{-7}$	445	319
10	60	0	7,10	5	$8{,}7\cdot10^{-4}$		$3{,}0\cdot10^{-7}$	$1{,}4\cdot10^{3}$	430
				24		$8{,}6\cdot10^{-4}$	$1{,}0\cdot10^{-7}$	$4{,}1\cdot10^{3}$	430
11	60	0	6,78	24	$1{,}15\cdot10^{-4}$	$1{,}08\cdot10^{-4}$	$4{,}3\cdot10^{-8}$	$1{,}34\cdot10^{3}$	373
12	90	0	4,79	5	$1{,}3\cdot10^{-4}$	$1{,}24\cdot10^{-4}$	$1{,}46\cdot10^{-7}$	445	325
13	90	0	6,82	5	$1{,}02\cdot10^{-4}$	$0{,}975\cdot10^{-4}$	$1{,}76\cdot10^{-7}$	277	404
14	90	0	6,77	24	$1{,}2\cdot10^{-4}$	$1{,}05\cdot10^{-4}$	$1{,}65\cdot10^{-7}$	296	607
15	90	0	7,80	5	$8{,}7\cdot10^{-4}$	$8{,}7\cdot10^{-4}$	$4{,}0\cdot10^{-7}$	$3{,}5\cdot10^{3}$	983

This series of experiments is carried out in an autoclave of teflon. Iodide-ion adsorption on the teflon surface experimentally is not found out, therefore at calculation in model equations the corresponding members have been equal to zero. As follows from comparison of the data in columns 10 and 11 of Table 38, calculated values, as well as in Table 37, they agree with experimental ones within the limits of the order magnitudes for the majority of experiments. The analysis of dataTable 37 and Table 38 allows to make the following conclusion. In the absence of irradiation:

At identical initial conditions calculation shows iodine PC growth with pH increase. At pH= 4-6 this tendency is expressed poorly, but it becomes more obvious at pH> 6, in experiment such dependence obviously is traced so;

Introduction in initial solution of iron-hydroxide sludge can cause both insignificant increase of iodine PC, and its appreciable decreasing if to proceed from experimental data. Calculation predicts PC

decrease in both cases. Probably, at temperature 60 ^{o}C heterogeneous oxidation of iodide-ion by trivalent iron proceeds.
Where irradiation:

- The iodine PC at identical pH, temperature and the moment of sampling is reduced on the order of value concerning experiments without irradiation PC calculated from $[I^{-}]_{aq}$);
- With introduction of hydroxide sludge in initial solution at identical temperature and pH~5 it is observed decrease of iodine PC. At 90 ^{o}C and 120 ^{o}C and sludge presence PC increases by 2-10 times.

Thus, fulfilled verification has confirmed availability of the developed calculated code and satisfactory agreement calculated and experimental data (to within the order of value).

3. Results by the end of the project duration

Earlier developed iodine model is modernized with reference to problems of the present work. The model is capable to predict iodine behaviour in containment during a chemical phase of severe accident with fusion of core and corium release beyond a reactor vessel. The calculation program (in programming language Visual Fortran Professional Edition 6.5) is developed. At modernization of model the description of the mechanism of molecular iodine hydrolysis is specified (4 reactions describing HOI dissosiation and ion I_3^- dissociation-recombination are entered). The kinetic equations describing adsorption of a iodide-ion by iron hydroxide are proposed and entered into model. Pre-test calculations of influence of I^--ion adsorption by FeOOH (iron sludge) on iodine volatility and iodine PC are carried out with use of constant values calculated from published experimental data.
Verification of iodine module and calculation code developed by us has shown, that they well describe influence of an irradiation, temperatures and pH on iodine release in gas phase in conditions of the experiments.
Thus, the fulfilled verification has confirmed availability of the developed calculation code and satisfactory calculated and experimental data agreement (to within the order of value) in view of the reached accuracy of measurements. The iodine model and a calculation code can be used for post-test calculations in the project №3345 and in general severe accident code.

Personnel Commitments

Name	Category	Days
Kritsky Vladimir	1	**20**
Ampelogova Natalia	1	**30**
BobrovYuri	1	**96**
Vasiliev Vladimir	1	**100**
Alemaskina Elena	2	**16**
Shmantsar Oleg	2	**95**
Bezlepkin Vladimir	1	**26**
Zatevakhin Mikhail	1	**6**
Blinova Lidia	1	**0**
Leontyev Yury	2	**10**
Semashko Sergey	2	**19**
Ivkov Igor	2	**0**
Frolov Andrey	2	**35**
Astafyeva Vera	2	**0**
Lebedev Leonid	2	**56**
Ryabova Anastasia	2	**54**
Ignatyev Alexey	2	**5**
Potapov Igor	2	**8**
Sidorov Valery	2	**0**
Alexeev Sergey	2	**0**
Krylov Yury	2	**0**

Fomina Yulia	3	**11**
Buzharov Nikolay	4	**6**
Azaryeva Nadezda	3	**15**

3. Summary of Personnel Commitments

	Number of persons	Total days	Total grants, USD
Category I	47	4086	124694
Category II	53	5287.5	131812.5
Category III	17	1175	22170
Category IV	1	20	400
Total	**118**	**10568.5**	**279076.5**

4. Presentation of project results

see Attachment 1. List of published papers and reports without abstracts
see Attachment 2. List of presentations at conferences and meetings without abstracts
see Attachment 3. Information on patents and copy rights

5. Co-operation with foreign collaborators

5.1. 11th Meeting of Contact Expert Group on Severe Accident Management (CEG-SAM). March 6-9, 2007 Dresden

5.2. The EVAN ISTC project progress meeting, Saint Petersburg, Russia, September 10, 2007

5.3. 12th Meeting of Contact Expert Group on Severe Accident Management (CEG-SAM), September 11-13, 2007, St. Petersburg

5.4. The EVAN ISTC project progress meeting, Budapest, Hungary, March 04, 2008

5.5. 13th Meeting of Contact Expert Group on Severe Accident Management (CEG-SAM), Budapest, Hungary, Hungarian Academy of Sciences KFKI, Atomic Energy Research Institute AEKI, March 5-7, 2008

5.6. Foreign collaborator Paul Bottomley visited the NPO CKTI test facility at 01.06.2007 for investigation of aerosol transport with a goal of inspection of workflow on Project #3345. From Russian side in the meeting took part:

1. Bezlepkin V.V.. – project manager, deputy director of SPb AEP.
2. Krektunov O.P. – зам. руководителя проекта deputy project manager, leading researcher NPO CKTI.
3. Zubkov A.A. – head of department #10 NPO CKTI.
4. Fokin B.S. – head of laboratory 102.
5. Lebedev M.E.. – leadind researcher, department 10.
6. Feldberg L.A. – head of laboratory 112.
7. Yurchenko A.E.- leading engineer. sector 292.

O.P.Krektunov familiarized mr. Bottomley with test facility construction and demonstrated equipment installed and explained its function with respect to investigation tasks. L.A.Feldberg told about optical methods of measurements used in the test facility. Then test facility was activated and its equipment was demonstrated in operation. In conclusion it was noted that works on Project # 3345 are fulfilled in accordance with Working plan and test facility is ready completely for planned tests performance.

5.7. Foreign collaborators Paul Bottomley (JRS-ITU, Germany) and Dr. Ari Auvinen (VTT, Finland) visited the NPO CKTI test facility for aerosol transport investigation 07.09.2007 fo inspection of workflow on Project #3345. From Russian side in the meeting took part:

1. Bezlepkin V.V.. – project manager, deputy director of SPb AEP.
2. Krektunov O.P. – deputy project manager, leading researcher NPO CKTI.
3. Zubkov A.A. – head of department #10 NPO CKTI.
4. Fokin B.S. – head of laboratory 102.
5. Lebedev M.E.. – leading researcher, department 10.
6. Feldberg L.A. – head of laboratory 112.
7. Semidetnov N,V.. – associate prof .of SPBMTU
8. Yurchenko A.E.- leading engineer. sector 292.

O.P.Krektunov familiarized collaborators with test facility construction and demonstrated equipment installed and explained its function with respect to investigation tasks. L.A.Feldberg and N.V.Semidetnov told about optical methods of measurements used in the test facility. Then test facility was activated and its equipment was demonstrated in operation.
The joint seminar of project participants and the contact expert group has been carried out
The exchange of scientific materials and reports and discussion of the obtained experimental results have been realized on EVAN ISTC project Progress Meeting (Saint-Petersburg , 9-10 September 2007).

6. Co-operation with CIS sub-contractors

Regular working co-operation with CIS sub-contractor has been organized.

7. Procurement

Work plan No.	Name	Status
	2-й квартал	
14	UPS PowerMan Real Smart 1500	Received
15	Computer	Received
17	Workstation №2 PC-3400	Received
18	Notebook Fujitsu-Siemens Amilo M-1451G 159500-003	Received
21	АЦП PCI-1718HGU	Received
23	Commutators; PCLD-789D	Received
29	Laboratory furniture	Received
31	PC: AMD Athlon64 X2 4200+Socket AM2, 2048 Mb, Video 256 Mb, DVD-CDRW, 400Gb HDD, mouse, keyboard, floppy	Received
32	LCD monitor 19"	Received
33	Motherboard ASUSTeK PSB Deluxe (P965) Processor Intel Core 2 Duo 2.13 GHz(BOX), Memory DDR2 1024 Mb Nanya PC6400 Video card XFX GeForce 8800GTX 575M 768Mb	Received
	3-й квартал	
7	digital oscilloscope EZ Digital DS-1080C	Received
11	ventilator AVDm – 3,5.2-02 (200 m3/h)	Received
13	thermohygrometer testo 625 with auxiliaries	Received
14	UPS PowerMan Real Smart 1500	Received
15	computer	Received
17	Server HP ProLiant ML310 T03 Monitor 19" Samsung 932B	Received
18	Notebook Fujitsu-Siemens Amilo M-1451G	Received

	159500-003	
19	Aire cap implosion protection AZD193.000	Received
20	differential manometer testo 512, 0... 20 GPa/Mbar, with auxiliaries	Received
21	ADC PCI-1718HGU	Received
22	Plate control –measure PRA-200, Producer - Halton Oy (Finland)	Received
23	Commutators PCLD-789D	Received
24	Covering thickness transducers	Received
25	Program supply for experiment automatization LabVIEW Development Systems	Received
29	Laboratory furniture	Received
	Аэрозольный генератор Pro ULV 1037 BP	Received
	Balance VLTE-500	Received
	Анализатор амплитуды импульсов (AAI)	Received
	4-й квартал	
5	Analog to digital converter (20 MHz): PCI 9812 - 4-CH	Received
7	digital oscilloscope EZ Digital DS-1080C	Received
11	ventilator AVDm – 3,5.2-02 (200 m3/h)	Received
13	thermohygrometer testo 625 with auxiliaries	Received
14	UPS PowerMan Real Smart 1500	Received
15	computer	Received
17	Server HP ProLiant ML310 T03 Monitor 19" Samsung 932B	Received
18	Notebook Fujitsu-Siemens Amilo M-1451G 159500-003	Received
19	Aire cap implosion protection AZD193.000	Received
20	differential manometer testo 512, 0... 20 GPa/Mbar, with auxiliaries	Received
21	ADC PCI-1718HGU	Received
22	Plate control –measure PRA-200, Producer - Halton Oy (Finland)	Received
23	Commutators PCLD-789D	Received
24	Covering thickness transducers	Received
25	Program supply for experiment automatization LabVIEW Development Systems	Received
29	Laboratory furniture	Received
	Aerosol generator Pro ULV 1037 BP	Received
	Balance VLTE-500	Received
	Pulse-Height Analyzer (PHA)	Received
	Vacuum cleaner Delvir	Received

8. Conclusion, Problems, Suggestions

During the course of the project the new research results will be obtained allowing to develop new up-to-date computer programs (codes) for nuclear power plants accident analysis. Enhancing the level of safety assessment for new NPP designs with up-to-date computer codes increase the competitiveness of the design at the market. Selling or promoting of the research product obtained during the project is possible within the framework of the cluster of research institutions involved in the applied R&D for NPP safety analysis.

Primarily, the Russian and foreign nuclear power engineering research and design institutions are demanding for results of the project. Foreign collaborators having submitted the support letters to ISTC are the main foreign consumers of the future results.

Later work plan and need for additional developments will depend on effectiveness of co-operation with the main potential end-users of the research results — foreign collaborators.

Most probable scenario for gaining income out of the project results will be international contracts for joint activities on safety assessment for nuclear power plants.

9. Attachment 1. List of published papers and reports

№	Document	Confidentiality	Title
1	Report	Non-classified	Analysis of calculation results for severe accident scenarios.
2	Report	Non-classified	Experimental studies of the low-volatile fission products release at the oxidation of suboxidized molten corium.
3	Report	Non-classified	Analytical investigation of fission products release from molten pool or core catcher.
4	Report	Non-classified	Experimental study of aerosols transport processes in the primary circuit equipment.
5	Report	Non-classified	Theoretical and computer modeling of aerosol transport in the primary circuit.
6	Report	Non-classified	Experimental investigations of containment parameters impact on volatile iodine content and correlation.
7	Report	Non-classified	Numerical and theoretical modeling of containment parameters impact on volatile iodine species content and correlation.

10. Attachment 2. List of presentations at conferences and meetings

10.1. The EVAN ISTC project progress meeting, Saint Petersburg, Russia,September 10, 2007

A. Frolov	Radioactive release during severe beyond-design-basis accidents at nuclear power plants with WWER reactors
I. Potapov	Analysis of FP buildup in fuel, FP release from fuel and molten pool (review of models).
V. Sidorov S.Tsaun	Analysis of conditions for release of radioacitve sources from reactor plant during severe accidents (LOCA and primary-to-secondary circuit leaks).
M. Zatevakhin I. Ivkov	Analysis of aerosol behavior inside containment during severe accidents.
S. Beshta	Experimental studies of fission product release from molten pool / core catcher
O.Tarasov	Theoretical analysis and computation of fission product release from molten pool / core catcher
O. Krektunov	Result of an experimental study of aerodynamic characteristics and processes of liquid aerosol transport in a vertical tube
V. Alipchenkov	Pre- and post-test analysis of experimental findings obtained at ATF facility
N. Ampelogova	Experimental studies of effects produced by in-containment parameters on content

	and ratio of volatile forms of iodine
Yu. Bobrov	Analytical modeling of effects produced by in-containment parameters on content and ratio of volatile forms of iodine. Pre- and post-test calculations.
Yu. Gorbachev	"Modeling of particle carryover from a surface in turbulent flow"
A. Ignatiev	"Numerical simulation of aerosol particles transport and deposition based on 3D hydrodynamic codes

10.2. The EVAN ISTC project progress meeting, Budapest, Hungary, March 04, 2008

V. Sidorov	Task 1. Assessment of results of severe accident sequences modeling
S. Bechta	Task 2. Experimental research on FP release from molten pool/core melt catcher
O. Tarasov	Task 3. Analytical investigation of fission products release from molten pool or core catcher
M. Lebedev	Task 4. Experimental study of processes aerosols deposition and resuspension in the primary circuit equipment
A. Ignatiev, Yu. Gorbachov	Task 5. Theoretical and computer modeling of aerosol transport in the primary circuit
N. Ampelogova	Task 6. Experimental investigations of containment parameters impact on volatile iodine content and correlation
N. Ampelogova, L. Lebedev	Task 7. Numerical and theoretical modeling of containment parameters impact on volatile iodine species content and correlation

10.3. V. Bezlepkin ."Status of the ISTC project #3345 "Ex-vessel source term analysis" (EVAN)", phase 1". 11th Meeting of Contact Expert Group on Severe Accident Management (CEG-SAM). March 6-9, 2007 Dresden

10.4. V. Bezlepkin. Status of the ISTC project #3345 "Ex-vessel source term analysis" (EVAN)", phase 1 (SPAEP). 12th Meeting of Contact Expert Group on Severe Accident Management (CEG-SAM), September 11-13, 2007, St. Petersburg

10.5. V. Bezlepkin. Final report on the ISTC project #3345 "Ex-vessel source term analysis" (EVAN)", phase 1. 13th Meeting of Contact Expert Group on Severe Accident Management (CEG-SAM), Budapest, Hungary, Hungarian Academy of Sciences KFKI, Atomic Energy Research Institute AEKI, March 5-7, 2008

11. Attachment 3. Information on patents and copy rights

Requests for patents and copy rights have not been submitted.

12. Attachment 4. Technology Implementation Plan

ISTC Project #3345

Source Term Assessment at Ex-vessel Stage of Severe Accident

Technology Implementation Plan

on the work performed from 01.01.2007 to 31.12.2007

Federal State Unitary Enterprise "St.Petersburg Research and Design Institute ATOMENERGOPROEKT"
(FSUE SPAEP)

191036, Russia, St.Petersburg, 2nd Sovetskaya street, 9/2a

Project Manager
SPAEP Deputy
Director for R&D

Vladimir Bezlepkin
Doctor of Science
(Power Engineering)

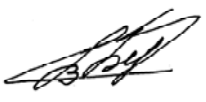

31.12.07

Signature / Date